

**UNIVERSITY OF PRETORIA**  
**FACULTY OF VETERINARY SCIENCE**  
**DEPARTMENT OF PARACLINICAL SCIENCES**

**TITLE OF THE RESEARCH PROJECT:**

**Pathology of complicated *Babesia rossi*-associated acute lung injury and respiratory distress syndrome in dogs**

**THE DEGREE:**

MMedVet (Pathology)

**AUTHOR:**

Dr Collin Martin

**STUDENT NUMBER:**

21075116

**CONTACT DETAILS:**

Address: Unit 27 La Bri, 94 Mopani Street, Hennopspark, 0157

Tel: 0835027040; Email: cmartin@webmail.co.za

**SUPERVISOR:** Prof. Andrew Leisewitz

**CO-SUPERVISOR:** Dr Sarah J. Clift

## ACKNOWLEDGEMENTS

This odyssey is finally at its end and there are so many people that helped and guided me along the journey that I need to thank.

Firstly, to my wife, Robyn, who listened patiently to the ramblings of a confused young man and helped make sense of life. You helped me see things from another point of view and stood by my side no matter the bumps in the road. The many late-night cups of coffee were greatly appreciated. I am a far better person with you and it's a privilege to be with you every day. I love you with all my heart baby girl.

To my mother, Retha, for instilling in me a love of animals that made me pursue a career in veterinary science.

To Tim, Angela, Lynn, Isabel, Llewellyn, Shayna, Melanie and the other staff at Blue Hills Veterinary Hospital for giving me start in veterinary science and teaching a fresh-faced, naive new graduate about being a real veterinarian.

To Sam, for being a friend and giving me the opportunity to pursue Veterinary pathology.

To Liza. My friend and mentor. You took a virtual pathologic idiot and turned me into a somewhat decent pathologist. How you did this I don't know. Your wisdom and patience are truly infinite.

To Sarah and Andrew, without your guidance and infinite patience, this lazy post graduate student probably would not have succeeded.

To my daughter Molly. You came along in the middle of this adventure and just made it so much more exciting. You completely changed my perspective on life. Now I get to be at your side, showing you the way through life. Picking you up when you fall down and that is truly a privilege.

And finally, to my late father, Les. Although you were not able to see me complete this sojourn, I know you are with me in spirit. Guiding me along the path of life as I will now do with Molly. I will miss your patient ear, the unexpected sage advice and your wickedly dry sense of humour. I will miss you dad. We all miss you!

## DECLARATION

I, **Collin Armand Martin**, hereby declare that the work on which this thesis is based is my own independent work and that neither the whole work nor part of it has been, is being, or shall be submitted for another degree at this or another university, institution for tertiary education or professional examination body.

---

Collin Martin

---

Date

## **ETHICS STATEMENT**

I, Collin Armand Martin, have obtained the necessary research ethics approval (V073-16) for the research described in this dissertation; I declare that I have obtained the ethical standards required in terms of the University of Pretoria's code of ethics for researchers and the policy guidelines for responsible research.

## TABLE OF CONTENTS

ACKNOWLEDGEMENTS .....	2
DECLARATION .....	3
ETHICS STATEMENT .....	4
TABLE OF CONTENTS.....	5
LIST OF FIGURES .....	8
LIST OF TABLES.....	11
ABREVIATION LIST .....	12
SUMMARY .....	14
CHAPTER ONE: INTRODUCTION .....	16
CHAPTER TWO: LITERATURE REVIEW .....	18
2.1. Expanded Definition of ALI/ARDS .....	18
2.2. Risk Factors for ALI/ARDS .....	21
2.3. Pathophysiology of ALI/ARDS .....	22
2.4. Temporal aspects of the pathology of ALI/ARDS .....	25
2.5. Macroscopic pulmonary pathology in ALI/ARDS .....	26
2.5.1. Macroscopic pulmonary pathology in complicated canine babesiosis .....	26
2.5.2. Macroscopic pulmonary pathology in human malaria-associated ALI/ARDS .....	27
2.5.3. Macroscopic pathology in murine malaria-associated ALI/ARDS .....	27
2.5.4. Macroscopic pathology of murine babesia-associated ALI/ARDS .....	28
2.6. Microscopic pulmonary pathology in ALI/ARDS .....	28
2.6.1. Microscopic pulmonary pathology in complicated canine babesiosis .....	29
2.6.2. Microscopic pulmonary pathology in human malaria-associated ALI/ARDS .....	31
2.6.3. Microscopic pulmonary pathology in murine malaria-associated ALI/ARDS .....	32
2.6.4. Microscopic pulmonary pathology in murine babesia-associated ALI/ARDS .....	33
2.7. Immunohistochemistry .....	34
2.8. Problem and Hypothesis .....	35
2.8.1. Problems .....	35
2.8.2. Hypotheses .....	35
2.9. Benefits arising from the experiment .....	35
2.10. Objectives .....	36
CHAPTER THREE: MATERIALS AND METHODS .....	36
3.1. Experimental design .....	36

3.1.1.	Model system and justification of the model .....	36
3.1.2.	Experimental animals: Inclusion criteria .....	36
3.1.3.	Experimental animals: Exclusion criteria .....	36
3.1.4.	Control animals: Exclusion criteria .....	36
3.1.5.	Source of Experimental animals .....	37
3.1.6.	Source of Control animals .....	37
3.1.7.	Post-mortem examination and sample collection .....	37
3.1.8.	Sample processing .....	37
3.1.9.	Tissue sections .....	38
3.1.10.	Immunohistochemistry technique .....	38
3.1.11.	Examination .....	39
3.2.	Data Analysis .....	39
3.3.	Experimental animals .....	40
3.4.	Staff.....	40
3.5.	Facilities .....	40
3.6.	Equipment .....	40
3.6.1.	Macropathology .....	40
3.6.2.	Routine Histology .....	40
3.6.3.	Immunohistochemistry .....	41
3.7.	Records.....	43
3.8.	Declaration of conflict of interest .....	43
3.9.	Ethical Considerations .....	43
CHAPTER FOUR: RESULTS .....		44
4.1.	Gross pathology .....	44
4.1.1.	Control cases.....	44
4.1.2.	Naturally infected <i>B. rossi</i> cases .....	44
4.2.	Histopathology.....	47
4.2.1.	Control cases.....	47
4.2.2.	Naturally infected <i>B. rossi</i> cases .....	50
4.3.	Immunohistochemistry .....	64
4.3.1.	Control cases.....	64
4.3.2.	Naturally infected <i>B. rossi</i> cases .....	66
5	CHAPTER FIVE: DISCUSSION.....	80
5.1.	Macroscopic pathology.....	80
5.2.	Histopathology.....	80
5.2.1.	Pulmonary oedema, endothelial cell activation and VCAM-1.....	81

5.2.2.	Inflammatory cell population.....	82
5.2.3.	Haemorrhage, fibrin exudation.....	85
5.2.4.	Thrombosis and other intravascular findings .....	85
5.2.5.	Cell death.....	86
5.2.6.	Other lesions.....	86
CONCLUSION .....		89
REFERENCES .....		91
APPENDICES .....		100
Appendix 1: O’Dell lung scoring system grading criteria <sup>69</sup> .....		101
Appendix 2: Modified O’Dell Lung scoring system for use in <i>Babesia</i> -associated ALI/ARDS .....		103
Appendix 3: Immunohistochemistry score sheet for <i>Babesia</i> -associated ALI/ARDS.....		106
Appendix 4: Informed consent.....		107
Appendix 5: Individual case reports.....		108
5.1.	Case 1.....	108
5.2.	Case 2.....	108
5.3.	Case 3.....	109
5.4.	Case 4.....	109
5.5.	Case 5.....	110
5.6.	Case 6.....	110
5.7.	Case 7.....	111
5.8.	Case 8.....	111
5.9.	Case 9.....	112
5.10.	Case 10 .....	112
5.11.	Case 11 .....	113

## LIST OF FIGURES

Figure 1: Human lung, hyaline membrane formation (Thick arrow) <sup>105</sup> .....	18
Figure 2: Normal (left) vs injured (right) alveolus. Note that the pathological sequence of events is triggered by activated alveolar macrophages and neutrophils (circled) <sup>105</sup> . 22	
Figure 3: Normal canine lung, inflated. Note the light pink, pillowy appearance in all lung lobes. Image obtained from the pathology database, Section of Pathology, Department of Paraclinical Science, Faculty of Veterinary Science, University of Pretoria. ....	26
Figure 4: Representative lungs from uninfected mice and mice infected with <i>Plasmodium chabaudi</i> AS (10 d post-infection), <i>Plasmodium berghei</i> strain NK65 (10 d post-infection), or <i>Plasmodium berghei</i> ANKA (7 d post-infection) were photographed. Note the swelling and dark brown discolouration (black star) in the 10 day post-infection sample <sup>98</sup> . ....	27
Figure 5: Histology of normal dog lung. Note the thin alveolar walls and absence of oedema and inflammatory cells within alveolar walls and lumens 400×. From the pathology database, Section of Pathology, Department of Paraclinical Science, Faculty of Veterinary Science, University of Pretoria. ....	28
Figure 6: Histopathology of the lungs during complicated canine babesiosis (H&E stain, ×200). Note the presence of haemorrhages (black star), hyaline membranes (block arrow), and congestion of capillaries (thin black arrows) <sup>17</sup> .....	30
Figure 7: A. Pulmonary histopathology in a fatal case of adult falciparum malaria. There is expansion of alveolar capillaries by sequestered parasitized erythrocytes and host inflammatory leukocytes (thin black arrow). Monocytes and neutrophils within alveolar septal capillaries (haematoxylin and eosin [H&E] staining, magnification × 400. B. More severe pulmonary histopathology from another fatal case of falciparum malaria with host leukocytes expanding the alveolar septa (thin black arrow), intra-alveolar haemorrhage and pulmonary oedema (black star), hyaline membrane formation (thick black arrow) as part of a picture of diffuse alveolar damage (H&E staining, magnification x200) <sup>92</sup> . ....	31
Figure 8: Lungs of <i>Plasmodium berghei</i> strain NK65-infected mice were dissected at 8, 10 and 12 days post-infection and sections were stained with H&E. Representative examples are shown (original magnification, ×20; scale bars, 100 μm) <sup>98</sup> . Note the progressive development of pulmonary oedema (black stars) along with leukocyte infiltration.....	32
Figure 9: Pulmonary histopathology in <i>Babesia</i> -infected mice. A. Section of lung from a WA-1 infected mouse showing a small pulmonary vein occluded by mononuclear inflammatory cells. B. Section of lung from a WA-1 infected mouse showing the presence of vacuolated alveolar macrophages in the alveolar lumens (arrows) <sup>34</sup> .....	33
Figure 17: Lung. Multifocal discrete, often coalescing pulmonary petechial and ecchymotic haemorrhages. ....	45
Figure 18: Lung. Severe diffuse pulmonary haemorrhage with atelectasis and multifocal emphysema.....	45
Figure 19: Lung, cut section. Severe pulmonary with oozing of fluid and froth. ....	46
Figure 20: Trachea, opened. Severe accumulation of pulmonary oedema/froth within the tracheal lumen.....	46



Figure 21: Case 4. Focal severe alveolar macrophage infiltration with pulmonary oedema (thick arrow) and mild interstitial expansion with mild perivascular lymphocytes and plasma cell accumulation (star). 200× magnification.....	51
Figure 22: Case 6. Interstitial mononuclear expansion (thin arrow) with endothelial cell activation and intravascular leukostasis (Thick arrow). 200× magnification.....	51
Figure 23: Case 9. Severe interstitial mononuclear expansion (Thick arrow) with scattered apoptosis (Thin arrow), atelectasis and pulmonary oedema (star). 400× magnification.....	52
Figure 24: Case 1. Severe mononuclear alveolar infiltrate (thick arrow) with haemorrhage and fibrin exudation extending into the alveolar ducts (thin arrow). 400× magnification.....	52
Figure 25: Case 1. Severe mononuclear alveolar infiltrate (thick arrow) with haemorrhage and fibrin exudation (Star) as well as endothelial cell activation (thin arrow), lymphocyte margination (triangle) and perivascular infiltration. 400× magnification.....	53
Figure 26: Case 2. Severe alveolar oedema (thin arrow) with moderate haemorrhage (thick arrow). 200× magnification.....	53
Figure 27: Case 1. Subpleural haemorrhage (thick arrow), Severe alveolar infiltrate with haemorrhage (thin arrow). 200× magnification.....	54
Figure 28: Case 1. Mild bronchiolar haemorrhage (thin arrow) with alveolar fibrin exudation (star) and mononuclear alveolar infiltrate (thick arrow). 200× magnification.....	54
Figure 29: Case 2. Perivascular lymphoplasmacytic cuffing (thick arrow) with alveolar oedema and haemorrhage (star) as well as endothelial cell activation (thin arrow). Also present is intravascular mononuclear leukostasis (triangle). 200× magnification.....	55
Figure 30: Case 8 - Intravascular haemosiderophages (thin arrows) and megakaryocytes (thick arrow). 400× magnification.....	55
Figure 31: Case 8. Moderate alveolar haemorrhage with fibrin (thick arrow) and endothelial activation (thin arrow). 400× magnification.....	56
Figure 32: Case 9. Severe interstitial mononuclear expansion, endothelial cell activation (thin arrow) with mild alveolar haemorrhage. 400× magnification.....	56
Figure 33: Case 9. Severe interstitial mononuclear expansion with endothelial cell activation and intravascular mononuclear leukostasis (thin arrow). Moderate alveolar haemorrhage and fibrin (star) and severe high protein content pulmonary oedema (thick arrow). Apoptotic cell (blocked arrow). 400× magnification.....	57
Figure 34: Case 10. Moderate endothelial cell activation (thin arrow). 200× magnification.....	57
Figure 35: Case 11. Moderate interstitial mononuclear expansion (thin arrow) with alveolar oedema (star). Large intravascular thrombosis with enmeshed large mononuclear cells (thick arrow). 200× magnification.....	58
Figure 36: Left. CD20 control section. Right. Case 7. CD20 positive B-lymphocytes and plasma cells within the alveoli and alveolar walls (arrows). 400× magnification.....	67
Figure 37: Left. CD3 control section. Right. Case 9. CD3 positive T-lymphocytes within the alveolar walls (arrow). 400× magnification.....	69
Figure 38: Left. Mum-1 control section. Absence of specific positive mature B-lymphocytes and plasma cells in the alveoli and alveolar walls. Right. Case 7.	

Scattered Mum-1 positive mature B-lymphocytes/plasma cells within the alveolar walls (arrow). 400× magnification. ....	71
Figure 44: Left. CD204 control section. Right. Case 8. CD204 positive alveolar macrophages in the alveoli (thin arrow) and positive macrophages/dendritic cells in the alveolar walls (thick arrow). 400× magnification. ....	73
Figure 40: Control. Pax-5. 400× magnification.....	75
Figure 48: Left. MAC387 control section. Right. Case 2. MAC387 positive monocyte-macrophages and rare neutrophils within the alveolar walls (thin arrow) and alveoli (thick arrow). 400× magnification. ....	77
Figure 51: Left. VCAM-1 control section. Positive vascular endothelium in the alveolar walls (thick arrow). 400× magnification. Right. Case 9. VCAM-1 positive endothelial cells in the alveolar walls (thick arrows) as well granular and cytoplasmic membrane labelling of intravascular mononuclear cells (thin arrow). 400× magnification. ....	78

## LIST OF TABLES

Table 1: Criteria for the diagnosis of veterinary Acute Lung Injury (ALI) and Acute Respiratory Distress Syndrome(ARDS) <sup>108</sup> .....	20
Table 2: Selected risk factors associated with the development of Acute Lung Injury and Acute Respiratory Distress Syndrome in veterinary patients. ....	21
Table 3: List of antibodies with target cell/process, supplier, type and clone and catalogue number .....	41
Table 4: Babesia related ALI/ARDS control cases summary score sheet A. Adapted severity scores <sup>73</sup> . ....	47
Table 5: Babesia related ALI/ARDS control cases summary score sheet B. Presence or absence of lesion <sup>73</sup> . ....	49
Table 6: Babesia related ARDS summary score sheet A. Severity of lesion .....	59
Table 7: Babesia related ARDS summary score sheet B. Presence or absence of lesion. ....	61
Table 8: Babesia related ARDS summary score sheet C. Lesion distribution. ....	61
Table 9: Immunohistochemistry control cases score summary sheet .....	64
Table 10: Summary of CD20 immunohistochemistry results in dogs naturally infected with <i>B. rossi</i> . ....	66
Table 11: Summary of CD3 immunohistochemistry in the lungs of dogs naturally infected <i>B. rossi</i> . ....	68
Table 12: Summary of Mum-1 immunohistochemistry results in the lungs of dogs naturally infected with <i>B. rossi</i> . ....	70
Table 13: Summary of CD204 Immunohistochemistry results in dogs naturally infected with <i>B. rossi</i> . ....	72
Table 14: Summary of Pax-5 immunohistochemistry results in the lungs of dogs naturally infected with <i>B. rossi</i> . ....	74
Table 15: Summary of MAC387 immunohistochemistry results in the lungs of dogs naturally infected with <i>B. rossi</i> . ....	76
Table 16: Summary of significant immunohistochemical results .....	79

## ABREVIATION LIST

**Ab**- Antibody  
**AHSV** – African Horse Sickness Virus  
**ALI** – Acute Lung Injury  
**ARDS** – Acute Respiratory Distress Syndrome  
**BALT** – Bronchial associated lymphoid tissue  
**CC** – Control Case  
**CHV** – Canine Herpes Virus  
**CXCL-10** - CXC Chemokine Ligand-10  
**C3H/HeN** – C3H/He mice  
**C57BL/6J** – C57 Black 6 Mouse – Jackson Laboratories  
**DPS** – Department of Paraclinical Science  
**EACC** – European American Consensus Committee  
**EqNALI/EqNARDS** - Equine Neonatal Acute Lung Injury / Equine Neonatal Acute Respiratory Distress Syndrome  
**FVS** - Faculty of Veterinary Science at the University of Pretoria  
**FFPE** - Formalin-Fixed, Paraffin-Embedded Tissue  
**H&E** – Haematoxylin and Eosin stain  
**HMGB-1** – High-mobility group box – 1 protein  
**HPF** – 400x magnification high power field.  
**ICAM-1** – Inter-cellular Adhesion Molecule – 1  
**IHC** - Immunohistochemistry  
**IL-1** – Interleukin 1  
**IL-4** – Interleukin 4  
**IL-6** – Interleukin 6  
**MA-ARDS** – Malaria-associated Acute Respiratory Distress Syndrome  
**MCP-1** – Monocyte chemotactic factor - 1  
**NE-ARDS**- Neonatal Acute Respiratory Distress Syndrome  
**OVAH** – Onderstepoort Veterinary Academic Hospital  
**PBANKA** - *Plasmodium berghei* ANKA  
**PBNK65** – *Plasmodium berghei* strain NK65  
**PCAS** - *Plasmodium chabaudi* AS  
**PIMS** – Pulmonary Intravascular Macrophages  
**SP** – Section of Pathology  
**SOP** – Standard Operating procedure  
**TC** – Test Case  
**TGF- $\beta$**  – Transforming Growth Factor – Beta  
**T<sub>H</sub>1** – T Helper 1  
**T<sub>H</sub>2** – T Helper 2  
**TNF- $\alpha$**  – Tumour Necrosis Factor - alpha  
**VetARDS** – Veterinary Acute Respiratory Distress Syndrome

**VetALI** – Veterinary Acute Lung Injury

**VE-Cadherin** – Vascular-Endothelial Cadherin

**VCAM-1** – Vascular Cell Adhesion Molecule – 1

**WA1** – *Babesia* type WA1 – Isolated from human in Washington State, United States of America.

## SUMMARY

### **THE PATHOLOGY OF COMPLICATED *BABESIA ROSSI*-ASSOCIATED ACUTE LUNG INJURY AND RESPIRATORY DISTRESS SYNDROME IN THE DOG**

*By*

**Collin Armand Martin**

<b>Supervisor:</b>	<b>Prof A L Leisewitz</b>
<b>Co-supervisor:</b>	<b>Dr. S J Clift</b>
<b>Department:</b>	<b>Paraclinical Sciences</b>
<b>Degree:</b>	<b>M.Med.Vet (Pathology)</b>

A proportion of *Babesia rossi* infections in dogs are classified as complicated. One of the most lethal complications is the acute lung injury (ALI) and acute respiratory distress syndrome (ARDS). Patients affected by this complication usually succumb within 24 hours and there are similarities between this disease and malaria associated ALI and ARDS in humans, both rapidly fatal conditions. Both diseases are caused by haemoprotozoal parasites transmitted by insect vectors, namely ticks for babesiosis and mosquitoes for malaria.

The pulmonary pathology of complicated babesiosis is poorly described and the aim of this study is to provide a thorough histomorphological analysis with immunohistochemical labelling of leukocytes to further define the immune cell population.

The left caudal lung lobes from 11 *Babesia rossi* infected dogs and 4 healthy controls were examined with standard light microscopy and immunohistochemical markers applied. Markers included CD204 (resident tissue macrophages and dendritic cells), MAC387 (monocyte-macrophages of bone marrow origin), CD3 (mature T-lymphocytes), CD20 (mature B-lymphocytes and normal plasma cells), Mum-1 (plasma cells) and PAX-5 (immature and mature B-lymphocytes).

Histopathology showed a severe increase in monocyte-macrophages within the alveolar walls and lumens. This was invariably accompanied by alveolar oedema as well as multifocal to coalescing areas of haemorrhage. Immunohistochemical labelling showed

a significant increase in MAC387, CD204 and CD3 positive cells in the infected cases compared to healthy control dogs.

This study provided novel insights into the pathology of and similarities between babesia and malaria associated ALI/ARDS in dogs and humans, respectively. Further fine ultrastructural examination of the pulmonary vascular endothelium is required in future studies.

## CHAPTER ONE: INTRODUCTION

Acute lung injury (ALI) and acute respiratory distress syndrome (ARDS) are clinical syndromes characterised by arterial hypoxaemia caused by pulmonary pathology that leads to a reduction in the efficiency of gaseous exchange<sup>105</sup>. Diagnosis of ALI and ARDS can only be reached if cardiac causes of dyspnoea have been ruled out<sup>105</sup>. It is important to realise that ALI and ARDS are on a continuum with ALI being less severe than ARDS, but as the pulmonary injury and hypoxaemia worsens, ALI progresses to ARDS.

Acute lung injury and ARDS are infrequently observed in veterinary medicine, but they are commonly fatal. It is not a diagnosis in and of itself but is rather the end result of a variety of diseases and conditions that are responsible for the underlying lung pathology. Recognising when the syndrome is present is important from a treatment and prognosis point of view. Acute lung injury and ARDS should be a differential diagnosis for any patient presenting with acute onset severe dyspnoea.

Acute lung injury and ARDS were first described by Ashbaugh et al<sup>6</sup> in 1967 in human patients. An adult respiratory distress syndrome was initially described but eventually the clinical term Acute Respiratory Distress Syndrome was coined because it was also found to occur in children<sup>102</sup>. Since these initial studies, a vast amount of research has been done as ALI /ARDS is still a leading cause of mortality in human medicine. It is estimated that 40 to 60% of human patients diagnosed with these syndromes, despite all the latest technological advances, will die as a result<sup>102</sup>. Acute lung injury and ARDS is one of the leading causes of death in human *Plasmodium spp.* infection (mostly *P. falciparum* and less commonly *P. vivax*<sup>5</sup>) and has been extensively studied<sup>94</sup>. Malaria and babesiosis are similar diseases in the respect that they are both caused by vector-borne protozoal parasites which share similar morphological and structural characteristics (both belonging to the phylum Apicomplexa, which have apical complexes allowing for host cell penetration), as well as disease pathogenesis (by invading erythrocytes) and evoke a similar host immune response<sup>13</sup>. Murine models exist for both *Plasmodium* and *Babesia* infection and the lesions observed show striking similarities and even a degree of cross-protection was observed in some cases<sup>15</sup>.

There numerous potential risk factors which may incur ALI/ARDS. One of the most common and well characterised is systemic bacterial infection or sepsis and septic shock<sup>90,12,101</sup> which occur in all species, especially in immunocompromised patients and gram negative infections whereby lipopolysaccharides or endotoxins are released into systemic circulation<sup>64</sup>.

The typical clinico-pathological hallmarks of uncomplicated canine babesiosis include lethargy, haemolytic anaemia with a water-hammer pulse, pyrexia and splenomegaly. The “atypical” or “complicated” form includes acute renal failure, immune-mediated haemolytic anaemia, rhabdomyolysis, cerebral signs, hepatopathy, haemoconcentration, disseminated intravascular coagulation, acute pancreatitis,



myocardial infarction as well as pulmonary oedema<sup>103,67</sup>. The symptoms observed with uncomplicated canine babesiosis are directly related to haemolytic anaemia whereas the complicated forms appear to be triggered by the host inflammatory response and cannot be directly attributed to haemolysis<sup>40</sup>. Maegraith et al. first described the pulmonary pathology in dogs that died from what we now refer to as “complicated” canine babesiosis as early as 1957<sup>60</sup>. In that paper, 25/34 patients showed some pulmonary pathology varying from slight hyperaemia to severe pulmonary oedema, especially in the fatal cases. Shock lung or acute interstitial pneumonia has long been recognised as a significant lesion in complicated canine babesiosis infection<sup>39</sup> but the pathology has never been properly investigated or described in detail.

This review will summarise what is known of the pathology at all levels (including the basic pathogenesis) of ALI/ARDS in both the human medical and veterinary literature.

## CHAPTER TWO: LITERATURE REVIEW

### 2.1. Expanded Definition of ALI/ARDS

Most research on ALI/ARDS has been done within the realm of human medicine and a joint European-American Consensus committee (EACC) was convened in 1992 in order to create a standardised definition for use by researchers and clinicians<sup>9</sup>. Acute lung injury is specifically defined as bilateral pulmonary damage in the absence of left-sided heart failure<sup>50</sup>. Causes and mechanisms of pulmonary damage/injury are vast and varied and will be covered separately (Sections 2.2 and 2.3). Regardless of cause, ALI often progresses to ARDS, which is typically characterised by worsening pulmonary hypertension, aggregation of neutrophils within the pulmonary vasculature, diffuse alveolar damage, permeability oedema and hyaline membrane formation<sup>64</sup>. Hyaline membranes (Figure 1) are accumulations of necrotic cellular debris, fibrin and surfactant that adhere to denuded alveolar basement membranes<sup>102</sup>.

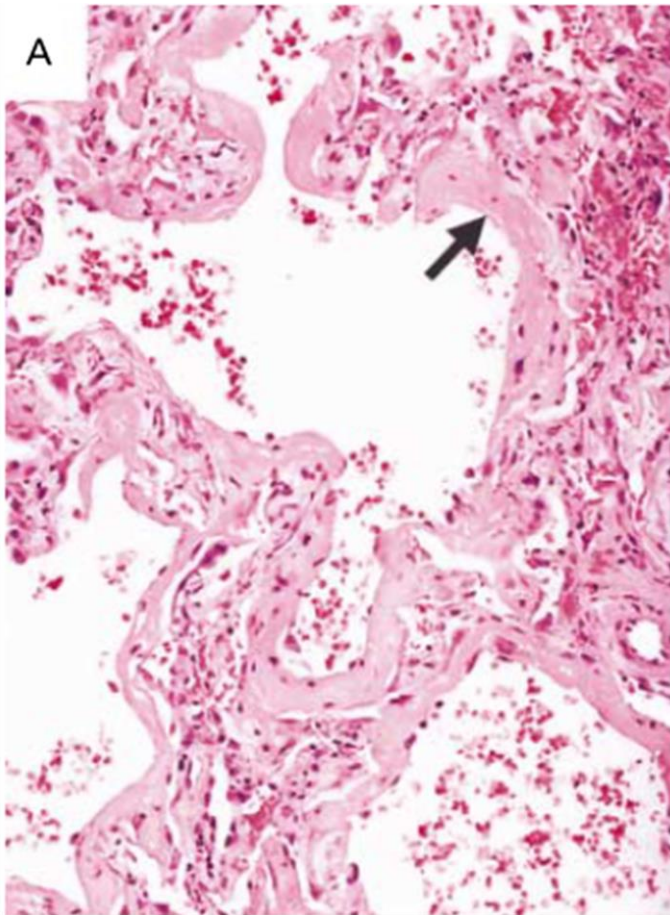


**Figure 1:** Human lung, hyaline membrane formation (Thick arrow)<sup>102</sup>.

A recent paper published by Wilkins et al<sup>105</sup> detailed a meeting between experts in the field of veterinary emergency and critical care who were tasked to come up with a consensus for ALI/ARDS that was specific for use in the veterinary field<sup>105</sup>. Three definitions emanated from the meeting. The first one refers specifically to equine neonates younger than 24 hours and is termed Neonatal Equine Respiratory Distress Syndrome (NERDS). The second definition pertains to equine neonates older than one

week of age termed Equine Neonatal Acute Lung Injury / Equine Neonatal Acute Respiratory Distress Syndrome (EqNALI/EqNARDS). The third definition, which is applicable to this review, is termed Veterinary Acute Lung Injury and Veterinary Acute Respiratory Distress Syndrome (VetALI/VetARDS). Delegates established that there was insufficient information to be species-specific (pertaining to the last definition) but they were able to develop a general definition for mammals. Using the EACC methodology, they proposed five criteria of which the first 4 are prerequisite for the diagnosis of VetALI/VetARDS. The fifth criterion was deemed exceedingly invasive, although highly recommended, and was therefore made optional. The salient points are presented in table 1.

**Table 1:** Criteria for the diagnosis of veterinary Acute Lung Injury (ALI) and Acute Respiratory Distress Syndrome (ARDS)<sup>105</sup>

<p>1.) Acute onset of tachypnoea and dyspnoea at rest</p> <p>a. Less than 72 hours duration</p>
<p>2.) Presence of known Risk factors</p>
<p>3.) Pulmonary capillary leakage without increased pulmonary capillary pressure</p> <p>a. No evidence of cardiac failure causing cardiogenic pulmonary oedema</p> <p>b. Thoracic radiographs: Bilateral diffuse thoracic infiltrates</p> <p>c. Computed Tomography: Bilateral Dependant Density</p> <p>d. Proteinaceous Fluid in the conducting Airways</p> <p>e. Increased Extravascular Lung Water</p>
<p>4.) Inefficient Gas Exchange</p> <p>a. Hypoxaemia</p> <p>i. Without assisted positive end expiratory pressure ventilation</p> <p>ii. Known Fraction of inspired Oxygen (FiO<sub>2</sub>)</p> <p>iii. Partial Pressure of alveolar Gas (PaO<sub>2</sub>) to fraction inspired oxygen ratio (FiO<sub>2</sub>) (Carrico index)</p> <p>1. VetALI it must be more than or equal to 300mmHg</p> <p>2. VetARDS it must be more than or equal to 200mmHg</p> <p>iv. Increased alveolar-arterial oxygen gradient</p> <p>v. Venous admixture</p> <p>b. Increased dead space ventilation</p>
<p>5.) Diffuse pulmonary inflammation.</p> <p>a. Neutrophilia and/or inflammatory biomarkers seen in transtracheal washes or bronchoalveolar lavages</p> <p>b. Molecular imaging using positron emission tomography</p>

In summary, these criteria include acute onset tachypnoea or dyspnoea within 72 hours, the presence of a known risk factor or risk factors for the development of ARDS, evidence of pulmonary capillary leakage without cardiogenic causes, proof of inefficient gaseous exchange as evidenced by hypoxaemia and finally, the presence of diffuse pulmonary inflammation.

## 2.2. Risk Factors for ALI/ARDS

Using the basic risk factors provided by Wilkins et al. in the Havemeyer working group, an expanded set of risk factors is provided in table 2<sup>105</sup> and the veterinary literature was used to add risk factors where possible. Risk factors can be regarded as either primary respiratory disorders that cause direct lung injury or are associated with systemic disorders or involvement where the lung injury is indirect<sup>19</sup>. This classification will be used in this review.

Acute lung injury and ARDS are most commonly observed with bacterial and aspiration pneumonias as well as in sepsis and shock<sup>73</sup> and the pulmonary injury is mediated by inflammatory cells and not the inciting cause per se. Thus sepsis would also be classified as indirect injury. Canine parvovirus is another indirect cause of ALI/ARDS as the parvovirus does not directly affect the respiratory epithelium or vascular endothelium. Rather immunosuppression, aspiration of vomitus, and secondary sepsis due to denuded intestinal mucosa with subsequent bacterial translocation, may result in bacterial pneumonia. Direct causes include those factors that damage to the blood-air barrier directly and would include African horse sickness virus, paraquat toxicity or smoke inhalation, etc.

**Table 2: Selected risk factors associated with the development of Acute Lung Injury and Acute Respiratory Distress Syndrome in veterinary patients.**

Risk Factor Category	Direct injury	Systemic involvement
<b>Infectious</b>		
<i>Viral</i>	African horse Sickness virus <sup>96,97</sup>	Canine Parvovirus <sup>93</sup>
	Respiratory syncytial virus <sup>86</sup>	
	Feline calici virus <sup>86</sup>	
	Canine herpes virus <sup>18</sup>	
<i>Protozoal</i>		Canine babesiosis <sup>17,62,39</sup>
		<i>Toxoplasma gondii</i> <sup>86</sup>
<i>Bacterial</i>		Bacterial Pneumonia <sup>73</sup>
		Sepsis and endotoxaemia <sup>19,86</sup>
<b>Metabolic</b>		Uraemia <sup>86</sup>
<b>Systemic inflammatory</b>		Acute necrotising pancreatitis <sup>58</sup>
		Massive bee envenomation <sup>100</sup>
		Snakebite hypersensitivity
<b>Severe Trauma</b>	Pulmonary contusion <sup>19</sup>	Long bone fracture <sup>72</sup>
	Airway obstruction <sup>21</sup>	Cranial trauma – Neurogenic
	Strangulation <sup>86</sup>	Electrocution <sup>21</sup>
	Lung lobe torsion and	
	Ventilator-induced injury <sup>86</sup>	
<b>Miscellaneous</b>	Near drowning <sup>22</sup>	Multiple blood transfusions <sup>91</sup>
	Thermal injuries such as smoke	Burn wounds <sup>16,87</sup>
	Aspiration of stomach contents –	
<b>Drugs</b>		Anaesthesia <sup>46</sup>
<b>Toxins</b>	Paraquat <sup>43</sup>	
	Chlorhexidine Gluconate <sup>35</sup>	
	Kerosene <sup>86</sup>	
<b>Genetics</b>		Dalmations <sup>42</sup>

### 2.3. Pathophysiology of ALI/ARDS

In essence, ALI/ARDS, independent of the inciting causes, involve a breakdown of the alveolar-capillary membrane, causing a disruption in the blood-air barrier. This membrane consists of two essential components, endothelial cells lining the alveolar capillaries and type I and type II pneumocyte epithelial cells that line the alveolus<sup>50</sup> as illustrated in figure 2 below.

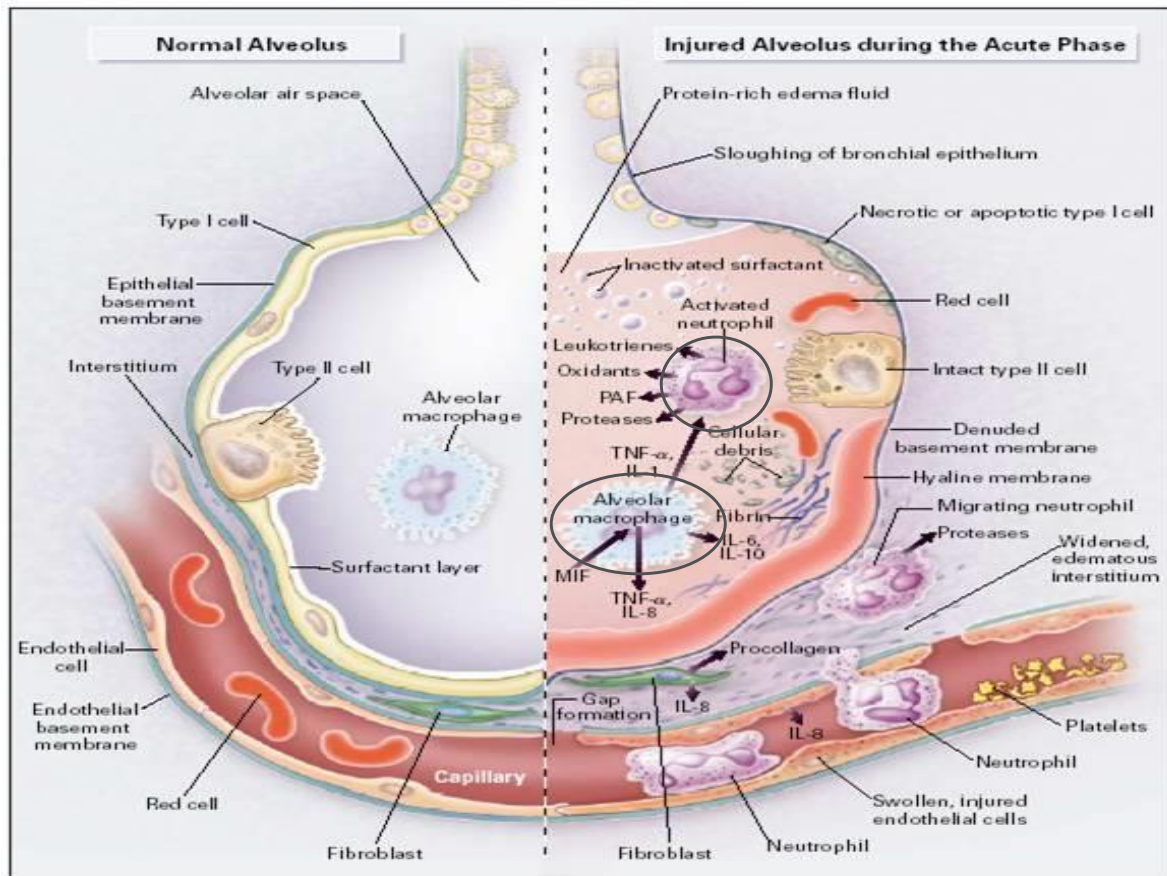


**Figure 2:** Normal (left) vs injured (right) alveolus. Note that the pathological sequence of events is triggered by activated alveolar macrophages and neutrophils (circled)<sup>102</sup>.

Type I pneumocytes are elongated, slender epithelial cells that line most of the alveolus whilst type II pneumocytes are fewer in number but are rounded and larger than type I pneumocytes. Type II pneumocyte functions include the manufacture of surfactant for maintenance of the structural integrity of the alveolus, the absorption of fluid within the alveolus and the production of epithelial basement membrane. Loss of surfactant would cause an increase in surface tension in the alveolus causing it to collapse, whilst the inhibition of fluid absorption would result in the development of alveolar oedema<sup>86,55</sup>. An additional cell type, namely the Clara cell, is present in the bronchiolar epithelium and they have a similar light microscopic appearance to type II pneumocytes. Clara cells are also referred to as secretory bronchiolar epithelial cells and they have numerous functions including the synthesis of surfactant, metabolism of xenobiotics and repair of the respiratory tract<sup>86</sup>. They are most abundant in the terminal bronchioles and respiratory bronchioles, especially in the rat, mouse, guinea pig and rabbit. In the cat and dog they make up over 95% of the epithelium in

respiratory bronchioles<sup>74</sup>. Clara cells also have specific features that are easy to identify ultrastructurally, including abundant agranular (smooth) endoplasmic reticulum in their apex and ovoid, membrane-bound cytoplasmic granules<sup>74</sup>.

Normally vascular endothelial cells and type I pneumocytes are tightly adhered to a shared, fused basement membrane, resulting in a narrow interstitial space, thereby minimising the distance over which gaseous exchange occurs. Gaseous exchange therefore has to take place across four cell membranes and a fused basement membrane. In humans the average thickness of the barrier is 2.2 $\mu\text{m}$ <sup>92</sup> whilst in dogs it is 1.78 $\mu\text{m}$ <sup>65</sup>. An additional advantage of such a thin and compact alveolar wall is that fluid does not leak easily into the alveolus. However, damage to any one of these alveolar wall components would obviously severely compromise lung function.

During ALI/ARDS the damage may be limited to either the pneumocytes or the endothelium or both components may be injured simultaneously. During indirect injury, disruption of the alveolar-capillary membrane is mediated by inflammatory cells, predominantly neutrophils and macrophages. The sequence of events often starts with macrophages (Figure 2)<sup>101,102</sup>. An insult precipitated by one or other risk factor occurs, which results in intra-alveolar macrophages secreting pro-inflammatory cytokines such as Interleukin-1(IL-1), Interleukin-6(IL-6), Interleukin-8(IL-8) and Tumour Necrosis Factor alpha (TNF- $\alpha$ )<sup>64</sup>. These pro-inflammatory cytokines cause endothelial activation which stimulates recruitment, vascular adhesion and extravasation of neutrophils into the interstitium by altering the membrane expression of selectins and other cell surface proteins. These same cytokines also activate the neutrophils themselves to release enzymes such as lecithinases, proteases, superoxide free radicals and more pro-inflammatory cytokines to perpetuate the process<sup>50</sup>. It has been postulated that ALI/ARDS is the result of an imbalance of pro- and anti-inflammatory mediators (which include interleukin-4 (IL-4), transforming growth factor – beta (TGF- $\beta$ ) etc.) as both types of mediators are always being produced, but certain disease states and conditions favour the action of the pro-inflammatory mediators<sup>26</sup>. Pro-inflammatory cytokine release causes severe local tissue damage which culminates in necrosis. With damage to the pneumocytes and/or endothelium, which may vary in severity from sub-lethal cell injury to irreversible necrosis, the blood-alveolar membrane disintegrates resulting in the extravasation of fluid into alveolar lumens with the development of non-cardiogenic pulmonary oedema. Type I pneumocytes are ten times less permeable than endothelial cells<sup>86</sup> but damage to these cells alone can cause excessive leakage of interstitial fluid into the alveolus. In human malaria-associated ARDS (MA-ARDS) resulting from primarily *Plasmodium falciparum* infection, the alveolar damage appears to be mediated primarily by monocytes, macrophages and lymphocytes instead of neutrophils<sup>94</sup>.

Direct injury to endothelial cells also occurs and endotheliotropic viruses, for example African horse sickness virus (AHSV)<sup>96</sup> or canine herpes virus (CHV) cause severe damage to the endothelial lining of the pulmonary vasculature resulting in acute interstitial pneumonia. In addition to direct damage, activation of cells in close association with the endothelium, specifically pulmonary intravascular macrophages

(PIMS), causes the release of inflammatory mediators including TNF- $\alpha$  and IL-1 which recruit leukocytes to the area and induce further indirect pulmonary injury<sup>11</sup>.

Pulmonary intravascular macrophages are not present in large numbers in all species. Large populations have been demonstrated in horses, ruminants and cats and in some other species but not (thus far) in canines<sup>106,20,11</sup>. They are large macrophages which attach to the luminal endothelium by means of membrane-adhesive complexes (best visualized via transmission electron microscopy), which distinguish them from normal circulating monocytes<sup>20</sup>. The presence of pulmonary intravascular macrophages has been postulated as an important factor in the pathogenesis of (indirect) lung injury in horses with AHSV as they produce pro-inflammatory mediators including IL-1, TNF- $\alpha$ , Leukotriene B4 and Thromboxane A2<sup>11</sup>. However, in anaesthetised sheep, a reduction in the PIM population resulted in attenuated/decreased severity of pulmonary hypertension and microvascular leakiness in response to endotoxin injury<sup>83</sup>. Similarly, a depletion in PIMS resulted in decreased pulmonary inflammation in calves infected with *Mannheimia haemolytica*<sup>80</sup>.

In recent years, much attention has been paid to endothelial cell activation. The mechanisms underlying endothelial activation are extremely complex. Broadly speaking, the term is used to imply phenotypical changes that the vascular endothelium undergoes, which result in a pro-inflammatory and/or pro-coagulant state. It usually occurs as a response to external stimuli and is considered fundamental to the progression of ALI and ARDS by many clinicians and investigators<sup>110</sup>.

Pro-inflammatory cytokines trigger endothelial cells to express cell surface protein receptors which aid in the recruitment of leukocytes by causing them to marginate, roll, adhere and transmigrate through the endothelium, thus allowing for the development of an inflammatory response in the associated tissues. These endothelial adhesion molecules include the selectin and selectin-ligand family such as E-selectin, P-selectin and CD34 (GlyCam-1) as well the integrin and integrin-ligand family such as intercellular adhesion molecule-1 (ICAM-1) and vascular cell adhesion molecule-1 (VCAM-1)<sup>50</sup>. CD31 is another molecule that is expressed on both endothelial and leukocyte cell surfaces and this allows for the homotypic interactions necessary for the transmigration of leukocytes across the endothelium<sup>50</sup>.

Immunohistochemical (IHC) markers have been developed to investigate endothelial activation in humans and animals. The use of IHC to detect ICAM-1 expression on endothelial cells has been used in canine models of myocardial infarction<sup>48</sup>. Intercellular adhesion molecule-1 and CXC Chemokine Ligand-10 (CXCL-10) have also been found to be expressed in murine models of MA-ARDS and decreasing the expression of these molecules in these models resulted in decreased leucocyte extravasation and less severe pulmonary pathology, resulting in increased survival rates<sup>94</sup>.

In studies that have looked at the pulmonary histopathology in cases of canine babesiosis, mention has been made of diffuse and marked peracute interstitial pneumonia, hyaline membranes, alveolar oedema and haemorrhage<sup>17</sup> as well as septal



vessel congestion and frank pulmonary oedema with haemorrhage<sup>60</sup>. No ultrastructural studies were found pertaining to the lung pathology in canine babesiosis.

In human cases of ARDS, the alveolar epithelium often shows severe pathology compared to the endothelium<sup>92</sup>. Microscopic pathology that has been described includes type I pneumocyte necrosis and sloughing leaving behind a denuded alveolar basement membrane, resulting in the development of hyaline membranes<sup>92,2</sup>. Type II pneumocytes are known to be much more resistant to injury than type I pneumocytes but they may still undergo necrosis. The end result is the loss of epithelial membrane integrity with the movement of interstitial fluid into the alveolus<sup>92</sup>.

#### **2.4. Temporal aspects of the pathology of ALI/ARDS**

In the human and veterinary literature, the type of lesion most commonly associated with ALI/ARDS is diffuse alveolar damage<sup>86,12,102</sup>. However, other pulmonary pathology such as diffuse interstitial pneumonia and non-cardiogenic pulmonary oedema can result in arterial hypoxaemia.

Diffuse alveolar damage can be grouped according to three temporal stages depending on the time that has elapsed since the initial insult and the subsequent chronological development of lesions<sup>12,90,92,102</sup>. More than one phase can be present at any one time. The three stages include an acute exudative stage, followed by a sub-acute proliferative stage and finally a chronic fibrotic stage.

Most research has been devoted to the acute stage and macroscopic pathology characterising the proliferative and fibrotic phases of ALI / ARDS is not often encountered in veterinary medicine or pathology due to the highly fatal nature of the acute phase. In human medicine, due to more advanced interventions and treatments that lead to increased survival times, a proliferative stage occurs when the intra-alveolar and interstitial exudates begin to organise<sup>92</sup>. The proliferative phase eventually leads to the fibrotic phase which is characterized heavy and grey lungs. A cobblestone appearance is also possible late in the disease due to irregular fibrosis<sup>12</sup>.

The pathology and pathophysiology of ALI/ARDS due to babesia and malaria infection have been extensively studied in humans<sup>94,89</sup> as well as in murine models<sup>32,1,59,84,95</sup>. A summary of the macroscopic and microscopic changes associated with this disease is presented below and will also be scored according to criteria established for fatal natural African Horsesickness virus in dogs<sup>70</sup>.

## 2.5. Macroscopic pulmonary pathology in ALI/ARDS

Normal dog lungs appear homogeneously light pink in colour and are well aerated as illustrated in figure 3 below.

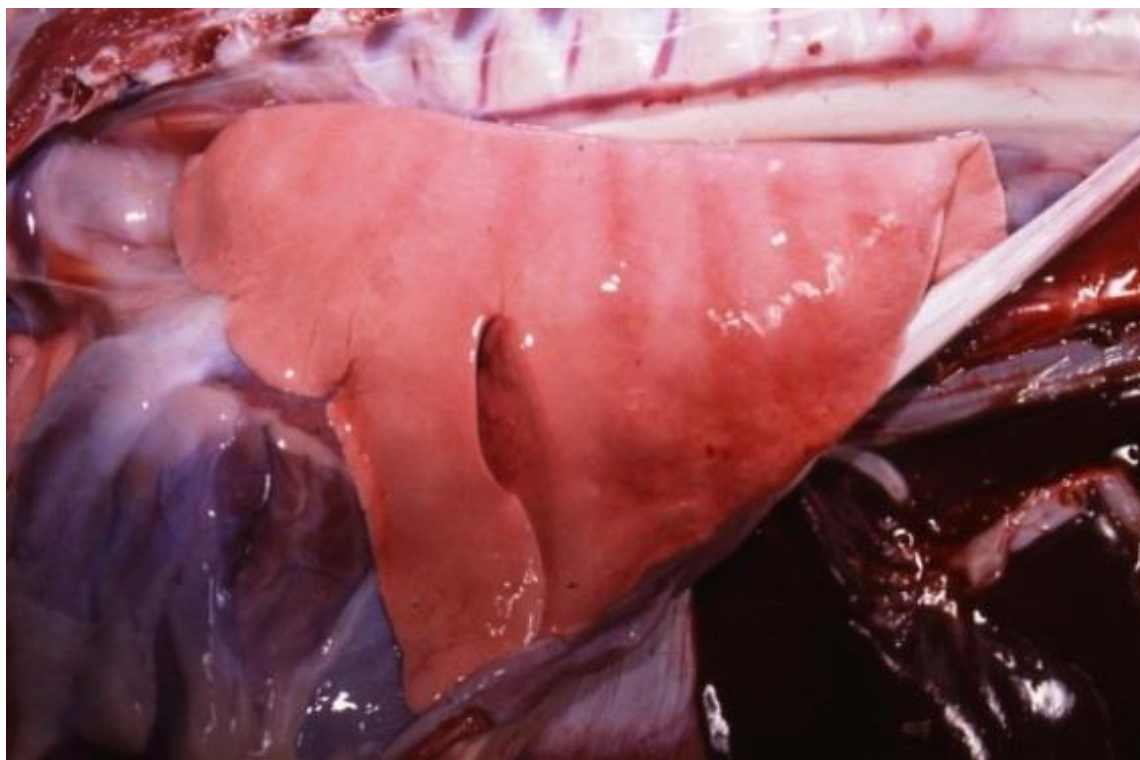


**Figure 3:** Normal canine lung, inflated. Note the light pink, pillowy appearance in all lung lobes. Image obtained from the pathology database, Section of Pathology, Department of Paraclinical Science, Faculty of Veterinary Science, University of Pretoria.

Macroscopic changes described for ALI/ARDS are similar to acute interstitial pneumonia<sup>64</sup>. The lesions tend to be generalised in distribution (often affecting all the lung lobes) or they may have a more dorso-caudal distribution. On opening the thoracic cavity, the lungs may fail to collapse and have distinct rib impressions on the pleural surface. The appearance of the lungs depends on the phase of injury. In the acute phase the lungs are diffusely red, the texture is elastic or rubbery and the cut surface may have a “meaty” appearance which would be dark red with an increased consistency. No exudate is visible in the bronchi or on the pleural surfaces and pulmonary oedema may be visible along with interstitial emphysema due to dyspnoea. The accumulation of cells and fluid would also significantly increase the weight of the lungs. In the chronic phase, the lungs may have a diffusely grey to mottled red appearance and would have significantly increased weight and a rubbery texture<sup>64</sup>.

### 2.5.1. Macroscopic pulmonary pathology in complicated canine babesiosis

The pulmonary pathology associated with complicated canine babesiosis has not yet been investigated thoroughly but was identified as early as 1957<sup>60</sup> and is a common complication<sup>39</sup>. The macropathology that has been described thus far includes mild hyperaemia and oedema<sup>60,17</sup>.

### 2.5.2. Macroscopic pulmonary pathology in human malaria-associated ALI/ARDS

In human MA-ARDS, similar macroscopic pathology was noted, but the oedema was severe. Lung weight was increased with occasional punctate/petechial pleural or intrapulmonary haemorrhages as well as pleural or pericardial serous effusion<sup>89</sup>.

### 2.5.3. Macroscopic pathology in murine malaria-associated ALI/ARDS

In a murine model of MA-ARDS using C57BL/6J mice infected with *Plasmodium berghei* strain NK65 exhibited swelling of the lungs as well as multiple petechiae (Figure 4)<sup>95</sup>.

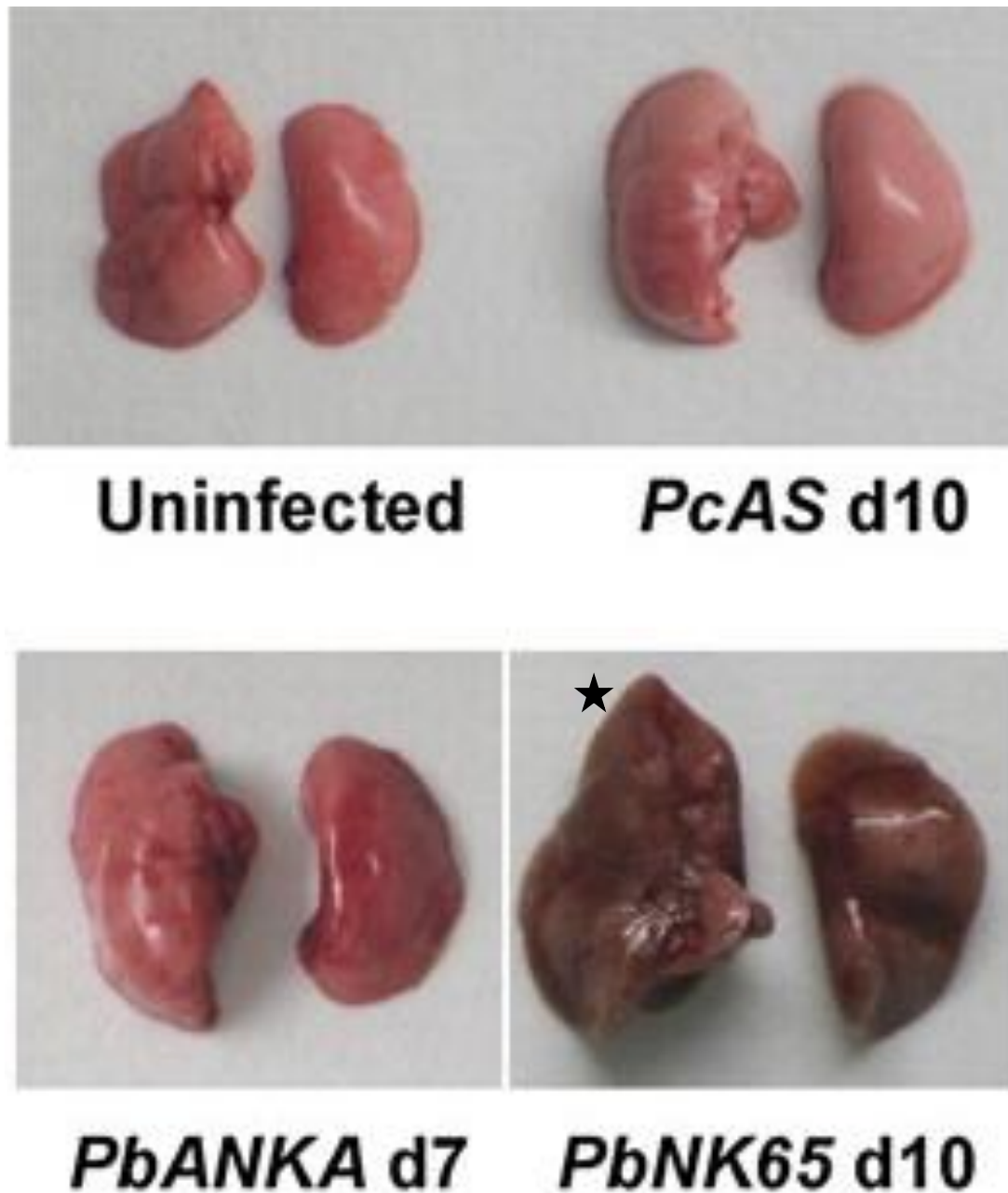


**Figure 4:** Representative lungs from uninfected mice and mice infected with *Plasmodium chabaudi* AS (10 d post-infection), *Plasmodium berghei* strain NK65 (10 d post-infection), or *Plasmodium berghei* ANKA

(7 d post-infection) were photographed. Note the swelling and dark brown discoloration (black star) in the 10 day post-infection sample<sup>95</sup>.

#### 2.5.4. Macroscopic pathology of murine babesia-associated ALI/ARDS

A model using C3H/HeN mice infected with WA-1 babesia showed pale lungs covered with petechiae while the trachea and bronchi were filled with serosanguinous fluid<sup>32</sup>.

### 2.6. Microscopic pulmonary pathology in ALI/ARDS

Figure 5 illustrates the histology of normal canine lungs in which it is important to note the absence of fluid and inflammatory cells within the alveoli, as well as the thin, one red blood cell-in-diameter thickness of the alveolar wall.

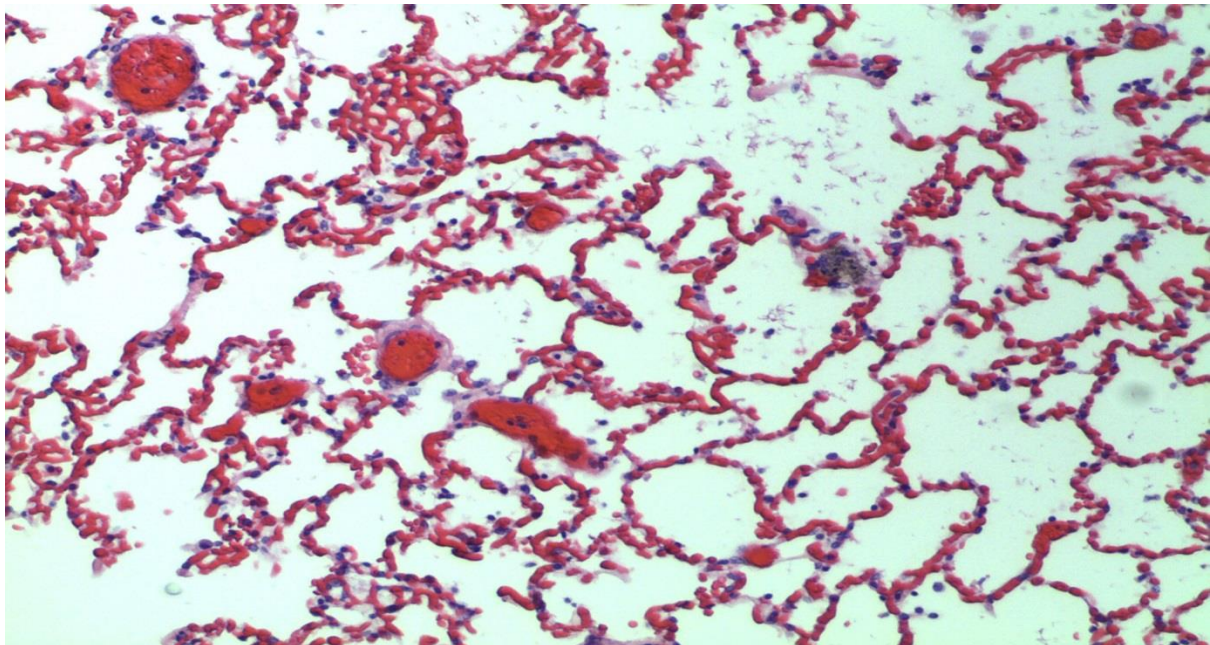


**Figure 5:** Histology of normal dog lung. Note the thin alveolar walls and absence of oedema and inflammatory cells within alveolar walls and lumens 400×. From the pathology database, Section of Pathology, Department of Paraclinical Science, Faculty of Veterinary Science, University of Pretoria.

The acute exudative of stage ALI/ARDS occurs within 12-24 hours of lung injury and is characterised by alveolar capillary congestion/hyperaemia, interstitial oedema and protein-rich alveolar oedema as well as intra-alveolar haemorrhage<sup>12,92,102</sup>. It is during this phase that the typical eosinophilic hyaline membrane develops. This linear membrane can be seen to line the walls of the alveoli and it consists of cellular debris, surfactant and plasma proteins including albumin, fibrinogen, immunoglobulins<sup>12</sup> and complement<sup>92</sup>. The alveolar ducts appear dilated<sup>92</sup>. Other changes include alveolar septal thickening with increased myxoid matrix produced by fibroblasts and myofibroblasts. The interstitium is infiltrated by macrophages, lymphocytes and plasma cells. The epithelial layer along the alveolar basement membrane is lost and attempts at healing result in epithelialisation (after 3-6 days), which marks the transition from the acute to the subacute proliferative phase. These regenerative epithelial cells can appear quite atypical, showing an increased nucleocytoplasmic ratio, karyomegaly, chromatin clumping as well as prominent, magenta nucleoli and mitotic figures<sup>12</sup>. Most veterinary patients present during this stage.

The subacute or proliferative phase is characterised by the spread of type II pneumocytes across the injured alveolar membranes where type I pneumocytes have undergone necrosis. A layer of plump cuboidal epithelium lining the alveoli is the most commonly recognised marker of this phase<sup>86</sup>, which can be seen from 2-6 days post injury<sup>86,12</sup>. Type II pneumocytes are much plumper (more cuboidal) than type I pneumocytes and hence gaseous exchange is adversely affected due to the increased distance between the alveolar air and intravascular erythrocytes. Type II pneumocytes are responsible for laying down new basement membrane in the event of basement membrane injury. They have the ability to differentiate into type I pneumocytes if the injurious agent is removed<sup>86</sup>. At this point healing may be complete if the initial insult was mild and of short duration, otherwise the lesion progresses to the chronic fibrotic stage.

The third and final stage is characterised histologically by the development of fibrovascular granulation tissue either in the alveolus or within the interstitium. Fibroblasts invade the oedema fluid from as early as three days post-injury<sup>86</sup> where they start to organise it into fibrous connective tissue. Collagen deposition by fibroblasts can start from 3-5 days after injured and complete fibrosis can be accomplished by day 14.

#### **2.6.1. Microscopic pulmonary pathology in complicated canine babesiosis**

Limited case reports and descriptions have been published since the initial Maegraith et al. study<sup>60</sup>. Lesions that have been reported include interstitial pneumonia, hyaline membrane formation, alveolar oedema and haemorrhage (figure 6)<sup>17</sup>. Mild thickening of the alveolar membranes was noted due to an increase in alveolar macrophages<sup>37</sup>.

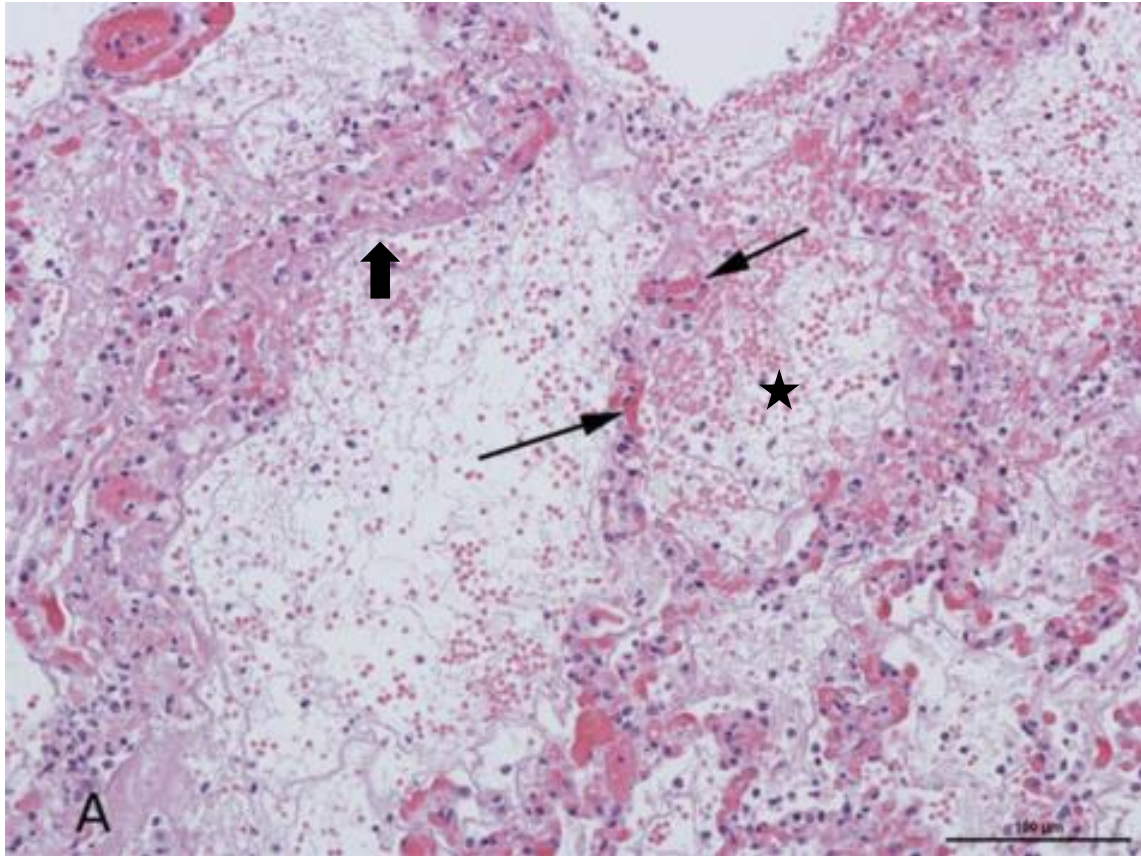


**Figure 6:** Histopathology of the lungs during complicated canine babesiosis (H&E stain, ×200). Note the presence of haemorrhages (black star), hyaline membranes (block arrow), and congestion of capillaries (thin black arrows)<sup>17</sup>.

### 2.6.2. Microscopic pulmonary pathology in human malaria-associated ALI/ARDS

Pulmonary histopathology in human MA-ARDS is characterised by congested alveolar septa with parasitized red blood cells, multifocal haemorrhages and widespread pulmonary oedema (Figure 7)<sup>85,89</sup>. Another less frequently encountered histological lesion includes hyaline membrane formation, but thrombosis and infarction are not generally observed<sup>89</sup>.

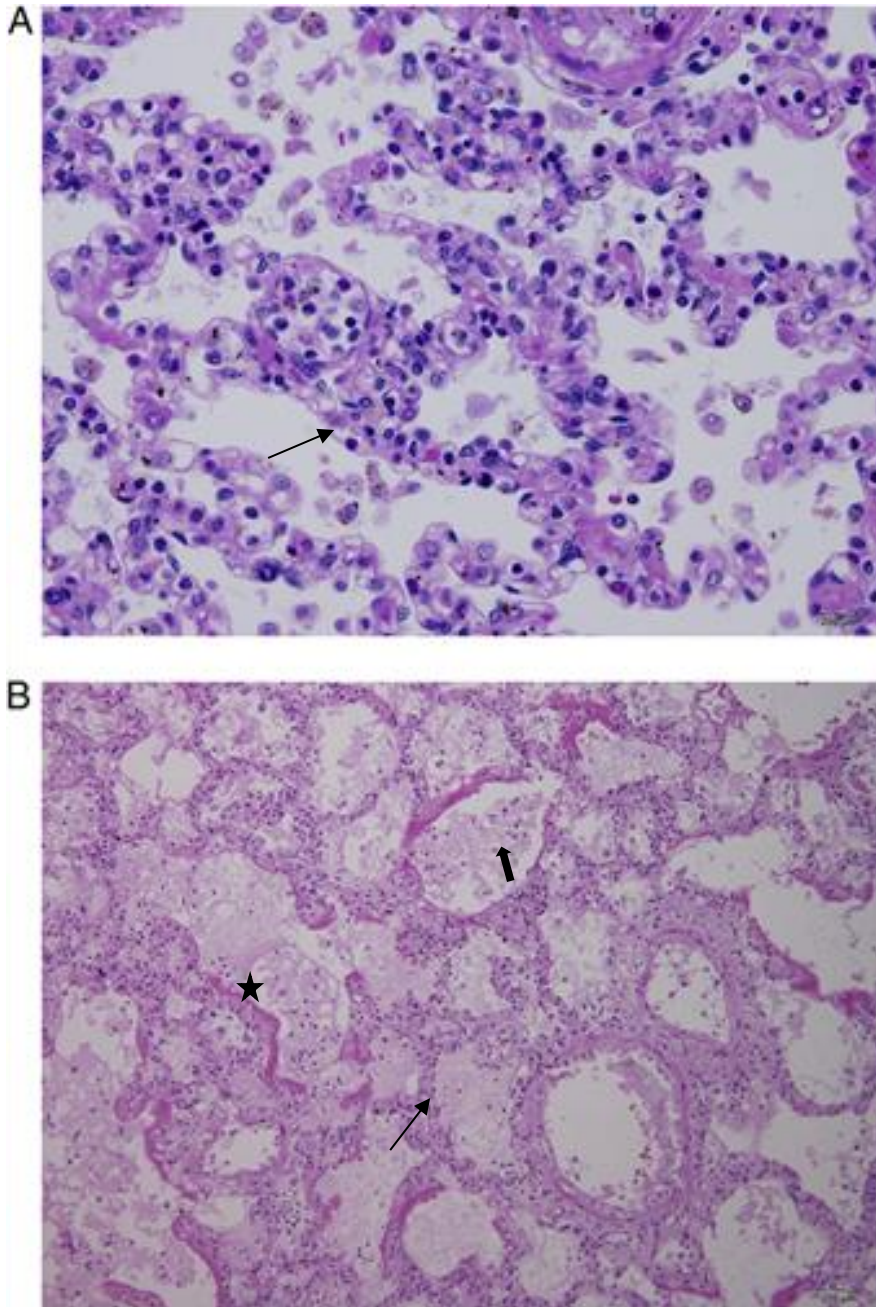


**Figure 7:** A. Pulmonary histopathology in a fatal case of adult falciparum malaria. There is expansion of alveolar capillaries by sequestered parasitized erythrocytes and host inflammatory leukocytes (thin black arrow). Monocytes and neutrophils within alveolar septal capillaries (haematoxylin and eosin [H&E] staining, magnification  $\times 400$ ). B. More severe pulmonary histopathology from another fatal case of falciparum malaria with host leukocytes expanding the alveolar septa (thin black arrow), intra-alveolar haemorrhage and pulmonary oedema (black star), hyaline membrane formation (thick black arrow) as part of a picture of diffuse alveolar damage (H&E staining, magnification  $\times 200$ )<sup>89</sup>.

### 2.6.3. Microscopic pulmonary pathology in murine malaria-associated ALI/ARDS

In a murine model of MA-ARDS using C57BL/6J mice infected with *Plasmodium berghei* strain NK65, frozen lung sections were evaluated at day 8 post-infection which showed interstitial oedema and severe leukocyte infiltration. By day 10 a prominent eosinophilic hyaline membrane was visible in the alveoli which is characteristic of ARDS (Figure 8). Mice that survived to day 12 showed severe hyaline membrane formation as well as widespread alveolar and interstitial leukocyte infiltration<sup>95</sup>.

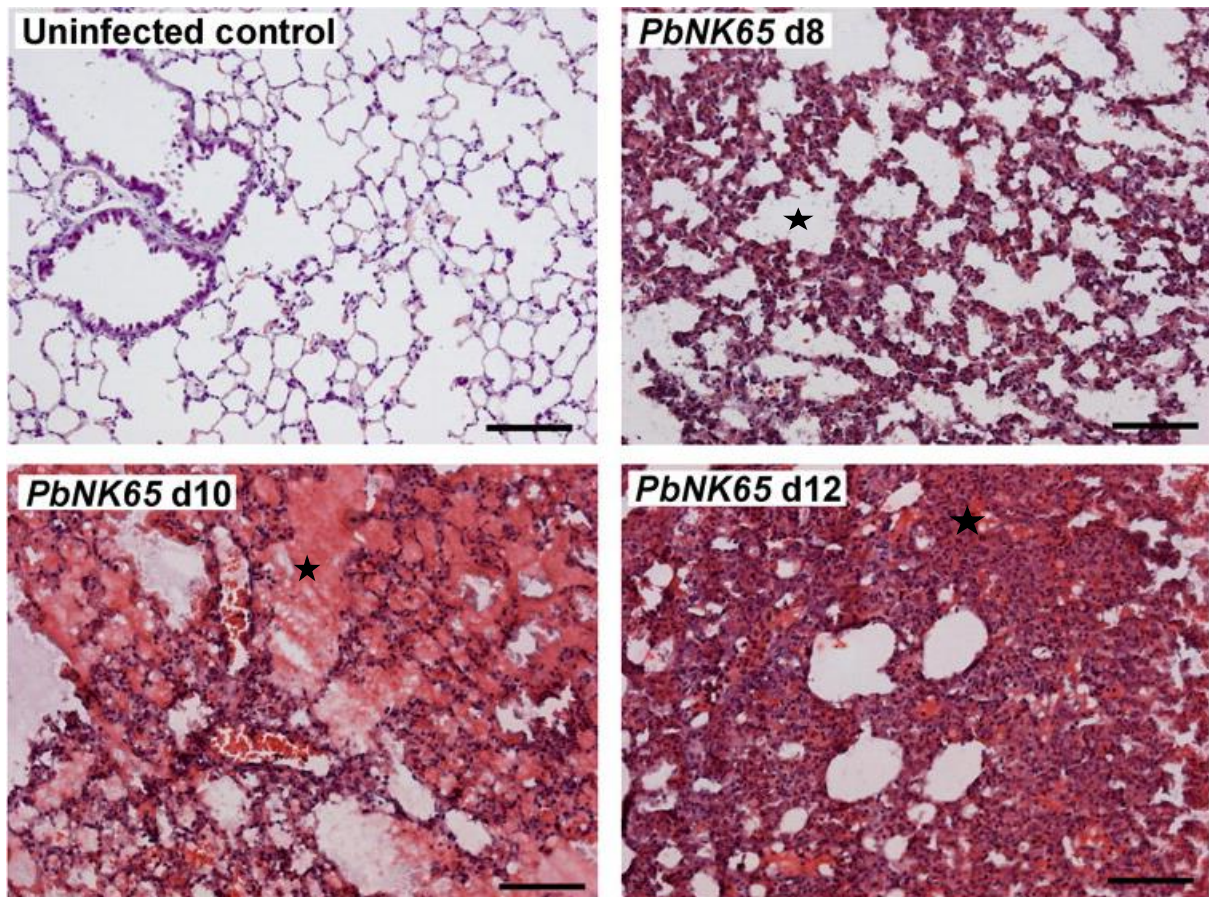


**Figure 8:** Lungs of *Plasmodium berghei* strain NK65-infected mice were dissected at 8, 10 and 12 days post-infection and sections were stained with H&E. Representative examples are shown (original magnification,  $\times 20$ ; scale bars, 100  $\mu\text{m}$ )<sup>95</sup>. Note the progressive development of pulmonary oedema (black stars) along with leukocyte infiltration.



#### 2.6.4. Microscopic pulmonary pathology in murine babesia-associated ALI/ARDS

The pulmonary histopathology observed in the murine C3H/HeN WA-1 babesia model included congested small- to medium-sized pulmonary veins which were lined by plump endothelial cells with marginated mononuclear cells and neutrophils. The perivascular stroma around the veins was expanded and had a lacy appearance (perivascular oedema) with scattered interstitial macrophages and lymphocytes (Figure 9A). The alveoli also contained homogenous eosinophilic fluid consistent with pulmonary oedema as well as vacuolated alveolar macrophages<sup>32</sup> (Figure 9B).

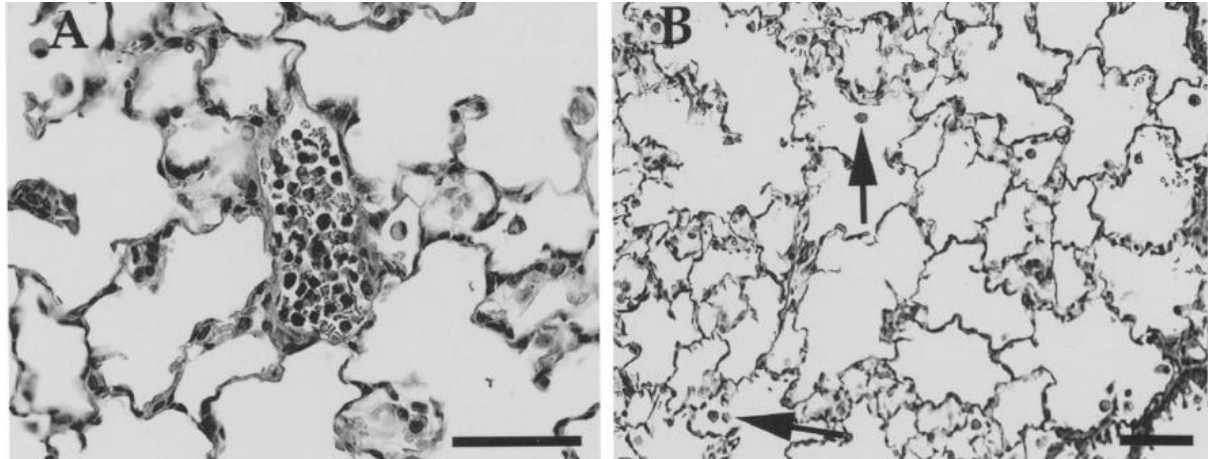


**Figure 9:** Pulmonary histopathology in *Babesia*-infected mice. A. Section of lung from a WA-1 infected mouse showing a small pulmonary vein occluded by mononuclear inflammatory cells. B. Section of lung from a WA-1 infected mouse showing the presence of vacuolated alveolar macrophages in the alveolar lumens (arrows)<sup>32</sup>.

## 2.7. Immunohistochemistry

Immunohistochemistry uses specific antibodies/immunoglobulins to label antigens of interest within tissue sections and was first utilised in 1941<sup>14</sup>. The immunoglobulin molecule has binding sites and can be tailored to recognise any required antigen. Immunoglobulins also have binding sites for other antibodies. It is these two properties which can be exploited in order to label antigens and allow their visualisation by means of light or fluorescent microscopy in tissue sections<sup>75</sup>.

This procedure therefore allows for the identification of cell types which normally cannot be differentiated with standard light microscopy e.g. B versus T lymphocytes. Another application is for the detection of the expression of various proteins on the surface of cell membranes or within the cytoplasm or nucleus of cells. These proteins include transcription factors, integrins or apoptotic markers amongst others. Immunohistochemistry enables the detection of normal versus altered phenotypic expression and the technique can therefore be used to enhance our understanding of pathogenesis<sup>76</sup>.

A great variety of mono- and polyclonal mouse, rabbit and goat antibodies have been generated and optimised for immunohistochemistry in formalin-fixed, paraffin-embedded (FFPE) dog tissues, especially during the last 25 years. What follows in table 3 below is a list of antibodies that were used to further investigate the pulmonary pathology (including underlying pathogenesis) associated with complicated *B. rossi* infection in dogs.

## 2.8. Problem and Hypothesis

From the literature review it is clear that although ALI/ARDS have been well researched and described in human medicine, there is very little on the pathology of ALI/ARDS in the veterinary literature. In addition, almost nothing has been described for babesia-associated ARDS beyond a few case reports with very cursory pathology descriptions.

### 2.8.1. Problems

- A. There is very little in the literature describing the pulmonary pathology associated with ALI/ARDS in dogs.
- B. There is no detailed description of the pulmonary pathology caused by complicated canine babesiosis in dogs.
- C. There is no comparison between the pulmonary pathology caused by *B. rossi* infection in dogs and that of human malaria and murine malaria and babesiosis.

### 2.8.2. Hypotheses

- A. The pulmonary injury in cases of complicated canine babesiosis will dovetail with the Havemeyer working group criteria for ALI/ARDS.
- B. The pulmonary histopathology in cases of complicated canine babesiosis will be very similar to what has been described in the murine babesia model.
- C. An inflammatory cellular infiltrate consisting primarily of mononuclear cells (macrophages / monocytes / lymphocytes) will be present within the alveolar interstitium.
- D. Immunohistochemistry using CD3, CD20, MAC387 and CD204 antibodies will quantify the extent and proportion these mononuclear cell populations in the inflammatory infiltrate.
- E. The pulmonary histopathology in complicated canine babesiosis will be similar to what has been described for human malaria-associated ALI/ARDS.
- F. The pulmonary histopathology in cases of complicated canine babesiosis will be very similar to what has been described in the murine model of malaria-associated pulmonary pathology.
- G. VCAM-1 expression on pulmonary endothelial cells will be upregulated during complicated canine babesiosis.

## 2.9. Benefits arising from the experiment

- A. The generation of detailed macroscopic and microscopic descriptions and possible elucidation of underlying pathophysiologic mechanisms of ALI/ARDS in complicated canine babesiosis. This will fill a significant gap in the knowledge and understanding of ALI/ARDS in dogs.
- B. A broader aim of the babesia work at Onderstepoort is to initiate a direct comparison between the dog disease and human malarial disease (especially at the pathological level). This study is the first step towards this comparison and it is envisaged that canine babesiosis may serve as a model for at least some aspects of human malarial disease.

- C. At least one high quality publication in an ISI journal will result from this work. A research abstract will be submitted for presentation as a poster or oral presentation at relevant local and international conferences.
- D. This research will be conducted in order to fulfil some of the requirements for the MMedVet (Pathology) degree.

### 2.10. Objectives

- A. To generate detailed macro- and microscopic as well as immunohistochemical pulmonary pathological descriptions for dogs that died of complicated babesiosis caused by *B. rossi*.
- B. To semi-quantify some of the different cell populations and processes within the lungs of dogs with canine babesiosis (including lymphocytes, macrophages, plasma cells, apoptotic cells and endothelial cells) using immunohistochemistry.

## CHAPTER THREE: MATERIALS AND METHODS

### 3.1. Experimental design

#### 3.1.1. Model system and justification of the model

- A. This project was a prospective cohort descriptive case control study on dogs that died naturally or were euthanased due to complicated *B. rossi* infection.

#### 3.1.2. Experimental animals: Inclusion criteria

- A. Eleven dogs of any body weight, age, breed and sex, naturally infected with *Babesia rossi* that were diagnosed with the infection based on a positive thin blood smear were included. Mono-infection with *B. rossi* was confirmed based on a PCR and reverse line blot assay which will exclude other haemoparasitic infections such as *Anaplasma* or *Ehrlichia spp.* as well as other *Babesia spp.* as per protocol VO34-14. Only dogs that died as a result of the infection or that were euthanized at the owner's request were included.
- B. Only animals that can be sampled within 18 hours to 24 hours of death were included.

#### 3.1.3. Experimental animals: Exclusion criteria

- A. Any animal received any treatment for babesia in the 4 weeks of life preceeding presentation tow the OVAH.
- B. Any animal that received any steroidal or non-steroidal treatment in the preceding 4 weeks preceding their presentation.
- C. Any animal that was suspected or confirmed to have any comorbid infectious disease.

#### 3.1.4. Control animals: Exclusion criteria

Dogs were not be selected for the control group if:

- A. Any blood parasite was diagnosed at a molecular level.

- B. Any significant co-morbid disease was diagnosed clinically or at the time of necropsy.

### **3.1.5. Source of Experimental animals**

- A. Cases selected for the experimental cohort were sourced from the OVAH and selected private veterinary practices in close proximity to the OVAH as well as from existing collaborators involved in a separate research project (protocol V034-14) managed by Professor Andrew Leisewitz.

### **3.1.6. Source of Control animals**

- A. The control cohort (CC's) included four dogs that were euthanized at a shelter or welfare organisation and the OVAH on humane grounds (protocol V034-14).

### **3.1.7. Post-mortem examination and sample collection**

A standard necropsy examination was performed within 18 hours of death at the PS, DPS, FVS, UP. Special emphasis was placed on acquiring representative lung tissue samples as quickly as possible before alveolar collapse or autolysis became significant. Photographs and detailed descriptions of the macroscopic pulmonary pathology were also performed to aid further interpretation of the histopathology as described below.

During post-mortem, two pieces of lung tissue from the cranial and caudal lobes from both left and right lung lobes measuring approximately 1cm<sup>3</sup> and representative of the overall macroscopic pathology were carefully collected into separate, labelled bottles containing 10% buffered-formalin using a sharp pair of scissors and knives to minimise tissue crush artefact. Both samples per lobe were evaluated to ensure homogeneity of the pulmonary pathology.

After fixation for 2-6 days, each FFPE lung sample was trimmed to a 5x5x2-3mm tissue section which was randomly selected from each case (including controls) for IHC using a simple random selection procedure provided the pulmonary pathology was homogenous per dog.

The left caudal lungs lobes were selected for closer examination. One sample per case was re-embedded into a test block with 6 cases per test block. Two separate test blocks were created for a total of 12 cases. All control lung sections were embedded into a single control block. The newly created wax blocks were carefully labelled with the correct case identification number to prevent misidentification. Slides generated from these blocks were processed and stained according to standard immunohistochemical procedures as described below.

### **3.1.8. Sample processing**

Formalin-fixed tissues were cut in by the primary investigator and placed in histology cassettes between 2-6 days after collection to facilitate immunohistochemical evaluation without the deleterious effect of over-fixation in formalin. Sections of

5x5x2-3mm were taken from the middle of each 1cm<sup>3</sup> sample to minimise tissue crush artefact. Tissue processing, embedding, sectioning and staining was performed according to Bancroft and Gamble<sup>7</sup>

In summary, the following were sampled and processed: eleven babesia-infected cases and four control cases.

A. Light microscopy:

- a. Eight x 1cm<sup>3</sup> lung samples per case in formalin (two samples per lobe for the cranial and caudal lobes of both the left and right lung lobes) for the babesia-infected cases.
- b. Four x 1cm<sup>3</sup> lung samples per case per case in formalin (one sample per lobe for the cranial and caudal lobes of both the left and right lungs) for the control cases.
- c. Four tissue cassettes/wax blocks per case for the babesia-infected and control cases.

B. Immunohistochemistry:

- a. Two tissue cassettes/wax blocks per six babesia-infected cases for immunohistochemistry.
- b. One tissue cassette/wax block per four control cases for immunohistochemistry.
- c. Total of three wax blocks for immunohistochemistry.

### 3.1.9. Tissue sections

- A. Four H&E stained sections per case x (eleven babesia-infected plus six control) cases = total of 64 H&E-stained sections.
- B. Seven antibodies x (Two babesia-infected plus one control) blocks for a total of 21 IHC-labelled sections

### 3.1.10. Immunohistochemistry technique

Routine immunoperoxidase staining was performed according to the standard operating procedures in the IHC laboratory, according to guidelines supplied by the manufacturer's specification sheets. In general, the procedure entailed manual processing using presented procedures<sup>76</sup>. In summary, 4µm-thick formalin fixed, paraffin-embedded sections were mounted on positively-charged Superfrost® glass slides. Routine deparaffinisation was performed using two changes of xylene whereafter the use of graded alcohol baths with distilled water was utilised for rehydration. 3% hydrogen peroxide in methanol was used to quench endogenous peroxidase activity for 15 minutes. Heat-induced epitope retrieval (HIER) was performed by microwaving in citrate buffer (pH 6) at 96°C and then allowed to cool on the bench to room temperature. Slides were rinsed in distilled water 3 times followed by 0.1 molar (M) phosphate buffer saline (PBS), pH 7.6, containing 0.1% bovine serum albumin (BSA), rinsing for 10 minutes follow by incubation with the primary antibody (table 3). Slides were rinsed again in distilled water followed by 10 minutes in PBS-BSA. Target antigens were then be detected using the BioComplex polymer system (Reference QD420-YKE, Lot QD420915) according to manufacturer's instructions. Sections were

subsequently exposed to one drop of DAB substrate (DAB buffer lot HK5200715) and DAB chromogen (lot HK1240515) (Vector Laboratories, Burlingame, California, USA) and counterstained with Mayer's Haematoxylin. Buffer and irrelevant mono- and polyclonal antibodies were substituted for the primary antibodies in the case of negative reagent controls. Positive controls were performed during the initial antibody optimisation and included reactive dog lymph node for lymphocyte, plasma cells and macrophages markers and normal puppy bone marrow for MAC387.

### 3.1.11. Examination

All H&E stained sections were examined using a light microscope with the aid of a histopathology checklist (Appendix 2). All subset of sections was also be checked by the co-supervisor in concert with the primary investigator.

## 3.2. Data Analysis

This study was primarily descriptive at the light microscopic level with additional immunohistochemistry. Samples from all four of the main lung lobes were examined and the lesions observed were relatively uniformly distributed throughout all four lobes, but the left caudal lobe showed the least variation. Thus, the left caudal lung lobes were selected for closer examination and description and IHC.

A recent dissertation by Nicolize O'Dell describing the pathology of natural African horsesickness virus infection in dogs created an objective histological lung scoring system<sup>70</sup> establishing semi-quantitative parameters for scoring lesion presence/absence, intensity and distribution (Appendix 1). A scoring sheet was adapted from this and used to score each of the naturally infected *B. rossi* cases as well as the control cases and is also available in the appendix 2. Briefly, the lung was divided into anatomical compartments and evaluated for inflammation, haemorrhage, congestion, apoptosis, endothelial cell activation, thrombosis and oedema. The anatomical regions include the alveolar wall, alveolar lumen, perivascular interstitium, peribronchiolar interstitium, bronchiolar lumen as well as sub-pleural interstitium. The scoring table was divided into three sections for ease of presentation. Sheet A contains lesion severity scores, sheet B, the presence or absence of lesion and Sheet C, the lesion distribution scores (Appendix 3).

For the various immunohistochemical stains, the number of positive cells for each of the major regions of interest (alveoli, alveolar walls and peribronchial interstitium) were determined for five 400× high-power fields and an average determined. The areas selected for examination were free of artefactual spaces and cracks and still had a recognisable anatomic structure. The same procedure was used on the normal control lungs to establish an average as well as a standard deviation which was subsequently used to create a normal range for non-diseased lungs. Immunohistochemical descriptions were used for stains where scoring was not applicable or appropriate.

### 3.3. Experimental animals

Not applicable as no experimental animals were utilised.

### 3.4. Staff

#### Staff

Category	Staff member	Description
Primary researcher	Dr Collin A Martin (Idexx Laboratories)	Post mortems, sample collection and analysis
Supervisor	Prof. Andrew Leisewitz (Department of Companion Animal Clinical Science, FVS)	Post mortems, sample collection
Co-supervisor	Dr Sarah J Clift (SOP, DPS, FVS)	Assistance with histopathology and IHC
	Dr Alischa Henning (SOP, DPS, FVS)	Post mortems
Histotechnologists	Mr. P Mokonoto (SOP, DPS, FVS)	Routine H&E slide preparation.
	Mrs N Timmerman (SOP, DPS, FVS)	Routine H&E slide preparation.
Immunohistotechnologist	Mrs RM Phaswane (SOP, DPS, FVS)	Immunohistochemical slide preparation

### 3.5. Facilities

The post mortem hall, histotechnology and immunohistochemistry laboratories at the SP, DPS, FVS, UP.

### 3.6. Equipment

#### 3.6.1. Macropathology

- A. Routine Post mortem equipment including knives, scalpels, cutting boards, scissors, shears and hacksaws.
- B. Photography using Apple® iPhone or Samsung® Galaxy S5.

#### 3.6.2. Routine Histology

- A. 10% buffered formalin bottles.
- B. Sundries (Latex gloves, cutting blades, microtome blades).
- C. Histology grade paraffin wax.
- D. Xylene and deionised water and H&E stain.
- E. Routine histological processing into wax blocks using the Shandon Excelsior tissue processor.
- F. Sectioning using a standard histopathology microtome.
- G. Routine staining using the Shandon® Varistain gemini automated H&E stainer.
- H. Glass cover slips.



- I. Mounting medium (Entellan™).
- J. Light microscopic analysis using an Olympus® BX43 microscope with an Olympus® DP72 camera mated to a computer equipped with Olympus® cellSens software image processing technology.

### **3.6.3. Immunohistochemistry**

- A. Tissue sections were mounted on Superfrost® glass slides.
- B. Glass cover slips.
- C. Mounting medium (Entellan™).
- D. Sundries (Latex gloves, cutting blades, microtome blades).
- E. Antibodies (please see table 3).

**Table 3:** List of antibodies with target cell/process, supplier, type and clone and catalogue number

Antibody	Target cells / process	Supplier	Dilution	Type (clone)	Catalogue number
CD20	Expressed by B-Lymphocytes and normal dog plasma cells <sup>44,38</sup> . This antibody will allow for quantification of B-lymphocytes and plasma cells within the region of interest.	Dako®	1:700	Mouse Monoclonal anti-human CD20cy B cell – (L26)	M0755, lot 110
CD204	Expressed by resident tissue macrophages as well as dendritic macrophages <sup>45</sup> . CD204-positive staining macrophages will be compared with MAC387 positive fixed and bone-marrow derived monocytes-macrophages and neutrophils.	Transgenic Inc.	1:400	Mouse monoclonal anti-human CD204 antibody	NBP2-03600
CD3	Expressed by T-Lymphocytes <sup>24,3</sup> . This antibody will allow for quantification of T-lymphocytes in a region of interest and will allow determination of the proportion of B- to T-Lymphocytes i.e. humoral vs. cell-mediated immunity.	Dako®	1:600	Polyclonal rabbit anti-human CD3	A0452
MAC387	Myeloid/histiocyte antigen expressed by circulating and tissue neutrophils, monocytes and reactive tissue macrophages and eosinophils but not dendritic cells <sup>10</sup> .	Dako®	1:800	Mouse Monoclonal antihuman myeloid/histiocyte antigen – (MAC387)	M0747
Mum1	Expressed in the late stages of B-lymphocyte development toward and including the plasma cell <sup>34</sup> . Many plasma cells may suggest a significant role for humoral immunity in the pathogenesis of ALI/ARDS in complicated babesiosis.	Dako®	1:50	Mouse Monoclonal anti-human Mum1 protein – (MUM1p)	M7259
PAX-5	Expressed in early B-cell lymphocyte development as well as naïve and mature B-lymphocytes except plasma cells <sup>34</sup> . This antibody will allow us to quantify the number of non-plasma cell B-lymphocytes in the region of interest.	BD Biosciences	1:50	Mouse Monoclonal Anti-Pax-5 antibody – (151-306)	610863
VCAM-1	Expressed on activated endothelial cells in order to facilitate leukocyte migration. The expression of VCAM-1 has been used as a marker of endothelial activation and is upregulated by TNF- $\alpha$ <sup>107</sup> . This molecule allows for the adhesion of leukocytes to endothelial cells, which may be one of the main triggering mechanisms for ALI/ARDS. It is a receptor for cytoadherence of malaria-infected red blood cells to endothelial cells in the lungs and central nervous system of humans <sup>71</sup> and in murine models <sup>23</sup> as well as human endothelial cell cultures co-cultured with malaria <sup>108</sup> .	Novus biologicals®	1:150	Mouse monoclonal antihuman VCAM1 – (3H10)	NBP2-03600

### **3.7. Records**

After completion of the study

- All FFPE, HE stained tissue sections are archived with Professor Andrew Leisewitz in his designated storage facility at the OVAH, FVS, UP.
- Photomicrographs, data collection sheets, excel tables and all related documents such as clinicopathologic findings were saved on external hard drives and on multiple DVD's belonging to the primary researcher and supervisors along with cloud-based backups such as Dropbox for all data files.
- The results of the project will be submitted in the form of a mini-dissertation as a requirement for the completion of a MMedVet (Pathology) degree at the FVS, UP.

### **3.8. Declaration of conflict of interest**

No conflicts of interest have been declared. Full funding has been received from an NRF research grant (Reference: CPRR13080726333, Grant No: 91572,31 March 2014) obtained by Professor Andrew Leisewitz.

### **3.9. Ethical Considerations**

Professor Andrew Leisewitz has already received authorisation from the Ethics committee as this project falls under a much larger protocol to investigate the use of canine babesiosis as a model or human malaria (V034-14).

## CHAPTER FOUR: RESULTS

### 4.1. Gross pathology

#### 4.1.1. Control cases

The majority of the control cases (CC's) showed lungs with a pale pink to slightly reddish colour with an elastic, pillowy texture (Fig 4).

#### 4.1.2. Naturally infected *B. rossi* cases

Lesions varied greatly between cases, but multifocal, often coalescing haemorrhages were a consistent finding resulting in a dark red, mottled appearance (Figure 10). Severe diffuse haemorrhage was noted in cases as well (Figure 11). There was always significant pulmonary oedema as evidenced by increased weight and consistency as well as oozing on cut section (Figure 12). Many cases also showed marked accumulation of thick tracheal froth (Figure 13).

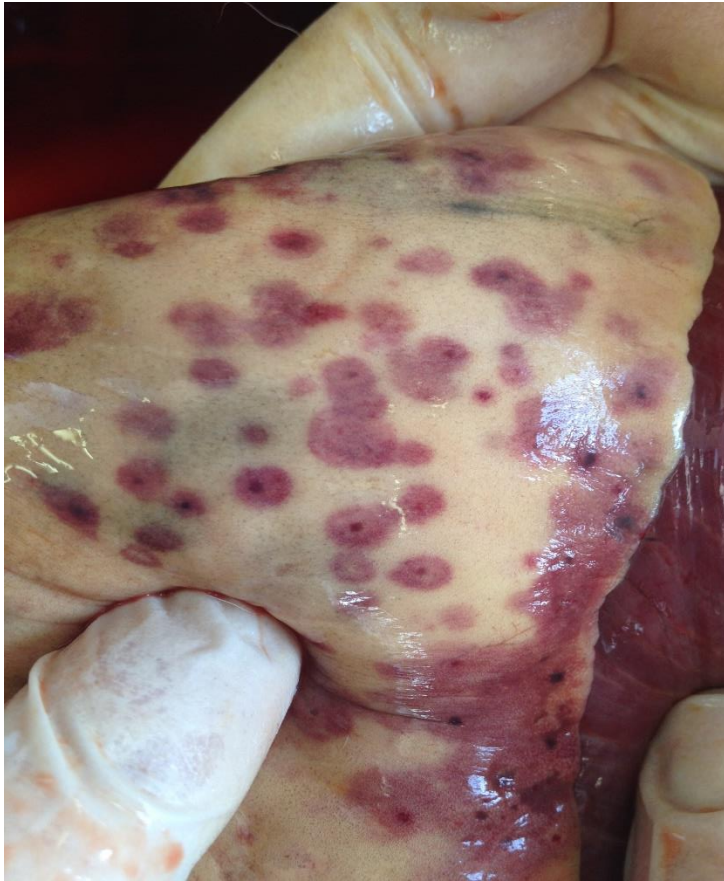


**Figure 10:** Lung. Multifocal discrete, often coalescing pulmonary petechial and ecchymotic haemorrhages.



**Figure 11:** Lung. Severe diffuse pulmonary haemorrhage with atelectasis and multifocal emphysema.



**Figure 12:** Lung, cut section. Severe pulmonary oedema with oozing of fluid and froth.

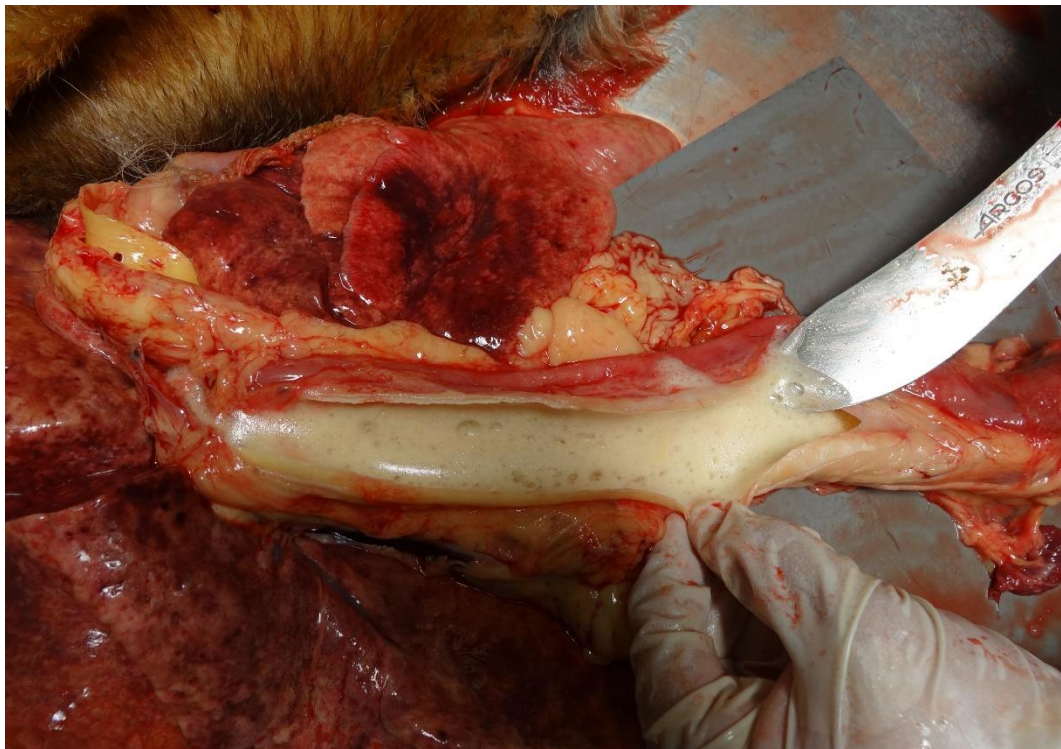


**Figure 13:** Trachea, opened. Severe accumulation of pulmonary oedema/froth within the tracheal lumen.

## 4.2. Histopathology

### 4.2.1. Control cases

#### 4.2.1.1. Standard H&E histological examination

Standard histological examination of the control lungs showed a normal appearance with thin alveolar walls and occasional mild congestion. There was minimal inflammatory infiltrate as well as any significant pulmonary oedema (Figure 5).

#### 4.2.1.2. O'Dell lung scoring system

The O'Dell lung scoring system<sup>70</sup> was applied to all the cases and the findings are summarised in Tables 4 and 5. Please refer to Appendix 1 for the grading criteria.

**Table 4:** Babesia related ALI/ARDS control cases summary score sheet A. Adapted severity scores<sup>70</sup>.

Parameter / Anatomical location	Number of cases with individual scores							
	Minimal (0)	%	Mild (1)	%	Moderate (2)	%	Severe (3)	%
<b>Autolysis</b>	4	100.0	0	0.0	0	0.0	0	0.0
<b>Congestion</b>	0	0.0	4	100.0	0	0.0	0	0.0
<b>Alveolar walls</b>								
Inflammatory cell infiltrate								
Monocyte-macrophages	4	100.0	0	0.0	0	0.0	0	0.0
Lymphocytes	4	100.0	0	0.0	0	0.0	0	0.0
Plasma cells	4	100.0	0	0.0	0	0.0	0	0.0
neutrophils	4	100.0	0	0.0	0	0.0	0	0.0
Eosinophils	4	100.0	0	0.0	0	0.0	0	0.0
Apoptosis	4	100.0	0	0.0	0	0.0	0	0.0
Microvascular endothelial cell activation								
Nuclear hypertrophy/activation	4	100.0	0	0.0	0	0.0	0	0.0
<b>Alveolar lumen</b>								
Inflammatory cell infiltrate								
Monocyte-macrophages	4	100.0	0	0.0	0	0.0	0	0.0
Lymphocytes	4	100.0	0	0.0	0	0.0	0	0.0
Plasma cells	4	100.0	0	0.0	0	0.0	0	0.0
neutrophils	4	100.0	0	0.0	0	0.0	0	0.0
Eosinophils	4	100.0	0	0.0	0	0.0	0	0.0
Fibrin	4	100.0	0	0.0	0	0.0	0	0.0
Haemorrhage	4	100.0	0	0.0	0	0.0	0	0.0
Oedema	4	100.0	0	0.0	0	0.0	0	0.0

<b>Perivascular interstitium</b>								
Inflammatory cell infiltrate								
Monocyte-macrophages	4	100.0	0	0.0	0	0.0	0	0.0
Lymphocytes	4	100.0	0	0.0	0	0.0	0	0.0
Plasma cells	4	100.0	0	0.0	0	0.0	0	0.0
neutrophils	4	100.0	0	0.0	0	0.0	0	0.0
Eosinophils	4	100.0	0	0.0	0	0.0	0	0.0
Fibrin	4	100.0	0	0.0	0	0.0	0	0.0
Haemorrhage	4	100.0	0	0.0	0	0.0	0	0.0
Oedema	4	100.0	0	0.0	0	0.0	0	0.0
Microvascular endothelial cell activation								
Nuclear hypertrophy/activation	4	100.0	0	0.0	0	0.0	0	0.0
Lymphatic vessel distension	4	100.0	0	0.0	0	0.0	0	0.0
<b>Subpleural interstitium</b>								
Inflammatory cell infiltrate								
Monocyte-macrophages	4	100.0	0	0.0	0	0.0	0	0.0
Lymphocytes	4	100.0	0	0.0	0	0.0	0	0.0
Plasma cells	4	100.0	0	0.0	0	0.0	0	0.0
neutrophils	4	100.0	0	0.0	0	0.0	0	0.0
Eosinophils	4	100.0	0	0.0	0	0.0	0	0.0
Fibrin	4	100.0	0	0.0	0	0.0	0	0.0
Haemorrhage	4	100.0	0	0.0	0	0.0	0	0.0
Oedema	4	100.0	0	0.0	0	0.0	0	0.0
<b>Peribronchiolar interstitium</b>								
Inflammatory cell infiltrate								
Monocyte-macrophages	4	100.0	0	0.0	0	0.0	0	0.0
Lymphocytes	4	100.0	0	0.0	0	0.0	0	0.0
Plasma cells	4	100.0	0	0.0	0	0.0	0	0.0
neutrophils	4	100.0	0	0.0	0	0.0	0	0.0
Eosinophils	4	100.0	0	0.0	0	0.0	0	0.0
Fibrin	4	100.0	0	0.0	0	0.0	0	0.0
Haemorrhage	4	100.0	0	0.0	0	0.0	0	0.0
Oedema	4	100.0	0	0.0	0	0.0	0	0.0
<b>Bronchiolar lumen</b>								
Inflammatory cell infiltrate								
Monocyte-macrophages	4	100.0	0	0.0	0	0.0	0	0.0
Lymphocytes	4	100.0	0	0.0	0	0.0	0	0.0
Plasma cells	4	100.0	0	0.0	0	0.0	0	0.0
neutrophils	4	100.0	0	0.0	0	0.0	0	0.0
Eosinophils	4	100.0	0	0.0	0	0.0	0	0.0



Fibrin	4	100.0	0	0.0	0	0.0	0	0.0
Haemorrhage	4	100.0	0	0.0	0	0.0	0	0.0
Oedema	4	100.0	0	0.0	0	0.0	0	0.0

**Table 5:** Babesia related ALI/ARDS control cases summary score sheet B. Presence or absence of lesion<sup>70</sup>.

Parameter / Anatomical location	Quantity of cases with individual scores			
	Present (1)	%	Absent (0)	%
<b>Alveolar walls</b>				
Thrombosis	0	0.0	4	100.0
<b>Alveolar Lumen</b>				
Hyaline membrane	0	0.0	4	100.0
<b>Pleural mesothelium</b>				
Hypertrophy/activation	0	0.0	4	100.0
<b>Peribronchiolar interstitium</b>				
Anthracosis	0	0.0	4	100.0

No haemorrhages were observed in the control sections. Hence Sheet C, pertaining to the lesion distribution was not applicable.

## 4.2.2. Naturally infected *B. rossi* cases

### 4.2.2.1. Standard H&E histopathology summary

The individual case reports in are Appendix 5 and the following generalised observations are based on those findings.

Within the alveolar spaces, almost all cases showed a marked increase in alveolar macrophages ([Figure 14](#),[Figure 17](#),[Figure 18](#)) which was often accompanied by severe pulmonary oedema ([Figure 14](#),[Figure 19](#), [Figure 26](#)) as well as multifocal to coalescing and occasionally focally extensive haemorrhage ([Figure 17](#),[Figure 18](#),[Figure 19](#),[Figure 21](#)). The alveolar macrophages were often foamy and contained small quantities of brown pigment consistent with haemosiderin.

The alveolar interstitium was often severely infiltrated by monocyte-macrophages results in increased alveolar wall thickness([Figure 14](#),[Figure 15](#),[Figure 16](#)). This was often combined with moderate to severe congestion and hyperaemia ([Figure 27](#)) as well as mononuclear leukostasis. Endothelial cell activation, characterised by plump endothelial cell nuclei, was also present ([Figure 24](#),[Figure 25](#),[Figure 26](#),[Figure 27](#)) and there was mild perivascular oedema as well.

Visible *B. rossi* intraerythrocytic piroplasm's were visible in three cases. Cell death characterised by visible karyorhexis and karyolysis were noted occasionally along with blastic cells as well as megakaryocytes ([Figure 23](#)).

The bronchioles often contained oedema, fibrin and haemorrhage ([Figure 21](#)) and occasionally a few neutrophils.

Perivascular lymphoplasmacytic cuffing was also noted in two cases ([Figure 22](#)) and there were prominent intravascular mononuclear leukostasis ([Figure 22](#)).

Intravascular haemosiderophages and megakaryocytes were also variably present. ([Figure 23](#)). Dark brown to black, refractive intracytoplasmic carbon pigment was noted in areas of the bronchial associated lymphoid tissue consistent with anthracosis.

Although not prominent, one case showed a large intravascular fibrin thrombus formation in bronchial vasculature ([Figure 28](#)). Atelectasis as well as occasionally scattered alveolar emphysema were noted, and a few scattered neutrophils but only in two cases.

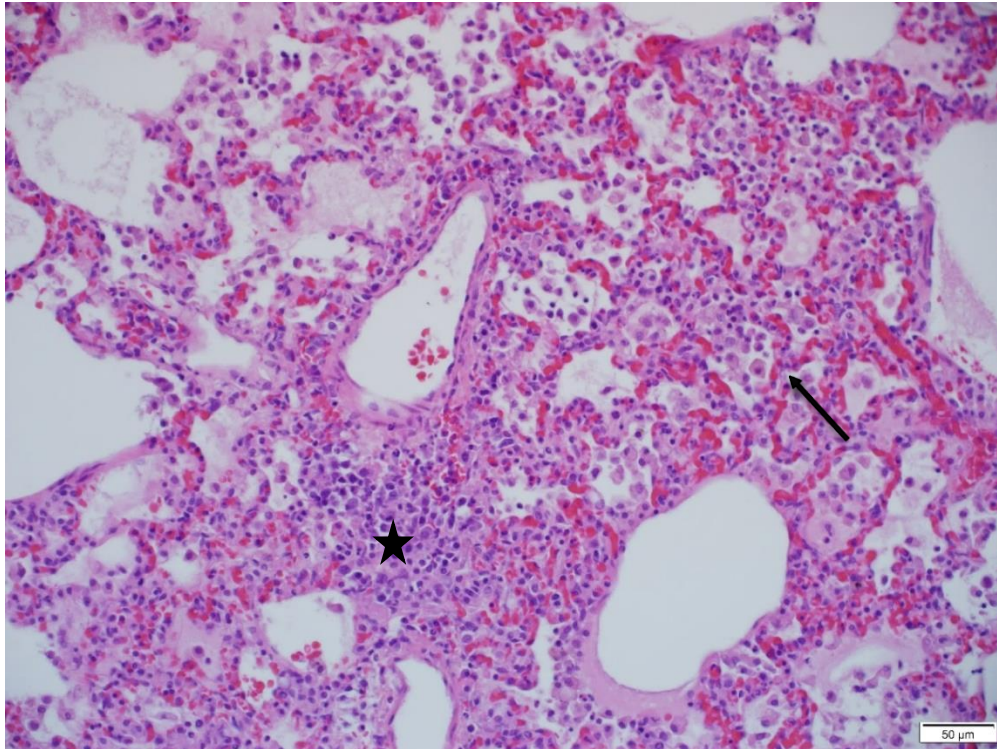


**Figure 14:** Case 4. Focal severe alveolar macrophage infiltration with pulmonary oedema (thick arrow) and mild interstitial expansion due to perivascular lymphocyte and plasma cell accumulation (star). 200× magnification.

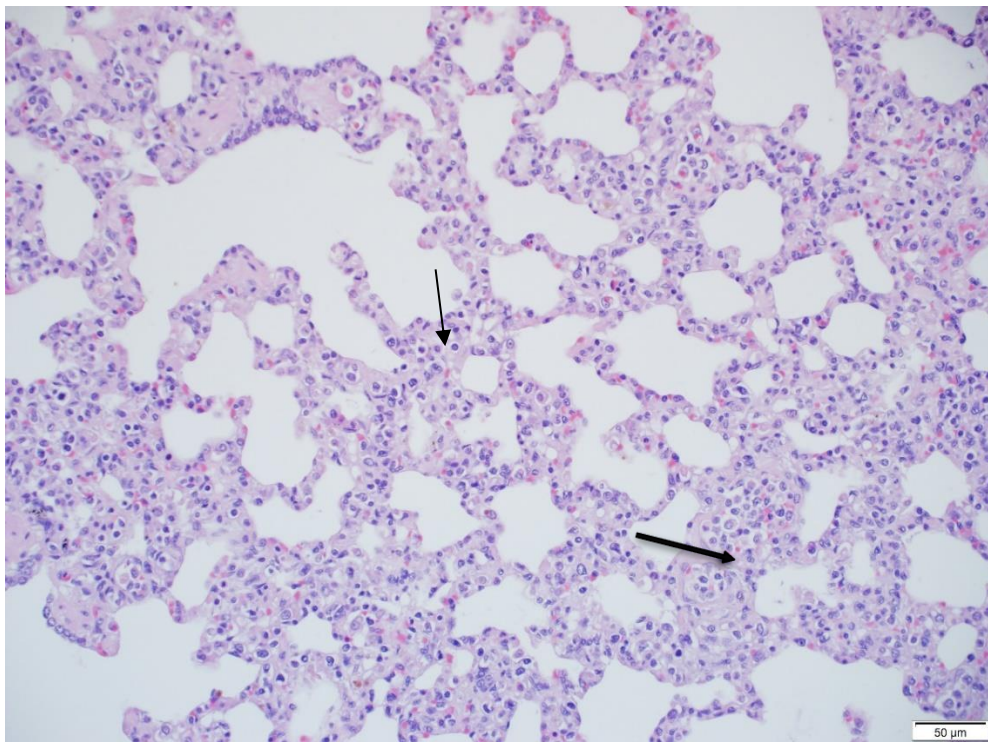


**Figure 15:** Case 6. Moderate thickening alveolar walls due to mononuclear leukocytic infiltration (thin arrow) with endothelial cell activation and leukostasis (Thick arrow). 200× magnification.

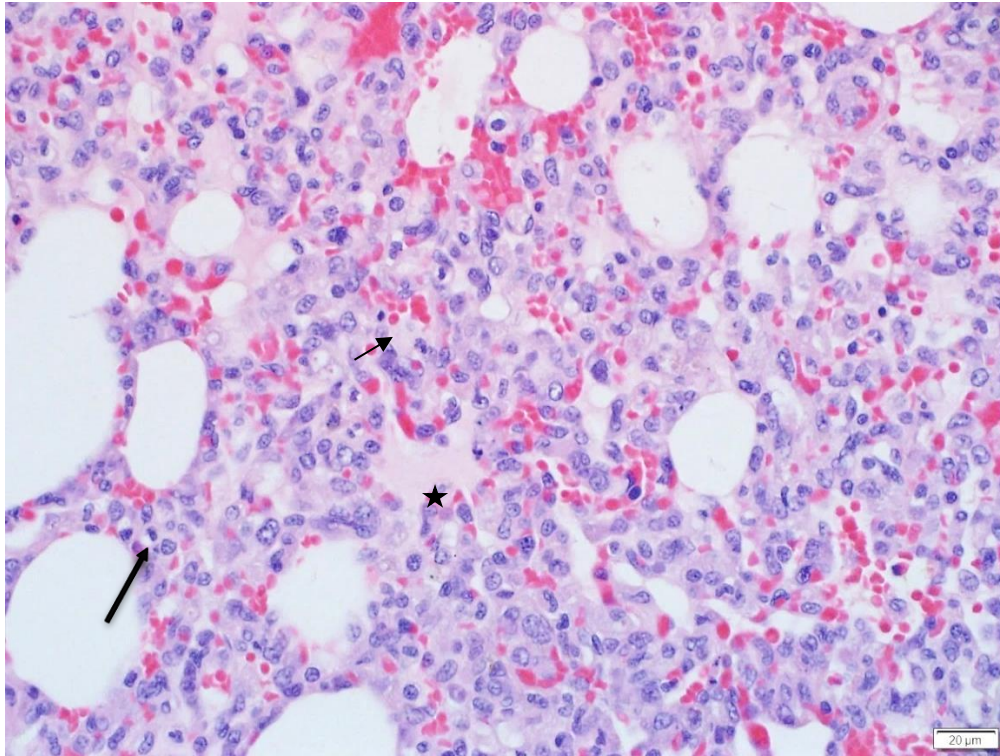


**Figure 16:** Case 9. Severe interstitial mononuclear expansion (Thick arrow) with scattered apoptosis (Thin arrow) and pulmonary oedema (star). 400× magnification.

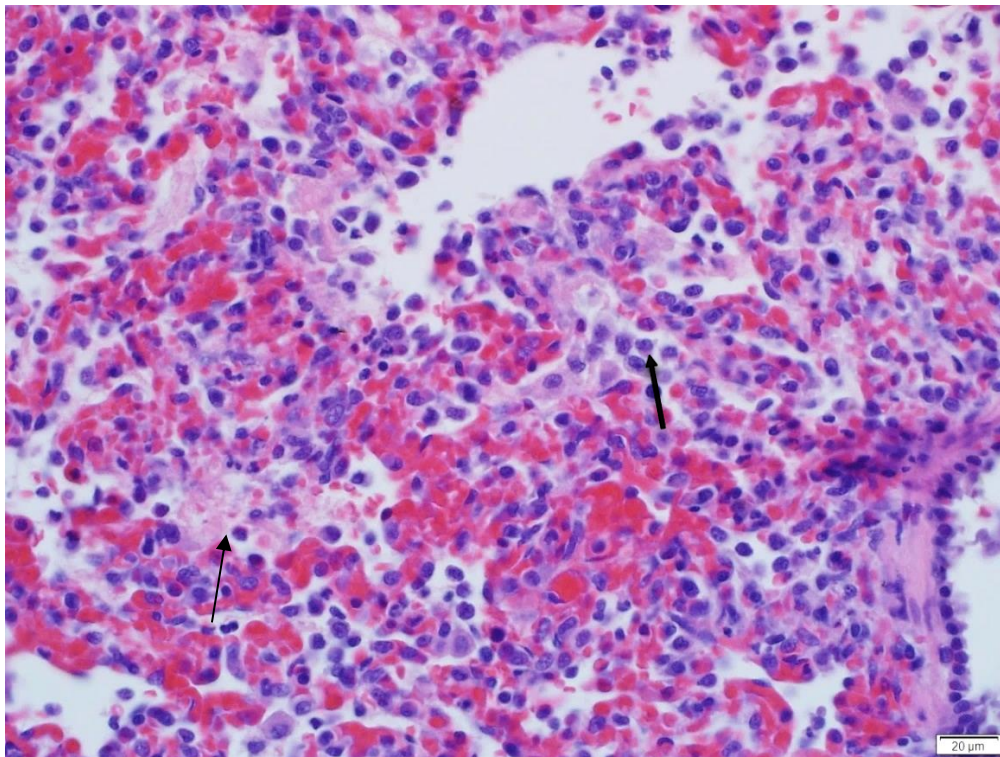


**Figure 17:** Case 1. Severe mononuclear alveolar inflammatory cell infiltrate characterised by alveolar macrophages and fewer neutrophils (thick arrow) with haemorrhage and fibrin exudation extending into the alveolar ducts (thin arrow). 400× magnification.

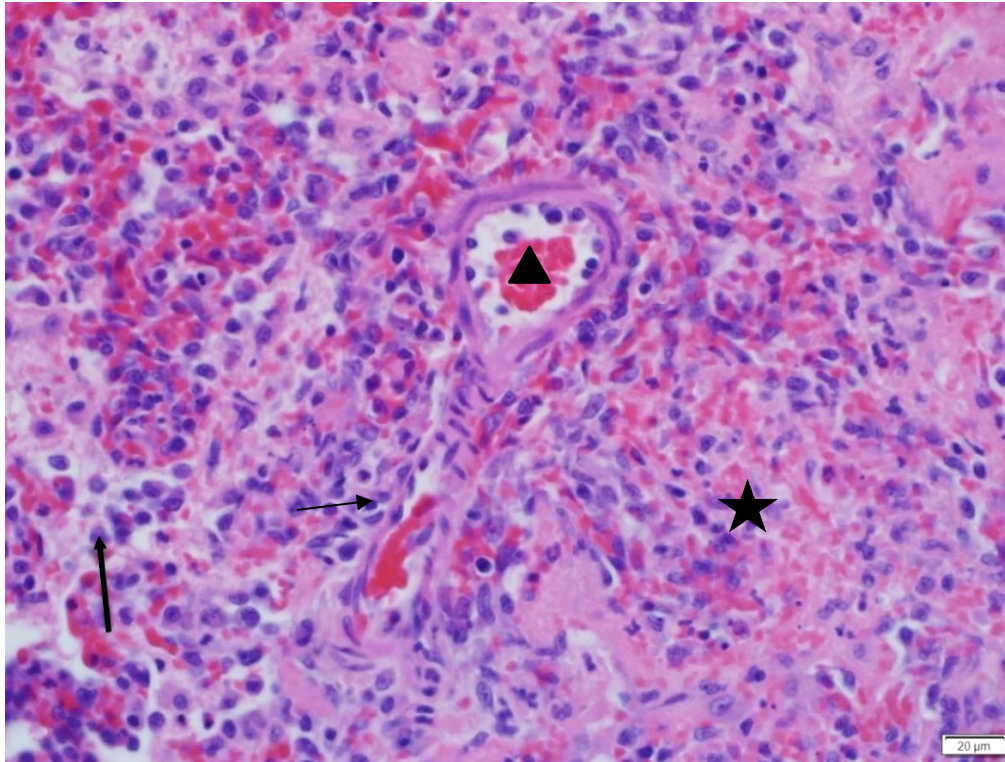


**Figure 18:** Case 1. Severe mononuclear alveolar inflammatory cell infiltrate (thick arrow) with haemorrhage and fibrin exudation (Star) as well as endothelial cell activation (thin arrow), lymphocyte margination (triangle) and perivascular infiltration. 400× magnification.

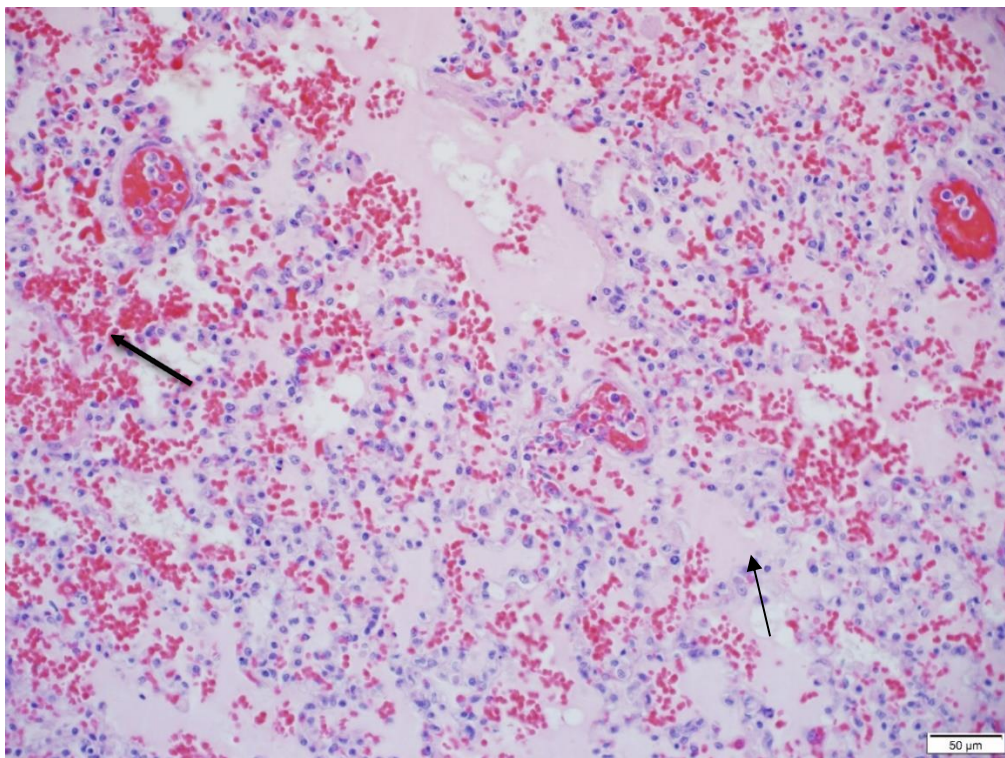


**Figure 19:** Case 2. Severe moderately protein rich alveolar oedema (thin arrow) with moderate haemorrhage (thick arrow). 200× magnification.

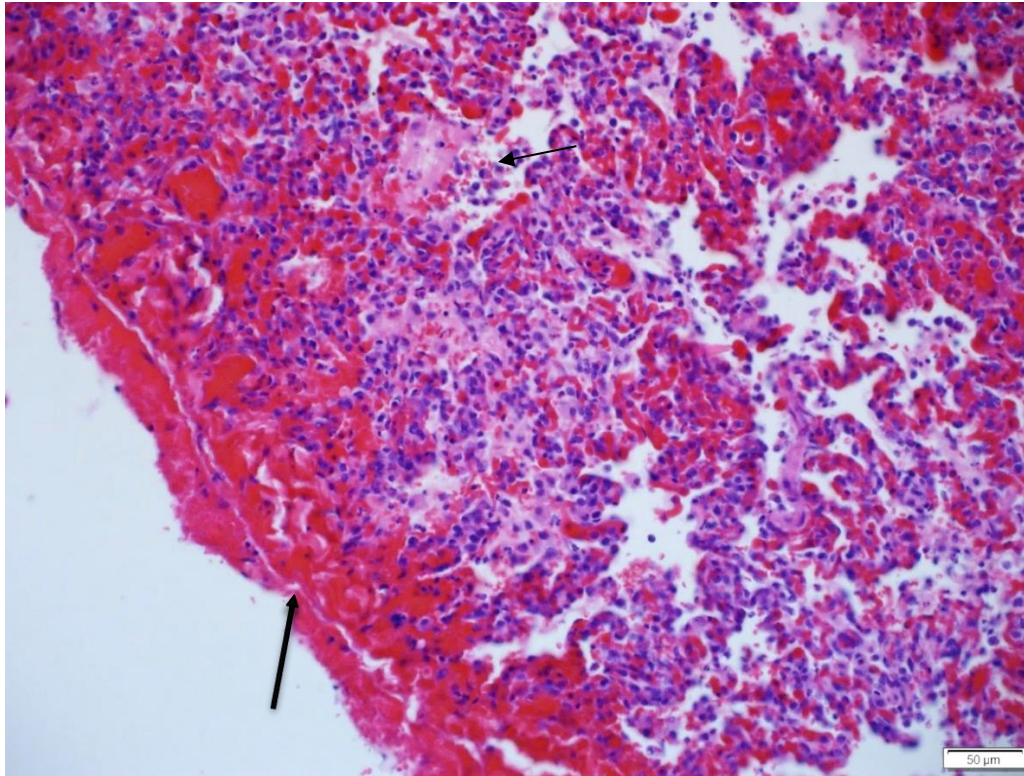


**Figure 20:** Case 1. Subpleural haemorrhage (thick arrow), Severe alveolar infiltrate with haemorrhage (thin arrow). 200× magnification.

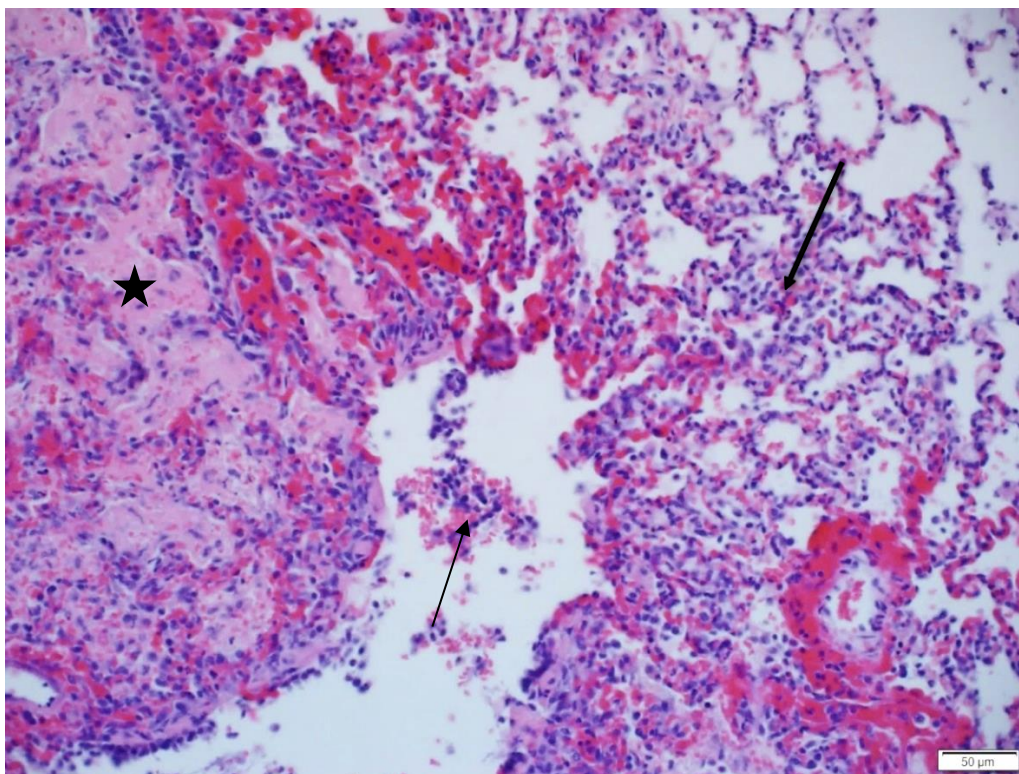


**Figure 21:** Case 1. Mild bronchiolar haemorrhage (thin arrow) with alveolar fibrin exudation (star) and moderate alveolar mononuclear cell infiltrate (thick arrow). 200× magnification.

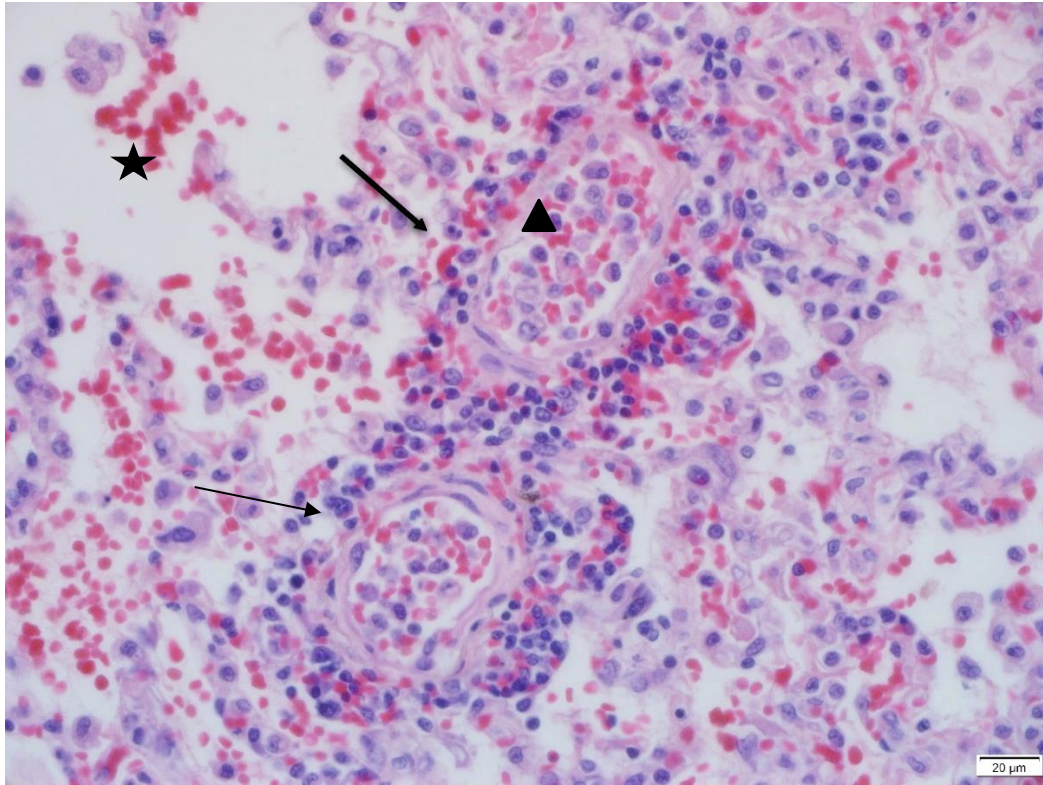


**Figure 22:** Case 2. Perivascular lymphoplasmacytic cuffing (thick arrow) with alveolar oedema and haemorrhage (star) as well as endothelial cell activation (thin arrow). Also present is intravascular mononuclear leukostasis (triangle). 200× magnification.

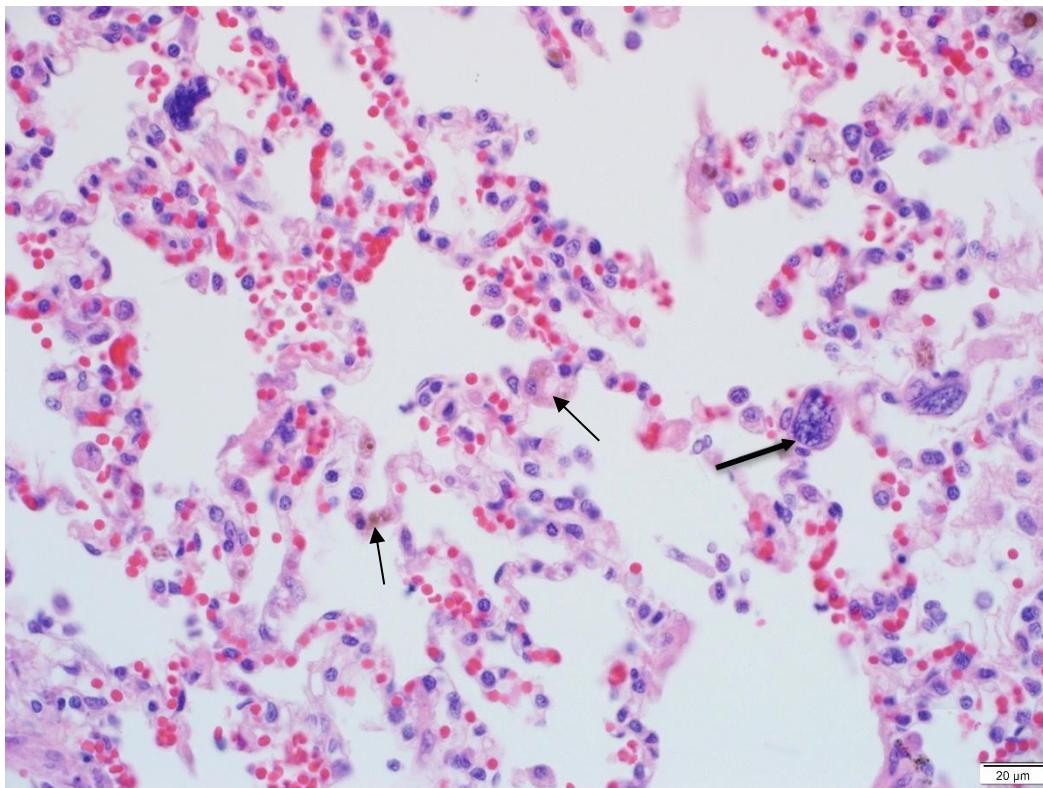


**Figure 23:** Case 8. Intravascular haemosiderophages (thin arrows) and megakaryocytes (thick arrow). 400× magnification.

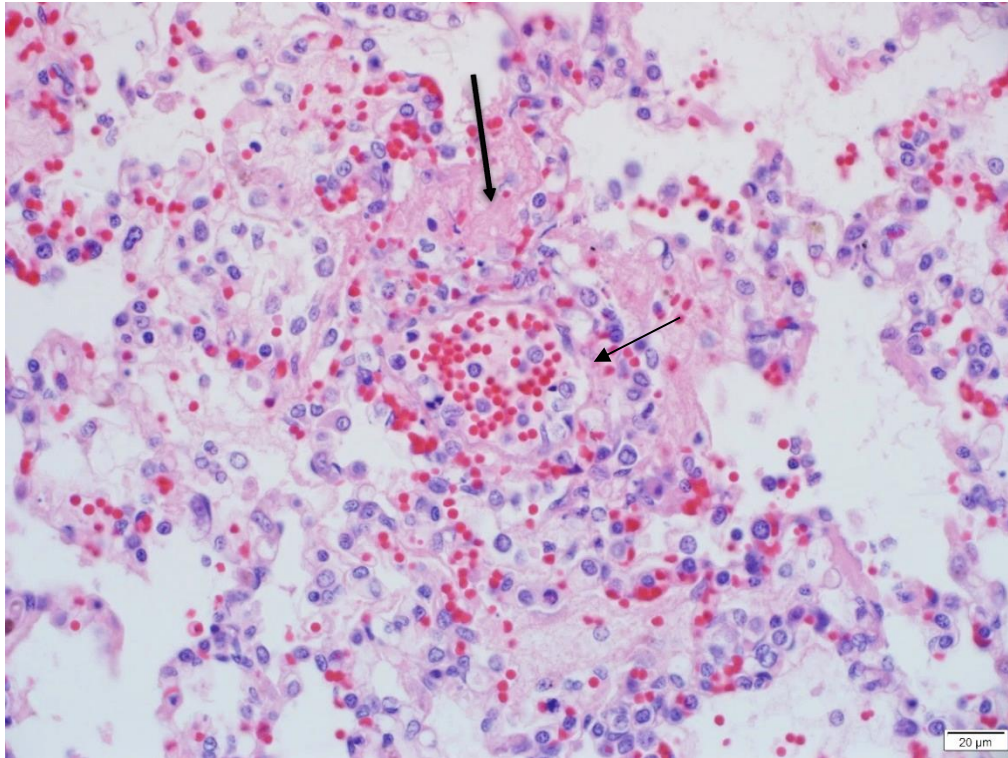


**Figure 24:** Case 8. Moderate alveolar haemorrhage with fibrin (thick arrow) and endothelial activation (thin arrow). 400× magnification.

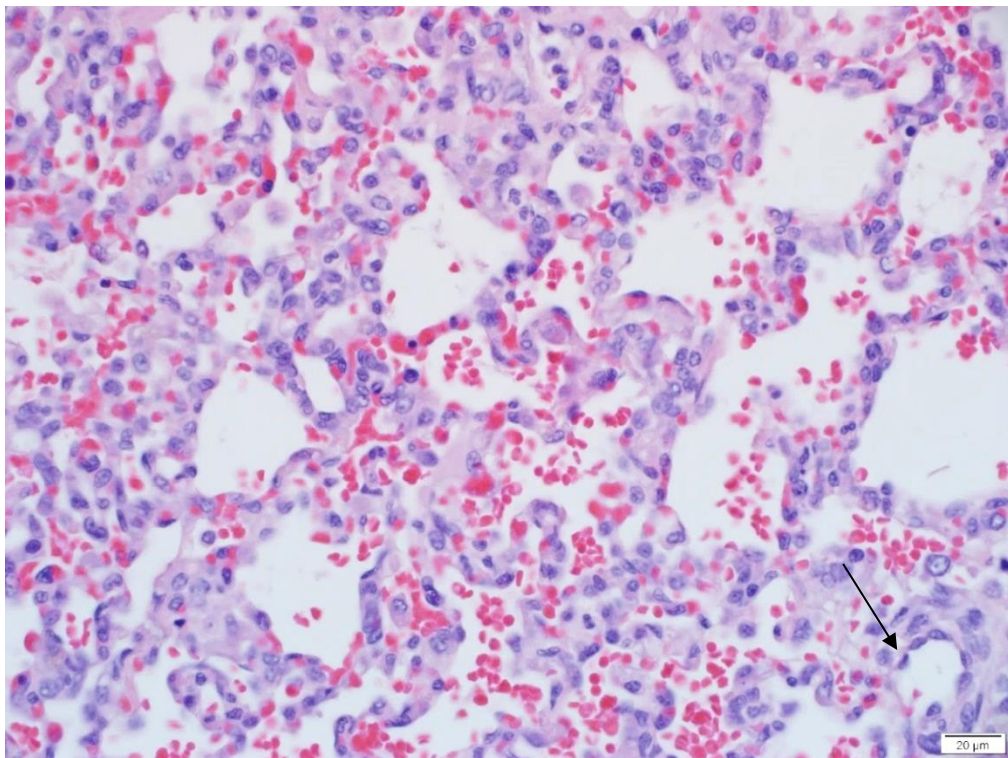


**Figure 25:** Case 9. Severe interstitial mononuclear expansion, endothelial cell activation (thin arrow) with mild alveolar haemorrhage. 400× magnification.



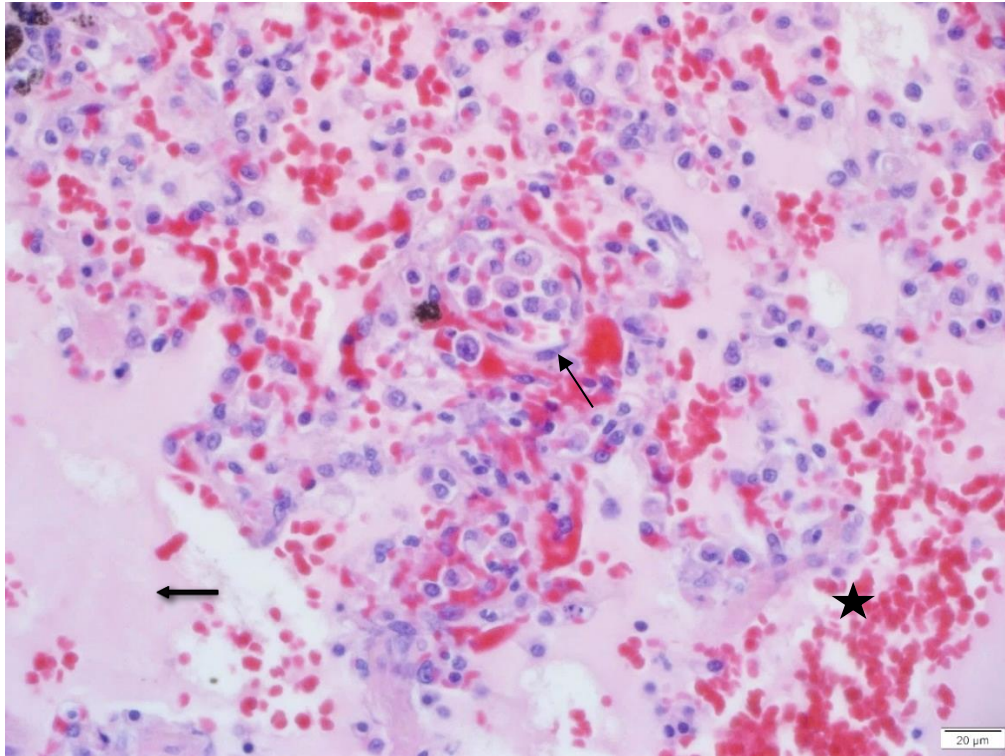


**Figure 26:** Case 9. Severe interstitial mononuclear expansion with endothelial cell activation and intravascular mononuclear leukostasis (thin arrow). Moderate alveolar haemorrhage and fibrin (star) and severe high protein content pulmonary oedema (thick arrow). 400× magnification.

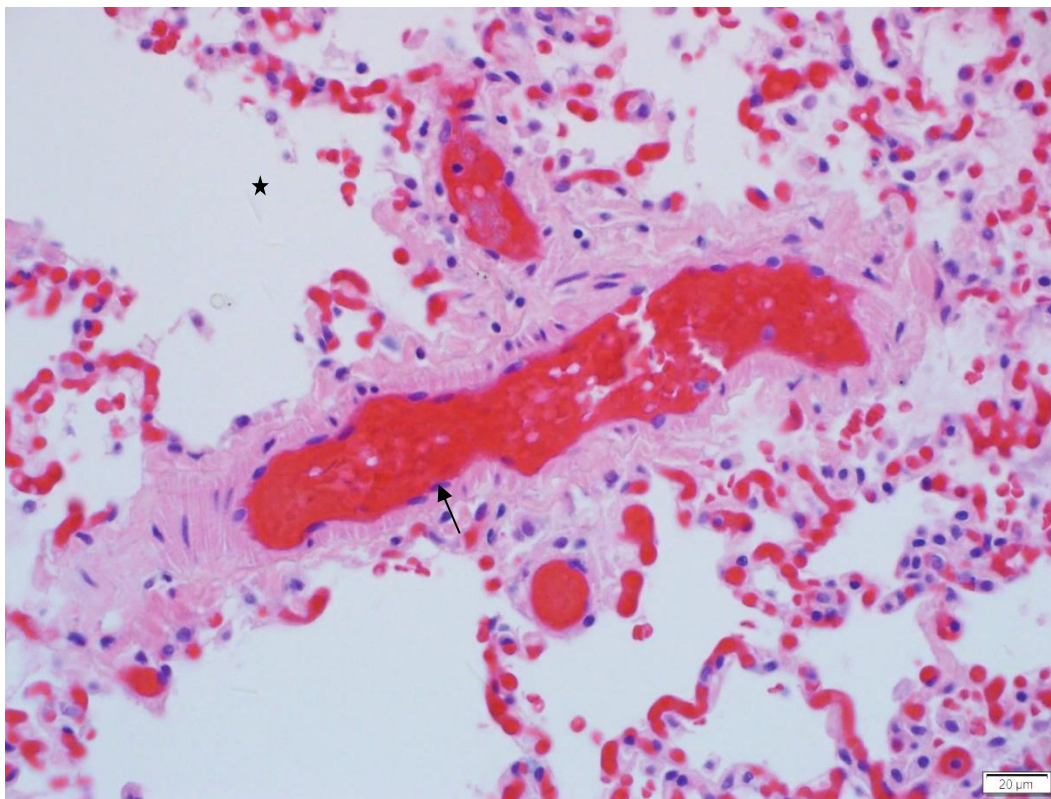


**Figure 27:** Case 10. Moderate endothelial cell activation and hyperaemia (thin arrow). 200× magnification.

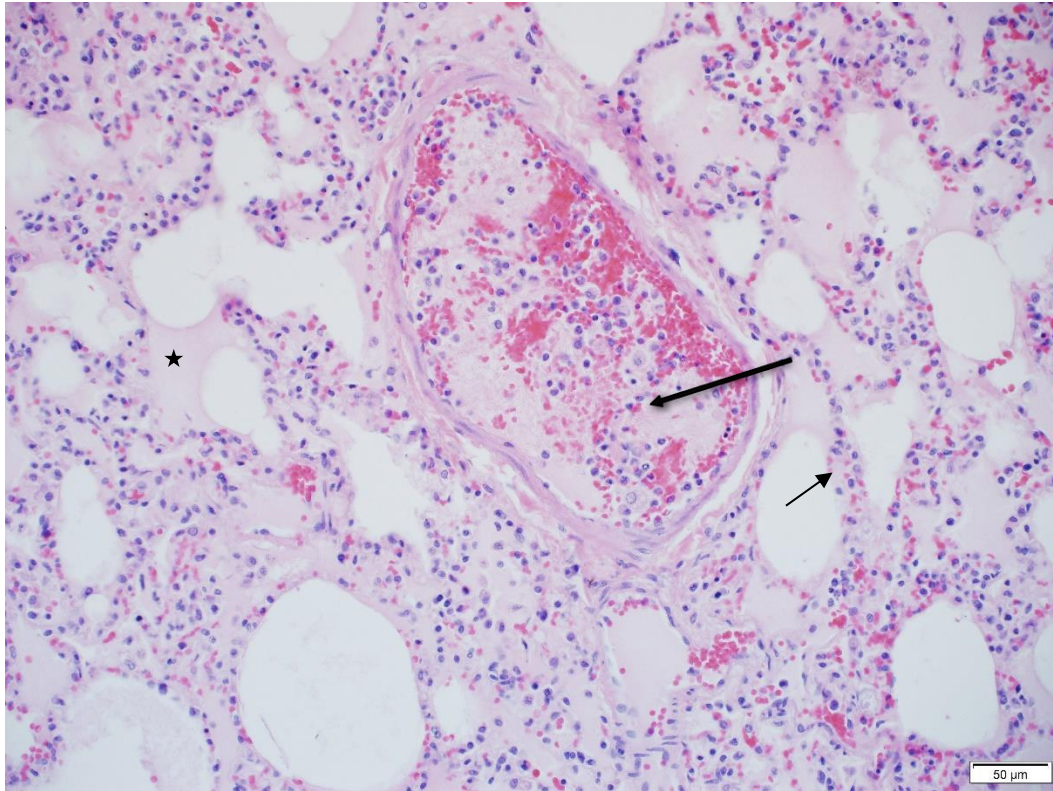


**Figure 28:** Case 11. Moderate interstitial mononuclear expansion (thin arrow) with alveolar oedema (star). Large intravascular thrombus with enmeshed large monocytes (thick arrow). 200× magnification.

#### 4.2.2.2. O'Dell lung scoring system

All the naturally infected *B. rossi* cases were scored using the reviewed O'Dell lung scoring system<sup>70</sup> and a summary is presented in tables 6-8. The grading criteria are available in Appendix 1.

**Table 6:** Babesia related ARDS summary score sheet A. Severity of lesion

Parameter / Anatomical location	Number of cases with individual score							
	Minimal (0)	%	Mild (1)	%	Moderate (2)	%	Severe (3)	%
<b>Autolysis</b>	11	100.0	0	0.0	0	0.0	0	0.0
<b>Congestion</b>	3	27.3	6	54.5	2	18.2	0	0.0
<b>Alveolar walls</b>								
Cell infiltrate								
Monocyte-macrophages	1	9.1	6	54.5	2	18.2	2	18.2
Lymphocytes	5	45.5	5	45.5	1	9.1	0	0.0
Plasma cells	9	81.8	2	18.2	0	0.0	0	0.0
neutrophils	11	100.0	0	0.0	0	0.0	0	0.0
Eosinophils	11	100.0	0	0.0	0	0.0	0	0.0
Apoptosis	2	18.2	8	72.7	1	9.1		0.0
<b>Microvascular endothelial cell activation</b>								
Nuclear hypertrophy/activation	0	0.0	3	27.3	6	54.5	2	18.2
<b>Alveolar lumen</b>								
Cell infiltrate								
Monocyte-macrophages	0	0.0	5	45.5	5	45.5	1	9.1
Lymphocytes	11	100.0	0	0.0	0	0.0	0	0.0
Plasma cells	11	100.0	0	0.0	0	0.0	0	0.0
neutrophils	9	81.8	2	18.2	0	0.0	0	0.0
Eosinophils	11	100.0	0	0.0	0	0.0	0	0.0
Fibrin	5	45.5	2	18.2	3	27.3	1	9.1
Haemorrhage	2	18.2	5	45.5	2	18.2	2	18.2
Oedema	0	0.0	2	18.2	1	9.1	8	72.7
<b>Perivascular interstitium</b>								
Cell infiltrate								
Monocyte-macrophages	6	54.5	3	27.3	2	18.2	0	0.0
Lymphocytes	6	54.5	3	27.3	2	18.2	0	0.0
Plasma cells	7	63.6	4	36.4	0	0.0	0	0.0
neutrophils	11	100.0	0	0.0	0	0.0	0	0.0
Eosinophils	11	100.0	0	0.0	0	0.0	0	0.0
Fibrin	9	81.8	2	18.2	0	0.0	0	0.0

Haemorrhage	9	81.8	2	18.2	0	0.0	0	0.0
Oedema	1	9.1	6	54.5	3	27.3	1	9.1
Microvascular endothelial cell activation								
Nuclear hypertrophy/activation	0	0.0	4	36.4	6	54.5	1	9.1
Lymphatic vessel distension	10	90.9	1	9.1	0	0.0	0	0.0
<b>Subpleural interstitium</b>								
Cell infiltrate								
Monocyte-macrophages	11	100.0	0	0.0	0	0.0	0	0.0
Lymphocytes	11	100.0	0	0.0	0	0.0	0	0.0
Plasma cells	11	100.0	0	0.0	0	0.0	0	0.0
neutrophils	11	100.0	0	0.0	0	0.0	0	0.0
Eosinophils	11	100.0	0	0.0	0	0.0	0	0.0
Fibrin	10	90.9	0	0.0	1	9.1	0	0.0
Haemorrhage	10	90.9	0	0.0	1	9.1	0	0.0
Oedema	6	54.5	5	45.5	0	0.0	0	0.0
<b>Peribronchiolar interstitium</b>								
Cell infiltrate								
Monocyte-macrophages	11	100.0	0	0.0	0	0.0	0	0.0
Lymphocytes	11	100.0	0	0.0	0	0.0	0	0.0
Plasma cells	11	100.0	0	0.0	0	0.0	0	0.0
neutrophils	11	100.0	0	0.0	0	0.0	0	0.0
Eosinophils	11	100.0	0	0.0	0	0.0	0	0.0
Fibrin	10	90.9	1	9.1	0	0.0	0	0.0
Haemorrhage	10	90.9	1	9.1	0	0.0	0	0.0
Oedema	11	100.0	0	0.0	0	0.0	0	0.0
<b>Bronchiolar lumen</b>								
Cell infiltrate								
Monocyte-macrophages	10	90.9	1	9.1	0	0.0	0	0.0
Lymphocytes	11	100.0	0	0.0	0	0.0	0	0.0
Plasma cells	11	100.0	0	0.0	0	0.0	0	0.0
neutrophils	11	100.0	0	0.0	0	0.0	0	0.0
Eosinophils	11	100.0	0	0.0	0	0.0	0	0.0
Fibrin	11	100.0	0	0.0	0	0.0	0	0.0
Haemorrhage	4	36.4	7	63.6	0	0.0	0	0.0
Oedema	2	18.2	7	63.6	2	18.2	0	0.0

Table 7: Babesia related ARDS summary score sheet B. Presence or absence of lesion.

Parameter / Anatomical location	Number of cases with individual scores			
	Present (1)	%	Absent (0)	%
<b>Alveolar walls</b>				
Thrombosis	2	18.2	9	81.8
<b>Alveolar Lumen</b>				
Hyaline membrane	0	0	11	100.0
<b>Pleural mesothelium</b>				
Hypertrophy/activation	1	9.1	10	90.9
<b>Peribronchiolar interstitium</b>				
Anthraxis	5	45.5	6	54.5

Table 8: Babesia related ARDS summary score sheet C. Lesion distribution.

Anatomical location/Parameter	Number of cases with individual scores							
	Focal	%	Multifocal	%	Coalescing	%	Diffuse	%
<b>Lesion distribution</b>	0	0.0	1	9.1	4	36.4	6	54.5
<b>Alveolar lumen</b>								
Distribution of Haemorrhage	0	0.0	7	77.8	1	11.1	1	11.1
<b>Perivascular interstitium</b>								
Distribution of Haemorrhage	0	0.0	2	100.0	0	0.0	0	0.0
<b>Subpleural interstitium</b>								
Distribution of haemorrhage	0	0.0	0	0.0	0	0.0	1	100.0
<b>Peribronchiolar interstitium</b>								
Distribution of Haemorrhage	0	0.0	1	100.0	0	0.0	0	0.0
<b>Bronchiolar lumen</b>								
Distribution of Haemorrhage	4	57.1	3	42.9	0	0.0	0	0.0

Autolysis was minimal in all the 11 samples. Congestion/hyperaemia was absent in 3/11 (27.3%) of cases while congestion was mild in 6/11 (54.5%) and moderate in 2/11 (18.2%) of cases.

Within the alveolar walls, the inflammatory cell infiltrate, apoptosis and microvascular endothelial activation was scored along with presence or absence of thrombosis. Monocyte-macrophage infiltration was severe in 2/11 (18.2%) of cases, moderate in 2/11 (18.2%), mild in 6/11 (54.5%) and absent in 1/11 (9.1%). Lymphocytes were moderate in 1/11 (9.1%), mild in 5/11 (45.5%) and absent in 5/11 (45.5%). Plasma cells were mild in 2/11 (18.2%) and absent in 9/11 (81.8%) of cases. Neutrophils and eosinophils were completely absent in all 11 cases. Cell death was moderate in 1/11 (9.1%), mild in 8/11 (72.7%) and not visible in 2/11 (18.2%) of cases. Nuclear hypertrophy/activation was severe in 2/11 (18.2%), moderate in 6/11 (54.5%) and mild in 3/11 (27.3%). Thrombosis was present in 2/11 (18.2%) and absent in 9/11 (81.8%) of cases.

Similar inflammatory cell infiltration parameters were also evaluated in the alveolar lumens along with fibrin, haemorrhage, oedema and hyaline membrane formation. Monocyte-macrophage infiltrations were severe in 1/11 (9.1%), moderate in 5/11 (45.5%) and mild in 5/11 (45.5%) of cases. Neutrophils were mild in 2/11 (18.2%) and absent in 9/11 (81.8%) of cases. Lymphocytes, plasma cells and eosinophils were absent in all cases. Fibrin was severe in 1/11 (9.1%), moderate in 3/11 (27.3%), mild in 2/11 (18.2%) and absent in 5/11 (45.5%) cases. Alveolar haemorrhage was severe in 2/11 (18.2%), moderate in 2/11 (18.2%), mild in 5/11 (45.5%) and absent in 2/11 (18.2%) cases. Additionally, haemorrhage was multifocal in 7/9 (77.8%), coalescing in 1/9 (11.1%) and diffuse in 1/9 (11.1%) cases in the histology sections. Oedema was severe in 8/11 (72.7%), moderate in 1/11 (9.1%) and mild in 2/11 (18.2%) cases. True hyaline membranes were not seen in any of the cases.

The perivascular interstitium was also evaluated for inflammatory cell infiltration, fibrin, haemorrhage, oedema, microvascular endothelial cell activation as well as lymphatic distension. Monocyte-macrophages infiltration was moderate in 2/11 (18.2%), mild in 3/11 (27.3%) and absent in 6/11 (54.5%) cases. Lymphocytic infiltration was moderate in 2/11 (18.2%), mild in 3/11 (27.3%) and absent in 6/11 (54.5%) cases. Plasmacytic infiltration was mild in 4/11 (36.4%) and absent in 7/11 (63.6%) cases. Neutrophils and eosinophils were absent in all cases. Fibrin exudation was mild in 2/11 (18.2%) and absent in 9/11 (81.8%) cases. Haemorrhage was mild in 2/11 (18.2%) and absent in 9/11 (81.8%). Distribution of haemorrhage was multifocal in both cases. Oedema was severe in 1/11 (9.1%), moderate in 3/11 (27.3%), mild in 6/11 (54.5%) and absent in 1/11 (9.1%) cases. Endothelial cell nuclear hypertrophy/activation was and severe in 1/11 (9.1%), moderate in 6/11 (54.5%) and mild in 4/11 (36.4%) cases. Lymphatic vessel dilation was absent in all but 1/11 (9.1%) in which it was mild.

The subpleural interstitium was evaluated for cellular infiltrate, fibrin, haemorrhage, oedema and mesothelial activation. No monocytes-macrophages, lymphocytes, plasma cells, neutrophils or eosinophils were present. Fibrin exudation was moderate in 1/11 (9.1%) and absent in 10/11 (90.9%) cases. Haemorrhage was absent in 10/11 (90.9%) and moderate in 1/11 (9.1%) cases which was multifocal. Oedema was mild in 5/11

(45.5%) and absent in 6/11 (54.5%) cases. Pleural mesothelial activation was only seen in 1/11 (9.1%) cases.

The peribronchiolar interstitium was also evaluated for cell infiltrate, fibrin, haemorrhage, oedema and anthracosis. Monocyte-macrophages, lymphocytes, plasma cells, neutrophils and eosinophils were absent in all cases. Fibrin was mild in (1/11) 9.1% and absent in 10/11 (90.9%) cases. Haemorrhage was absent in 10/11 (90.9%) and mild in (1/11) 9.1 % cases and the distribution was multifocal. Oedema was absent in all cases. Anthracosis was present in 5/11 (45.5%) and absent in 6/11 (54.5%) cases.

The bronchiolar lumens were evaluated for cell infiltrate, fibrin, haemorrhage and oedema. Monocyte-macrophages were mild in 1/11 (9.1%) and absent in 10/11 (90.9%) cases. No lymphocytes, plasma cells, neutrophils or eosinophils were present. No fibrin exudate was visible either. Haemorrhage was absent in 4/11 (36.4%) and mild in 7/11 (63.6%) cases and the distribution was focal in 4/7 (57.1%) and multifocal in 3/7 (42.9%) cases.

### 4.3. Immunohistochemistry

#### 4.3.1. Control cases

Immunohistochemistry was performed on the control cases and the results are summarised in table 9.

**Table 9:** Immunohistochemistry control cases score summary sheet

Marker	Region	Average number of positive cells / HPF	Standard Deviation	Minimum	Max
CD20	Alveolar	0	0.0	0	0
	Alveolar wall	0	0.0	0	0
	Peribronchial	0	0.0	0	0
CD3	Alveolar	0	0.0	0	0
	Alveolar wall	0	0.0	0	0
	Peribronchial	0	0.5	0	1
MUM-1	Alveolar	0	0.2	0	0
	Alveolar wall	0	0.4	0	1
	Peribronchial	0	0.0	0	0
CD204	Alveolar	7	4.7	3	12
	Alveolar wall	5	4.2	1	10
	Peribronchial	0	0.8	0	1
PAX-5	Alveolar	0	0.0	0	0
	Alveolar wall	0	0.0	0	0
	Peribronchial	0	0.0	0	0
MAC387	Alveolar	1	0.6	0	1
	Alveolar wall	9	5.9	3	15
	Peribronchial	3	3.6	0	7

Based on the control group, the following normal distributions were established using an average over all 4 cases with one standard deviation in each of the three regions of interest.

There were virtually no CD20-positive B-lymphocytes and normal plasma cells per 400X high power field (HPF) in either alveolar lumens, alveolar walls or peribronchial regions. There were scarce to any CD3 positive T-lymphocytes in the alveolar lumens and alveolar wall region, but the standard deviation was 0.5 in the peribronchial regions. Therefore, anything up to 1 CD3 positive T-lymphocyte per HPF was considered normal. There were no Mum-1 positive mature B-lymphocytes or plasma cells in the alveoli but they were present in the alveolar walls and peribronchial regions. The standard deviation was 0.4 in the alveolar wall and up to 1 Mum-1 positive mature B-cells and plasma may be seen per HPF in these regions. There was an average of 7 CD204 positive macrophages or dendritic cells per HPF in the alveoli with a standard deviation of 4.7. The normal ranges comprised between 3 and 12



CD204 positive macrophages and dendritic cells per HPF. The alveolar wall has an average of 5 CD204 positive macrophages and dendritic cells per HPF and a standard deviation of 4.2. The normal range was between 1 to 10 CD204 positive macrophages and dendritic cells per HPF. The peribronchial interstitium showed very few positive cells with 0 per HPF on average, but the standard deviation was 0.8, therefore, up to one CD204 positive macrophage and dendritic cell per HPF was considered normal. PAX-5 positive lymphocytes were extremely scarce and showed virtually no positive staining cells in any of the regions of interest. On average, there was 1 MAC387 positive leukocyte per HPF in the alveoli and the standard deviation was 0.6. Up to one MAC387 positive leukocyte per HPF may be considered normal. On average, there were 9 MAC387 positive leukocyte per HPF in the alveolar walls with a standard deviation of 5.9. The resulting a normal range is from 3 to 15 MAC387 positive leukocytes per HPF. On average, there were 3 MAC387 positive leukocytes per HPF in the peribronchiolar regions with a standard deviation of 3.6. Therefore, normal range is between 0 and 7 MAC387 positive leukocytes per HPF.

VCAM-1 immunohistochemistry was also performed on the control sections which showed strong positive staining of the endothelium in the alveolar capillaries forming almost parallel lines in a diffuse distribution.

### 4.3.2. Naturally infected *B. rossi* cases

#### 4.3.2.1. CD20

The CD20 immunohistochemistry results are summarised in Table 10.

**Table 10:** Summary of CD20 immunohistochemistry results in dogs naturally infected with *B. rossi*.

		Case Average positive cells / HPF	Control Range	
			Min	Max
Case 1	Alveolar	4.4	0	0
	Alveolar wall	0.2	0	0
	Peribronchial	1	1	1
Case 2	Alveolar	2.4	0	0
	Alveolar wall	0	0	0
	Peribronchial	1	1	1
Case 3	Alveolar	7.4	0	0
	Alveolar wall	0	0	0
	Peribronchial	0.8	1	1
Case 4	Alveolar	1.8	0	0
	Alveolar wall	7.6	0	0
	Peribronchial	0.8	1	1
Case 5	Alveolar	1	0	0
	Alveolar wall	0.4	0	0
	Peribronchial	0	1	1
Case 6	Alveolar	0.8	0	0
	Alveolar wall	2.4	0	0
	Peribronchial	0.6	1	1
Case 7	Alveolar	1.8	0	0
	Alveolar wall	6.2	0	0
	Peribronchial	0.6	1	1
Case 8	Alveolar	3.6	0	0
	Alveolar wall	6.4	0	0
	Peribronchial	0.2	1	1
Case 9	Alveolar	0.8	0	0
	Alveolar wall	3.8	0	0
	Peribronchial	0.2	1	1
Case 10	Alveolar	0.2	0	0
	Alveolar wall	0.2	0	0
	Peribronchial	0	1	1
Case 11	Alveolar	0	0	0
	Alveolar wall	0.6	0	0
	Peribronchial	0.2	1	1
Total average	Alveolar	2.2	0	0
	Alveolar wall	2.5	0	0
	Peribronchial	0.5	0	1

There were 0 to 7.4 CD20 positive B-lymphocytes and plasma cells per HPF with an average of 2.2 in the alveoli (Figure 29) which is a 2.2× increase compared to the controls (Figure 29) in this region. The alveolar walls ranged from 0 to 7.6 positive B-lymphocytes and plasma cells per HPF with an average of 2.5 which is 2.5× increase compared to the controls (Figure 29). In the peribronchial regions, there were between 0 and 1 positive B-lymphocytes and plasma cells with an average of 0.5 and this falls within the ranges observed in the control group.

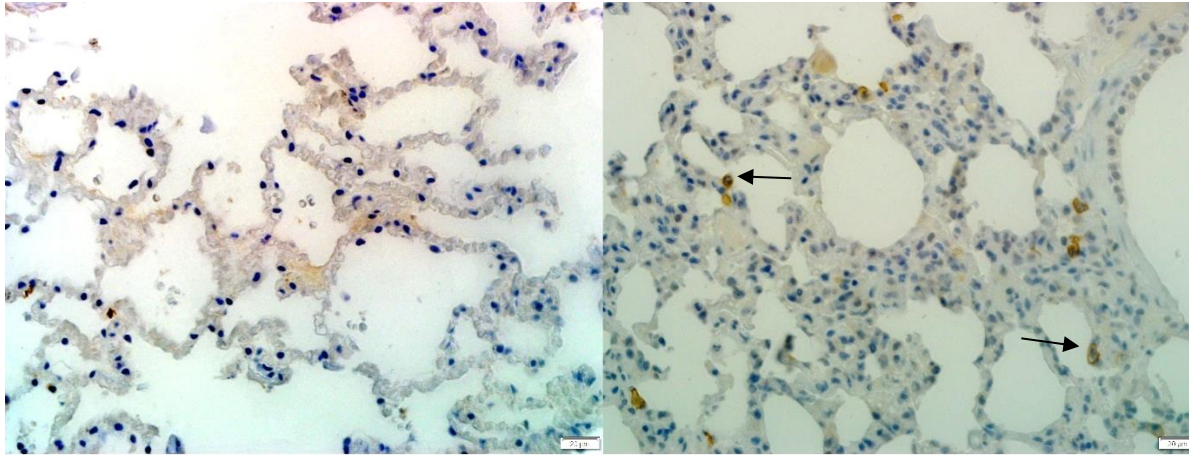


**Figure 29:** **Left.** CD20 control section. **Right.** Case 7. CD20 positive B-lymphocytes and plasma cells within the alveoli and alveolar walls (arrows). 400× magnification.

#### 4.3.2.2. CD3

The CD3 immunohistochemistry results are summarised in table 11.

**Table 11:** Summary of CD3 immunohistochemistry in the lungs of dogs naturally infected *B. rossi*.

		Case Average positive cells / HPF	Control range	
			Min	Max
Case 1	Alveolar	0	0	0
	Alveolar wall	8.4	0	0
	Peribronchial	0.2	0	1
Case 2	Alveolar	0	0	0
	Alveolar wall	1.4	0	0
	Peribronchial	0.2	0	1
Case 3	Alveolar	0	0	0
	Alveolar wall	18.6	0	0
	Peribronchial	0.2	0	1
Case 4	Alveolar	0	0	0
	Alveolar wall	6.2	0	0
	Peribronchial	0	0	1
Case 5	Alveolar	0	0	0
	Alveolar wall	0	0	0
	Peribronchial	0	0	1
Case 6	Alveolar	0	0	0
	Alveolar wall	4	0	0
	Peribronchial	0.2	0	1
Case 7	Alveolar	0	0	0
	Alveolar wall	29.4	0	0
	Peribronchial	0	0	1
Case 8	Alveolar	0	0	0
	Alveolar wall	15.4	0	0
	Peribronchial	0.4	0	1
Case 9	Alveolar	0	0	0
	Alveolar wall	38.4	0	0
	Peribronchial	0	0	1
Case 10	Alveolar	0	0	0
	Alveolar wall	1.2	0	0
	Peribronchial	0	0	1
Case 11	Alveolar	0	0	0
	Alveolar wall	13.4	0	0
	Peribronchial	0	0	1
Total average	Alveolar	0.00	0	0
	Alveolar wall	12.40	0	0
	Peribronchial	0.11	0	1

Within the alveoli, there were no CD3 positive T-lymphocytes in any of the naturally infected cases, which correlates with the normal control cases (Figure 30). The alveolar walls possessed from 1.4 to 29.4 CD3 positive T-lymphocytes per HPF with an average of 12.4 (Figure 30). This is a 12.4× increase compared to the normal range established in the controls. Between 0 to 0.4 CD3 positive T-lymphocytes per HPF were seen in the peribronchial regions, which was within the normal range established in the controls.

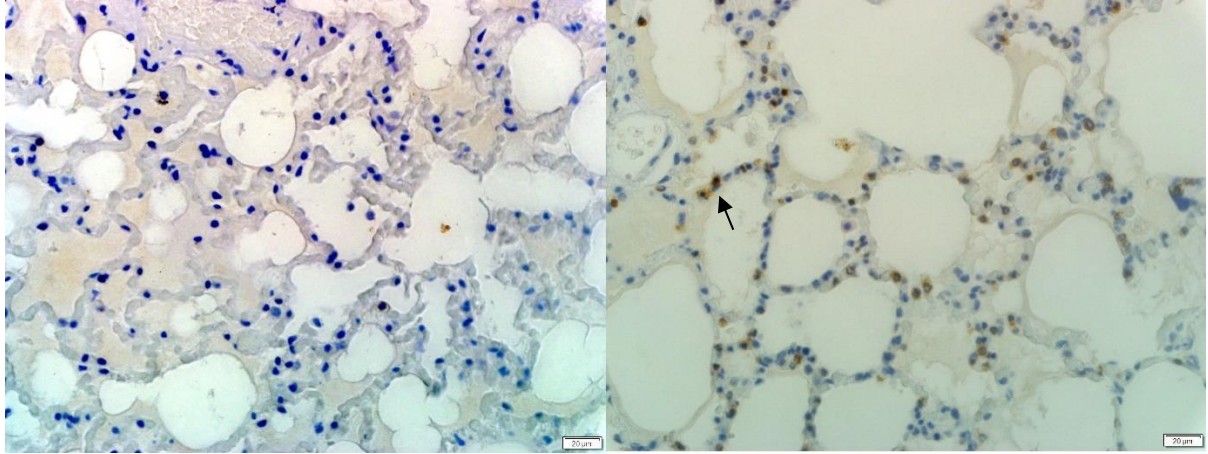


**Figure 30:** **Left.** CD3 control section. **Right.** Case 9. CD3 positive T-lymphocytes within the alveolar walls (arrow). 400× magnification.

### 4.3.2.3. Mum-1

The Mum-1 immunohistochemistry results are summarised in table 12.

**Table 12:** Summary of Mum-1 immunohistochemistry results in the lungs of dogs naturally infected with *B. rossi*.

		Case Average positive cells / HPF	Control range	
			Min	Max
Case 1	Alveolar	0	0	0
	Alveolar wall	0	0	1
	Peribronchial	0.2	0	0
Case 2	Alveolar	0	0	0
	Alveolar wall	0	0	1
	Peribronchial	0	0	0
Case 3	Alveolar	0	0	0
	Alveolar wall	5.2	0	1
	Peribronchial	2.8	0	0
Case 4	Alveolar	0	0	0
	Alveolar wall	1	0	1
	Peribronchial	1	0	0
Case 5	Alveolar	0	0	0
	Alveolar wall	0	0	1
	Peribronchial	0	0	0
Case 6	Alveolar	0	0	0
	Alveolar wall	0.4	0	1
	Peribronchial	0.2	0	0
Case 7	Alveolar	0	0	0
	Alveolar wall	5.2	0	1
	Peribronchial	2.2	0	0
Case 8	Alveolar	0	0	0
	Alveolar wall	5.4	0	1
	Peribronchial	0.6	0	0
Case 9	Alveolar	0	0	0
	Alveolar wall	0	0	1
	Peribronchial	0	0	0
Case 10	Alveolar	0	0	0
	Alveolar wall	0	0	1
	Peribronchial	0	0	0
Case 11	Alveolar	0	0	0
	Alveolar wall	0	0	1
	Peribronchial	0	0	0
Total average	Alveolar	0.0	0	0
	Alveolar wall	1.6	0	1
	Peribronchial	0.6	0	0

There were no Mum-1 positive mature B-lymphocytes and/or plasma cells in the alveolar lumens which correlates with the normal controls (Figure 31). The alveolar walls results range between 0 and 5.4 per HPF with an average of 1.6 which is a 0.6× increase compared to the controls (Figure 31). The peribronchial regions varied between 0 to 2.8 Mum-1 positive mature B-lymphocytes and/or plasma cells with an average of 0.6 which is a 0.6× increase over control cases.

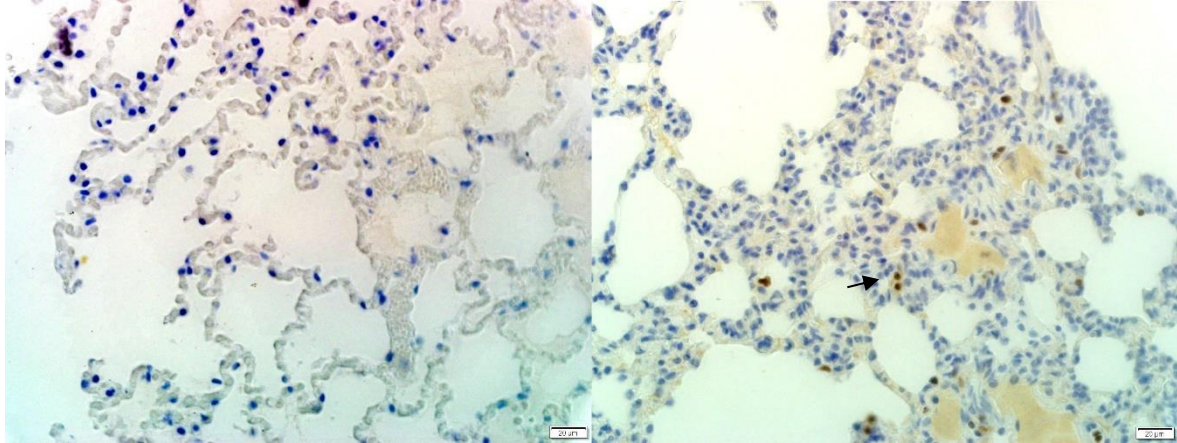


**Figure 31:** **Left.** Mum-1 control section. Absence of specific positive mature B-lymphocytes and plasma cells in the alveoli and alveolar walls. **Right.** Case 7. Scattered Mum-1 positive mature B-lymphocytes/plasma cells within the alveolar walls (arrow). 400× magnification.

#### 4.3.2.4. CD204

The CD204 results are summarised in table 13.

**Table 13:** Summary of CD204 Immunohistochemistry results in dogs naturally infected with *B. rossi*.

		Case Average positive cells / HPF	Control range	
			Min	Max
Case 1	Alveolar	7.6	0	2
	Alveolar wall	0.2	0	0
	Peribronchial	0	0	1
Case 2	Alveolar	4.6	0	2
	Alveolar wall	4	0	0
	Peribronchial	0.2	0	1
Case 3	Alveolar	12.2	0	2
	Alveolar wall	4.2	0	0
	Peribronchial	0	0	1
Case 4	Alveolar	5	0	2
	Alveolar wall	8.6	0	0
	Peribronchial	0.2	0	1
Case 5	Alveolar	5.8	0	2
	Alveolar wall	3.4	0	0
	Peribronchial	0	0	1
Case 6	Alveolar	10	0	2
	Alveolar wall	11.2	0	0
	Peribronchial	1.2	0	1
Case 7	Alveolar	0	0	2
	Alveolar wall	0.4	0	0
	Peribronchial	0	0	1
Case 8	Alveolar	11	0	2
	Alveolar wall	7.2	0	0
	Peribronchial	0.6	0	1
Case 9	Alveolar	6.8	0	2
	Alveolar wall	5.2	0	0
	Peribronchial	0	0	1
Case 10	Alveolar	10.6	0	2
	Alveolar wall	2.4	0	0
	Peribronchial	1.2	0	1
Case 11	Alveolar	8	0	2
	Alveolar wall	12	0	0
	Peribronchial	0.6	0	1
Total average	Alveolar	7.4	0	2
	Alveolar wall	5.3	0	0
	Peribronchial	0.4	0	1



The number of CD204-positive macrophages and/or dendritic cells in alveoli ranged from 0 to 12.2 per HPF with an average of 7.4 which is a 3.9× increase compared to the normal controls (Figure 32). The alveolar wall scores ranged from 0.2 to 12 per HPF with an average of 5.3 which is a 5.3× increase compared to the normal controls (Figure 32).

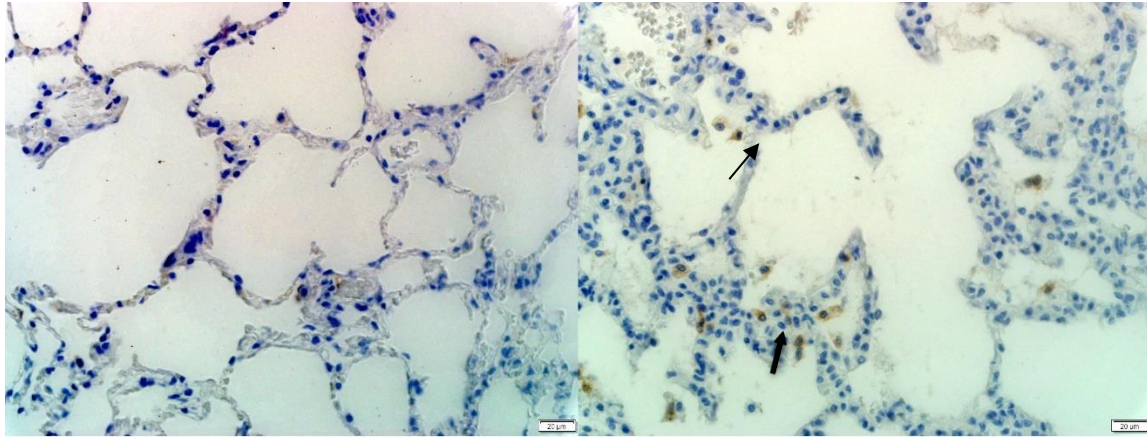


**Figure 32:** **Left.** CD204 control section. **Right.** Case 8. CD204 positive alveolar macrophages in the alveoli (thin arrow) and positive macrophages/dendritic cells in the alveolar walls (thick arrow). 400× magnification.

#### 4.3.2.5. PAX5

The PAX-5 immunohistochemistry is summarised in table 14.

**Table 14:** Summary of Pax-5 immunohistochemistry results in the lungs of dogs naturally infected with *B. rossi*.

		Case Average positive cells / HPF	Control range	
			Min	Max
Case 1	Alveolar	0	0	0
	Alveolar wall	0	0	0
	Peribronchial	0	0	0
Case 2	Alveolar	0	0	0
	Alveolar wall	0	0	0
	Peribronchial	0	0	0
Case 3	Alveolar	0	0	0
	Alveolar wall	0	0	0
	Peribronchial	0	0	0
Case 4	Alveolar	0	0	0
	Alveolar wall	0	0	0
	Peribronchial	0	0	0
Case 5	Alveolar	0	0	0
	Alveolar wall	0	0	0
	Peribronchial	0	0	0
Case 6	Alveolar	0	0	0
	Alveolar wall	0	0	0
	Peribronchial	0	0	0
Case 7	Alveolar	0	0	0
	Alveolar wall	0	0	0
	Peribronchial	0	0	0
Case 8	Alveolar	0	0	0
	Alveolar wall	0	0	0
	Peribronchial	0	0	0
Case 9	Alveolar	0	0	0
	Alveolar wall	0	0	0
	Peribronchial	0	0	0
Case 10	Alveolar	0	0	0
	Alveolar wall	0	0	0
	Peribronchial	0	0	0
Case 11	Alveolar	0	0	0
	Alveolar wall	0	0	0
	Peribronchial	0	0	0
Total average	Alveolar	0	0	0
	Alveolar wall	0	0	0
	Peribronchial	0	0	0

There were no Pax-5 specific positive B-lymphocytes were observed in any of the regions of interest which corresponds to the controls (Figure 33).

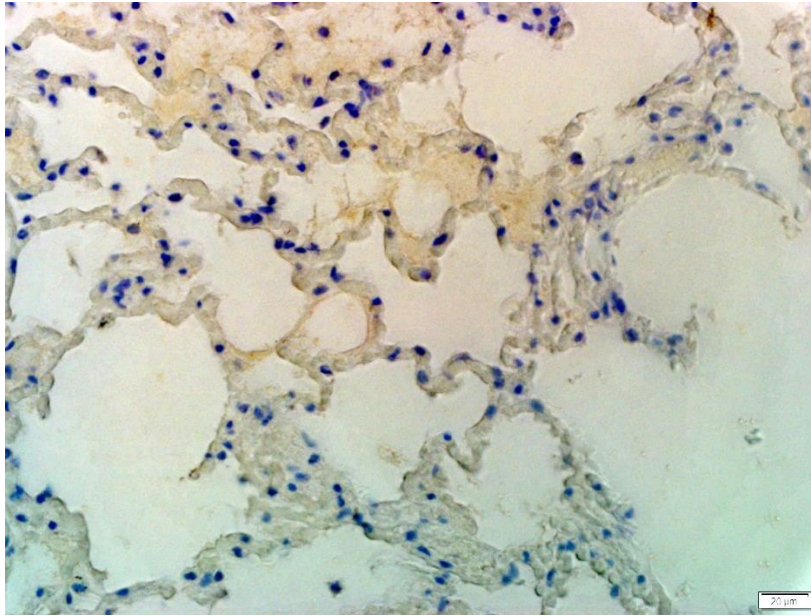


**Figure 33:** Control. Pax-5. 400× magnification

#### 4.3.2.6. MAC387

The MAC387 results are summarised in table 15.

**Table 15:** Summary of MAC387 immunohistochemistry results in the lungs of dogs naturally infected with *B. rossi*.

		Case Average positive cells / HPF	Control range	
			Min	Max
Case 1	Alveolar	53.6	0	1
	Alveolar wall	26.2	3	15
	Peribronchial	4.4	0	7
Case 2	Alveolar	4	0	1
	Alveolar wall	75.2	3	15
	Peribronchial	5.6	0	7
Case 3	Alveolar	1.6	0	1
	Alveolar wall	64.8	3	15
	Peribronchial	1	0	7
Case 4	Alveolar	1.2	0	1
	Alveolar wall	62	3	15
	Peribronchial	1	0	7
Case 5	Alveolar	2.6	0	1
	Alveolar wall	46	3	15
	Peribronchial	0.4	0	7
Case 6	Alveolar	1.2	0	1
	Alveolar wall	65.8	3	15
	Peribronchial	2.2	0	7
Case 7	Alveolar	1.6	0	1
	Alveolar wall	60.2	3	15
	Peribronchial	1.6	0	7
Case 8	Alveolar	1.4	0	1
	Alveolar wall	140.4	3	15
	Peribronchial	1.4	0	7
Case 9	Alveolar	2.6	0	1
	Alveolar wall	55.2	3	15
	Peribronchial	1	0	7
Case 10	Alveolar	1.6	0	1
	Alveolar wall	58.8	3	15
	Peribronchial	1.2	0	7
Case 11	Alveolar	58.6	0	1
	Alveolar wall	0.8	3	15
	Peribronchial	0.8	0	7
Total average	Alveolar	11.8	0	1
	Alveolar wall	59.6	3	15
	Peribronchial	1.9	0	7

Within the alveoli, the MAC387 positive bone marrow derived monocytes-macrophages and scarce neutrophils ranged from 1.2 to 58.6 per HPF with an average of 11.8 which is 10.8× above the normal range established in the controls (Figure 34). The alveolar walls ranged between 0.8 to 140.4 with an average of 59.6 which is a 4×increase compared to the normal controls (Figure 34). The peribronchial regions ranged between 0.4 and 4.4 with an average of 1.9 which falls within the normal range established in the control sections.

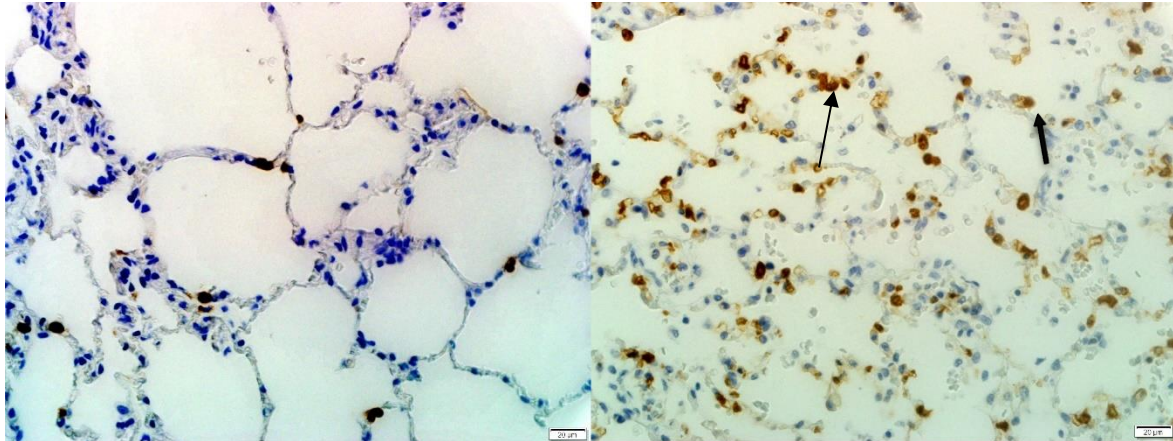


**Figure 34:** **Left.** MAC387 control section. **Right.** Case 2. MAC387 positive monocyte-macrophages and rare neutrophils within the alveolar walls (thin arrow) and alveoli (thick arrow). 400× magnification.

#### 4.3.2.7. VCAM-1

VCAM-1 immunohistochemistry was also performed. Across most cases, there was intense staining of VCAM-1 positive vascular endothelial cells in alveolar walls forming almost parallel lines in most instances. The staining pattern in the test cases was essentially similar to that in the controls (Figure 35). The naturally infected cases did show granular membranous positivity in intravascular mononuclear cells (Figure 35).

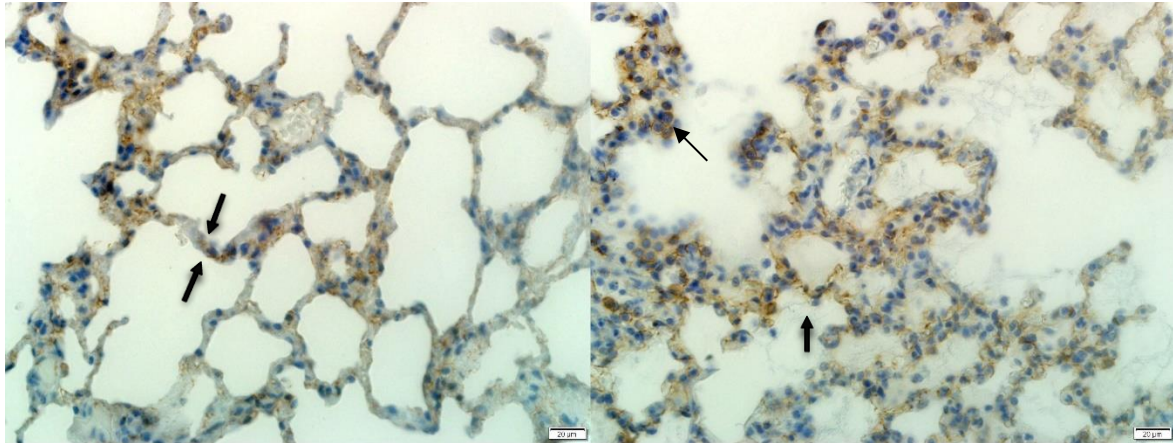


**Figure 35:** **Left.** VCAM-1 control section. Positive vascular endothelium in the alveolar walls (thick arrow). 400× magnification. **Right.** Case 9. VCAM-1 positive endothelial cells in the alveolar walls (thick arrows) as well granular and cytoplasmic membrane labelling of intravascular mononuclear cells (thin arrow). 400× magnification.

#### 4.3.2.8. Immunohistochemistry overview

The naturally infected *B. rossi* cases showed significant increases in MAC387 positive monocyte-macrophages and rare neutrophils, CD204 positive macrophages/dendritic cells and CD3 positive T-lymphocytes when compared to the normal control lungs. Milder increases in CD20 positive B-lymphocytes and plasma cells were also noted. The significant results are summarised in [Table 16](#).

**Table 16:** Summary of significant immunohistochemical results

		Average positive cells / HPF	Control range		Increase magnitude
			Min	Max	
<b>MAC387</b>	<b>Alveolar</b>	11.8	0.0	1.2	10.8x increase
	<b>Alveolar wall</b>	59.6	3.0	14.8	44.6x increase
	<b>Peribronchial</b>	1.9	0.0	7.0	Normal
<b>CD204</b>	<b>Alveolar</b>	7.4	0.0	1.9	3.9x increase
	<b>Alveolar wall</b>	5.3	0.0	0.4	5.3x increase
	<b>Peribronchial</b>	0.4	0.0	1.1	Normal
<b>CD3</b>	<b>Alveolar</b>	0.0	0.0	0.0	Normal
	<b>Alveolar wall</b>	12.4	0.0	0.0	12.4x increase
	<b>Peribronchial</b>	0.1	0.0	0.7	Normal
<b>CD20</b>	<b>Alveolar</b>	2.2	0.0	0.0	2.2x increase
	<b>Alveolar wall</b>	2.5	0.0	0.0	2.5x increase
	<b>Peribronchial</b>	0.5	0.4	0.9	Normal

## 5 CHAPTER FIVE: DISCUSSION

### 5.1. Macroscopic pathology

At the macroscopic level, there was some variability but most cases in this series showed moderate to severe multifocal pulmonary haemorrhages. Petechial and subpleural ecchymotic haemorrhages were also occasionally noted but not consistently. Severe pulmonary oedema, as evidenced by oozing of fluid on cut section as well as copious, often blood tinged, tracheal froth was present as well. Consequently, the lungs were often heavy with a slightly increased consistency. Acute interstitial pneumonia with oedema, congestion and multifocal haemorrhage was reported in 16 of 25 (64%) post mortems conducted the largest case series of *B. rossi* infected dogs<sup>53</sup>. It also showed pleural and pericardial effusions in 9/25 (36%) and 4/25 (16%) of cases on post mortem<sup>53</sup>. That study only evaluated macroscopic post-mortem changes and an older study that demonstrated the multisystemic nature of the disease in 91 complicated cases of the disease, 32 died (35%) and 18 of 91 (20%) died due to respiratory failure<sup>103</sup>. Although it was not evaluated as part of this study, arterial blood gas analysis evaluating acid-base and lung function has been studied in *B. rossi* infection, the classic findings of ARDS were not commonly diagnosed<sup>54</sup>. This was probably due to the fact that the time of arterial blood collection in these cases was many hours before death whilst ARDS (associated with widespread alveolar flooding and tracheal foam) appears to be a terminal event. ALI seems very common as many cases dying of organ failures in complicated canine babesiosis other than lung failure, demonstrate pulmonary pathology consistent with ALI<sup>54</sup>. The most common blood gas disturbance seen in severe disease is respiratory alkalosis mixed with metabolic acidosis which is consistent with primary metabolic and pulmonary pathology<sup>54</sup>.

The described changes were similar to the macroscopic pathology noted in human malaria-associated ARDS where severe oedema and intrapulmonary haemorrhages were described<sup>89</sup>. ARDS has been described in 8% of 139 cases of human *B. microti* infection<sup>104</sup>. Murine malaria-associated ARDS in C57BL/6J mice infected with *Plasmodium berghei* NK65 showed petechial haemorrhages<sup>95</sup>. The pathology noted in a murine model of babesia associated ALI/ARDS in C3H/HeN mice infected with WA-1 babesia shows petechiations with serosanguinous fluid in the trachea and bronchi<sup>32</sup> which is similar to the haemorrhage and pulmonary oedema noted in canine babesiosis.

### 5.2. Histopathology

In general, the histopathological sections all showed multifocal haemorrhages and severe pulmonary oedema correlating with the macroscopic findings. The inflammatory population was predominantly mononuclear macrophages as determined by MAC387 and CD204 immunohistochemistry. The inflammation was seen predominantly in the



alveolar walls with a 4× increase in MAC387 positive cells and 5.3× in CD204 positive cells compared to normal controls.

### **5.2.1. Pulmonary oedema, endothelial cell activation and VCAM-1**

Severe oedema was present in 72.7% of cases, moderate in 9.1% and mild in 18.2% of cases. Pulmonary oedema is the most consistent feature of babesia-associated ARDS. This correlates with the human-malaria associated ARDS<sup>89</sup>, murine model of MA-ARDS C57BL/6j<sup>95</sup> mice infected with *Plasmodium berghei* and murine model of babesiosis, C3H/HeN mice infected with WA-1 babesia<sup>31,32</sup>.

The pathogenesis of the pulmonary oedema is classified as non-cardiogenic meaning that there is no indication of pulmonary hypertension or increased hydrostatic pressure associated with congestive heart failure<sup>105</sup>. This implies a breakdown in the blood-air barrier probably as result of disruption of the endothelial cell layer, pneumocyte layer or both. Endothelial activation and injury would be the most logical triggering mechanism especially in this study.

In this study, endothelial activation was present in all cases, being moderate in 54.5% of cases, mild in 27.3% of cases and severe in 18.2% of cases. Since direct injury by *B. rossi* parasites is unlikely as they have no mechanism to directly affect vascular endothelium, the injury was likely mediated by pro-inflammatory cytokines released from activated macrophages (IL-8, IL2, TNF-α etc.). This has been shown in circulation in *B. rossi* infections previously<sup>52,27</sup>. In human medicine, cases of sepsis can also display ALI/ARDS<sup>36</sup> which is ascribed to pulmonary endothelial cell dysfunction. TNF-α and other mediators induce cytoskeletal contraction and increase vascular permeability<sup>61</sup> thus contributing to the pulmonary oedema observed in all cases of ALI/ARDS. The tight junctions between adjacent endothelial cells prevent neutrophil migration and vascular leakage<sup>51</sup>. One of the major components of the this tight junction is Vascular-Endothelial-cadherin (VE-Cadherin) which forms complexes between adjacent endothelial cells<sup>51</sup>. Endocytosis of the VE-cadherin during sepsis results in gaps between the endothelial cells which can increase permeability<sup>51</sup> and also contribute to pulmonary oedema formation. Another potential mechanism to increase paracellular gaps is high-mobility group box-1 protein (HMGB-1)<sup>69</sup>. This is a proinflammatory mediator which induces expression of VCAM-1 and ICAM-1<sup>25</sup>. One study found an increase in plasma HMGB-1 in dogs infected with babesiosis compared to healthy dogs at admission and again at 6 days after treatment<sup>49</sup>. Additionally, this study also found an increase in serum VCAM-1 concentrations at admission in dogs with complicated babesiosis compared to uncomplicated presentation<sup>49</sup>. It seems likely therefore that an increase in these pro-inflammatory mediators may also be involved in destabilisation of the pulmonary endothelial layer in canine babesia-associated ALI/ARDS.

The VCAM-1 antigen is expressed on activated endothelial cells and it facilitates leukocyte migration and is upregulated by TNF-α<sup>107</sup> and HMGB-1<sup>25</sup>. It is important in the cyto-adherence of malaria-infected red blood cells to endothelial cells in the lungs and central nervous system of humans<sup>71,108</sup> and in mice<sup>23</sup>. In this study however, there was no clear difference in staining pattern between the controls and experimental cases but of interest, was the visible granular staining noted on the cytoplasmic

membranes of intravascular mononuclear cells in the infected dog lungs. Research has shown that VCAM-1 can be expressed on cells other than endothelium eg. tissue macrophages, dendritic cells and even Kupfer cells in the liver in human patients<sup>47</sup> which may explain this finding. This might also explain the increase in serum VCAM-1 levels noted by Kuleš et al<sup>49</sup> but this requires further investigation.

Serum proinflammatory cytokine profiles have been performed on blood from dogs infected with *B. rossi*<sup>27,52</sup>. One study showed significant differences between IL-6, IL-8, IL-10, Monocytic Chemotactic factor-1(MCP-1) and TNF- $\alpha$ <sup>52</sup>, while another found significant differences between IL-10 and MCP-1 between infected and healthy dogs<sup>27</sup>. IL-6, MCP-1 and TNF- $\alpha$  levels were significantly higher in dogs that died compared to those that survived<sup>52,27</sup>. IL-8 levels appeared to decrease in infected cases<sup>27,52</sup>. Another study also showed an increase in serum C-reactive protein, soluble ICAM-1 and von Willbrand factor<sup>8</sup>. This confirms a pro-inflammatory cytokine milieu but does not identify a single factor or consistent constellation of factors that are responsible for or correlated with complicated cases. A multifactorial pathogenesis seems likely.

The endothelial glycocalyx may be worthy of further investigation in *B. rossi* infected dogs with ALI/ARDS. It is an important regulator of endothelial barrier function<sup>61</sup> and in cases of human sepsis, leukocytes do interact with and degrade this layer<sup>79</sup>. Further investigation will require ultrastructural examination of the alveolar walls.

## **5.2.2. Inflammatory cell population**

### **5.2.2.1. Monocyte-macrophages**

Monocyte-macrophages were the predominant cell population noted in the regions of interest. Within the alveolar walls, monocyte-macrophage infiltration was severe in 18.2%, moderate in 18.2%, mild in 54.5% and absent in 9.1%. Within the alveolar lumen macrophages were severe in 9.1% of cases, moderate in 45.5% and mild in 45.5%. A severe mononuclear leukostasis was noted in the cases as well and there were often rafts of adhered mononuclear cells present in the larger bronchial vasculature. Most cases showed a moderate to severe increase in the interstitium and within the alveolar capillaries, which was associated with an increased alveolar wall thickness. Further classification of this cell population was performed with CD204 and MAC387 immunohistochemistry.

CD204 is expressed in resident and tissue macrophages as well as dendritic cells<sup>45</sup>. CD204 immunohistochemistry for macrophages/dendritic cells showed an increase in alveolar macrophages of 7.4 $\times$  over the normal controls as well as 5.3 $\times$  and 0.4 $\times$  increase in the alveolar walls and peribronchial regions respectively. The results suggest that during canine babesia-related ALI/ARDS, there is a noteworthy increase in these cells, especially in the alveolar lumen and alveolar wall. Since this is a marker of resident and tissue macrophages, there is clear stimulation of these cells to proliferate in situ and there was a noticeable increase in mitotic frequency in some cases. The source of the stimulation is probably proinflammatory cytokine related and is further discussed below.

MAC387 labels myeloid/histiocyte antigens expressed by circulating and tissue neutrophils, monocytes and reactive tissue macrophages and eosinophils but not dendritic cells<sup>9</sup>. MAC387 immunohistochemistry for bone marrow-derived monocyte-macrophages and polymorphonuclear leukocytes showed a major 10.8× increase compared to the controls in the alveolar lumen and a 4× increase in the alveolar walls compared to the controls. Since neutrophils were minimally observed in the samples, most of these cells were probably bone marrow derived circulating histiocytes. There was clearly significant extravasation of these cells into the alveolar lumens, likely in response to alveolar wall injury and subsequent haemorrhage, fibrin exudation and oedema. Their presence within the alveolar walls also may indicate a role in the immune reaction. They are an important source of cytokines for activation of the acute inflammatory response as a component of the innate immune system and also trigger the adaptive immune response<sup>109</sup>.

In most cases of ARDS, activation of alveolar macrophages with subsequent release of pro-inflammatory cytokines (IL-1, IL-8, TNF- $\alpha$  etc) is considered an essential step in the pathogenesis<sup>101,102</sup>. It is unclear how intravascular haemoprotozoan parasites such as *Babesia rossi* or *Plasmodium falciparum* cause activation of these alveolar macrophages but given that there are activated monocytes within the intravascular compartment, proinflammatory cytokine release from these cells is highly likely. There may be spill over into the alveolar compartment along with likely endothelial cell activation and possible injury, leading to oedema, fibrin exudation and subsequent activation of alveolar macrophages. Another possibility is that the macrophages are not activated by the pro-inflammatory cytokines directly, but are triggered by the haemorrhage, fibrin and pulmonary oedema which was consistently observed in these cases in a futile attempt to clean up the spillage and restore function. This seems less likely given that a pro-inflammatory cytokine milieu is noted in babesia cases<sup>52,27</sup>. Of interest, increased bronchial interleukin-33 expression and decreased  $\gamma$ -epithelium sodium channel was noted in human cases of severe malaria with pulmonary oedema<sup>4</sup> and it may be of use to investigate these markers in canine babesiosis as well.

In a murine model of malaria-associated ARDS C57BL/6j mice infected with *Plasmodium berghei*, interstitial oedema and leukocyte infiltration was present on Day 8. By Day 10 eosinophilic hyaline membranes were present<sup>95</sup>. The type of leukocyte encountered in the murine model were not established but are likely to be mononuclear cells similar to that seen in canine babesia-associated ARDS. The oedema was also consistent between the two species. It is interesting that the dominant inflammatory cell response in classical human ALI/ARDS is the neutrophil (where bacteria and trauma are the most common triggers<sup>63</sup>). This draws a clear distinction between the pathogenesis of a hemoprotozoa macrophagic inflammation as an ARDS trigger and the more common triggers observed in humans.

#### **5.2.2.2. T-lymphocytes**

Although 45.5% of cases showed no visible lymphocytes, 45.5% of cases showed mild lymphocyte infiltration while 9.1% showed moderate infiltration. Together, the, CD3

and CD20 immunohistochemistry showed significantly more lymphocytes than initially observed with H&E staining. This suggests that lymphocytes may play a role in the interstitial inflammatory response in canine babesiosis.

CD3 immunohistochemistry for T-lymphocytes showed a major 12.4× increase in CD3-positive T-lymphocytes in the alveolar walls. This suggests that T-lymphocytes may be playing a significant role in the inflammation. T-lymphocytes are an essential component in cell-mediated immunity and may be activated in two ways (possibly occurring via the classical pathway with T-helper 1 (T<sub>h</sub>1) cells releasing IL-2 or IFN-λ or alternatively, but less likely via T-helper 2 (T<sub>h</sub>2) macrophages<sup>109</sup>). Cytotoxic T-lymphocytes (CTL) are also activated via the T<sub>h</sub>1 pathway by the presentation of antigens on major histocompatibility complex-class I (MHC-1) with a co-stimulatory signal from an antigenic presenting cell<sup>82</sup>. Activated CTL's can release perforins and granzymes inducing apoptosis in targeted cells and thus may be cause of the apoptosis (noted in some cases) but may also directly damage the vascular endothelium. The major increase in T-lymphocytes is interesting. In a recent study evaluating the peripheral lymphocyte phenotype in dogs naturally infected with *Babesia rossi*, dogs with complicated babesiosis showed a drop in CD3+ lymphocytes compared to cases with uncomplicated babesiosis<sup>77</sup>. The authors speculated that there may be functional immune suppression due to apoptosis or redistribution of the effector T-lymphocytes, or a combination of these and other mechanisms<sup>77</sup>. Although there was some apoptosis in these cases, the clear increase in T-lymphocytes in the pulmonary tissue suggests that redistribution of lymphocytes may be a significant cause of the drop in peripheral T-lymphocytes cells noted in the previous study. In the spleen of dogs affected by canine babesiosis, there was no significant difference in the T-lymphocyte populations in infected vs control cases<sup>33</sup>. It would stand to reason that the spleen, being the primary organ responsible for clearing haemoprotzoan parasites, would become hyperplastic and the lack of an appreciable increase in T-cells may be due to rapid redistribution or indeed may be due to accelerated apoptosis.

### **5.2.2.3. B-lymphocytes**

There was a 2.2× increase of CD20 positive B-cells and/or plasma cells compared to controls in the alveolar walls. Within the alveolar walls, there was 2.5× increase compared to the controls. Therefore, most cases of canine babesia-associated ALI/ARDS showed an increase in CD20+ cells.

These CD20 positive cells represented B-lymphocytes which with more chronic *Babesia rossi* infection, will likely mature into plasma cells to produce opsonising antibodies.

Mum-1 immunohistochemistry (which highlights mature B-cells especially plasma cells) showed a 0.6x increase on average within the alveolar walls and 0.6× increase in the peribronchial regions was not significant and was likely secondary to the overall inflammation. Meaning the majority of CD20+ cells were probably B-lymphocytes and not plasma cells. Pax-5 immunohistochemistry (which highlights immature B-

lymphocytes) was also performed and showed virtually no positive staining cells any of the regions of interest. B-lymphocytes would appear to be playing a minimally important role in the acute phase of this disease as the number of B-cell and plasma cells are raised slightly but not to the significance of T-cells. However suboptimal Pax-5 staining may also be a possibility to consider<sup>81</sup>.

#### **5.2.2.4. Neutrophils**

Only two cases showed mild neutrophil infiltration within the alveolar lumens, possibly secondary to fibrin exudation, endothelial injury and proinflammatory cytokines.

In the murine model of babesiosis, C3H/HeN mice infected with WA-1 babesia, there were plump endothelial cells with marginated mononuclear cells and neutrophils<sup>32</sup>. However, neutrophils were prominent in the murine model whereas they were mostly absent here. Neutrophils would not appear to be a major contributor to pulmonary injury caused by babesiosis in dogs. Their presence can indicate secondary bacterial infection/bronchopneumonia.

#### **5.2.2.5. Other inflammatory cells**

Mild perivascular lymphoplasmacytic infiltrates were also noted in a few samples but this is likely probably part of the overall general inflammation.

### **5.2.3. Haemorrhage, fibrin exudation**

While haemorrhage was mild in 45.5% of cases, severe in 18.2% of cases, moderate in 18.2% of cases and severe in 18.2% of cases. The distribution of haemorrhage was multifocal in 77.8%, coalescing in 11.1% and diffuse in 11.1%. Most cases showed some form of haemorrhage which corresponds with the macroscopic pathology.

Fibrin exudation into the alveolar lumen was absent in 45.5%, moderate in 27.3% , mild in 18.2% and severe in 9.1% of cases. Fibrin exudation is seen in approximately half of cases although why it is seen less than haemorrhage is not clear. It is possible that some of the dogs were also in disseminated intravascular coagulation<sup>28</sup> (another potential complication of *Babesia rossi* infection) and that severe coagulation factor depletion (through consumption) left insufficient to cleave fibrinogen. Alternatively, there was activation of the fibrinolytic system causing fibrinolysis and dissolution.

### **5.2.4. Thrombosis and other intravascular findings**

Although not a prominent finding, two of the cases (18.2%) did show evidence of intravascular thrombosis. Hypercoagulability is another potential complication of canine babesiosis<sup>56,28</sup>, but it is uncertain if this thrombosis was secondary to the pulmonary injury, induced hypercoagulability or a combination of both. A scintigraphic

perfusion study of the lungs of uncomplicated cases of *B. rossi* infection also did not demonstrate obvious pulmonary thromboembolic disease<sup>88</sup>.

Intra-erythrocytic *Babesia* parasites were visible in two cases but others showed no evidence of parasitaemia, this was likely due to anti-babesial treatment as the parasitaemia clears within 24 hours of diminazine aceturate treatment<sup>41</sup>. Occasional intravascular megakaryocytes were also noted but this is not uncommon with systemic infections due to bone-marrow hyperplasia and shifting of immature blastic cells into systemic circulation. Large, immature blastic cells were also noted within the interstitium and intravascular compartments.

Vascular congestion or hyperaemia was judged to be mild in 54.5%, moderate in 18.2%, and absent in 27.3% of cases. This is likely as a result of inflammatory cytokine release (ie. more consistent with hyperaemia), cardiac failure or a combination. This could link with myocardial haemorrhages common in fatal cases as well as elevated cardiac troponin levels which have also been reported, especially in complicated disease<sup>57</sup>.

#### **5.2.5. Cell death**

Cell death noted in the alveolar walls and alveolar lumen was mild in 72.7%, absent in 18.2% and moderate in 9.1% of cases. The cause of the cell death was also not clear, but given the highly activated nature of the monocyte-macrophages and lymphocytes, it is likely apoptosis from a combination of the intrinsic/mitochondrial pathway (due to cell injury from phagocytosis of oedema, erythrocytes and fibrin) and extrinsic/death receptor pathway (cytokine release from activated intravascular monocytes such as TNF- $\alpha$ )<sup>109</sup>. Apoptosis/cell death was not obvious within the endothelial cells in these cases but death of the endothelium is certainly a potential mechanism for the development of pulmonary oedema in ALI/ARDS in sepsis<sup>63</sup>. There are currently in-depth investigations into the pathophysiology of apoptosis, especially in human and animal models of sepsis. These studies showed that LPS treated macrophages released microparticles that contain caspase-1 as well as gasdermin-D which have the capacity to cause endothelial cell apoptosis<sup>78,66</sup>. In the current study, monocytes-macrophages were the main inflammatory cells noted within the interstitium and intravascular compartment and there may well be similarities between babesia-related ALI/ARDS and human sepsis and even MA-ALI/ARDS but further work is necessary, especially ultrastructural examination of the endothelium and inter-endothelial junctions.

#### **5.2.6. Other lesions**

The following lesions were only minor or inconsistent findings in the case series or were found to be absent.

##### **5.2.6.1. Perivascular interstitium**

Looking at the perivascular interstitial compartment, the cell infiltrate was mild to moderate and consisted mostly of monocytes and macrophages as well as lymphocytes and the occasional plasma cell. Monocyte-macrophages were mild in 27.3%, moderate

in 18.2% and absent in 54.5% of cases. Lymphocytes were mild in 27.3% and moderate in 18.2% and absent in 54.5% of cases. Plasma cells were mild in 36.4% and absent in 63.6% of cases. Fibrin and haemorrhage were mild in 18.2% of cases and absent in 81.8% while oedema was mild in 9.1% and absent in 9.1% of cases. The distribution of the haemorrhage was multifocal in 100% of cases with haemorrhage. The inflammatory component in this compartment likely represents reaction to the alveolar wall and alveolar lumen inflammation, which is further reinforced by the fact that microvascular endothelial activation was present in all cases, being moderate in 54.5%, mild in 36.4%, and severe in 9.1% of cases. Lymphatic vessel distension was only observed in 9.1% of cases.

#### **5.2.6.2. Bronchiolar lumens and peribronchiolar interstitium**

The bronchiolar lumens showed minimal change but 9.1% of cases showed mild monocyte-macrophage infiltration but there was more significant haemorrhage and oedema. 63.6% did show mild haemorrhage while 36.4% of cases showed no haemorrhage. Within the cases with haemorrhage, 57.1% showed focal and 42.9% multifocal lesions. There was no visible fibrin deposition. Oedema, as expected, was more significant with 63.6% showing mild, 18.2% moderate and 18.2% of cases showing no oedema. These changes are likely spillage from the alveolar lesions and are not primary. Anthracosis was present in 45.5% of cases but this was an incidental finding. Unremarkable changes were noted in the peribronchiolar interstitium with only 9.1% of cases showing mild haemorrhage and fibrin deposition with a multifocal distribution.

#### **5.2.6.3. Subpleural interstitium**

The subpleural interstitium was mostly unremarkable but 9.1% of cases did show moderate haemorrhage and fibrin deposition with a diffuse distribution. Mild oedema was noted in 45.5% of cases. 9.1% of samples did show hypertrophy of the pleural mesothelium. These changes are also likely only secondary to the primary alveolar and alveolar wall pathology.

#### **5.2.6.4. Hyaline membrane formation**

The formation of hyaline membranes was not observed in this case series but in the murine model infected with *P. berghei* NK65, they were only seen on day 10 post infection<sup>95</sup>. Canine patients with babesia associated ARDS usually succumb within 24 hours of presentation, long before day 10 post-infection which suggests that true hyaline membrane formation does not have enough time to develop in dogs. It may be of interest to examine lung sections from a dogs who were able to survive long enough for hyaline membrane development, but this is only likely in patients who are placed on mechanically assisted ventilation. Due to the inherently grave prognosis associated with ALI/ARDS combined with the expense of treatment, this is not often performed. Ventilator-induced lung injury would also likely complicate the histological picture.





## CONCLUSION

At both the macroscopic and histological level, *B. rossi* associated pulmonary pathology was similar among the disease cases, despite their lack of genetic homogeneity. Most cases showed severe high protein content pulmonary oedema as well as moderate to severe, multifocal to coalescing alveolar haemorrhages and fibrin exudation. The haemorrhage and oedema extended into the alveolar ducts and bronchioles. Alveolar walls were diffusely thickened due to a marked increase in cells of the monocyte-macrophage lineage. There was a marked increase in MAC387 positive bone marrow derived monocytes and macrophages and CD204 positive macrophages as well CD3 positive T-lymphocytes compared to the healthy controls indicating a role for both tissue and bone-marrow derived macrophages as well as T-lymphocytes in babesia-related ALI/ARDS. Neutrophils did not play a significant role in the inflammation. A role for sequestered parasitized red cells could not be established but seems unlikely.

This study also confirmed that the lung injury caused during natural complicated *Babesia rossi* infection in dogs fulfils the criteria for the definitions of acute lung injury and acute respiratory distress syndrome<sup>105</sup>. There was evidence of diffuse pulmonary inflammation as well as presence of a risk factor, *B. rossi*. The remaining criteria (acute onset of tachypnoea, proof of inefficient gas exchange and pulmonary capillary leakage without increased pulmonary capillary pressure) can only be confirmed clinically. The lung pathology in the current study was similar to murine malaria-associated ARDS in C57BL/6J mice infected with *Plasmodium berghei* NK65<sup>95</sup>, the murine model of babesia associated ALI/ARDS in C3H/HeN mice infected with WA-1 babesia<sup>32</sup> as well as human malaria-associated ALI/ARDS<sup>89,85</sup> and human babesiosis<sup>98,99</sup>. The MA-ALI/ARDS cases showed thickened alveolar septa, multifocal haemorrhages and severe, widespread oedema<sup>89,85</sup>. Hyaline membranes<sup>89</sup> were not a feature in this study, probably due to the acute nature of the respiratory pathology and decreased survival of the dogs. As in human malaria-associated ARDS, thrombosis and infarction were also rarely observed in canine babesiosis.

There were a few important shortcomings in this study. Only lethal cases were included in this case series, so it is possible that sublethal pulmonary injury may be present in some cases of treated complicated and uncomplicated canine babesiosis that survive. Ante-mortal lung function data such arterial blood gas and pulse oximetry was not available for these cases. Due to the rapid progression of this type of severe pulmonary disease, investigation of other biochemical markers such as lactate or oxygen saturation for early detection and treatment may be beneficial. All these cases were treated prior to death which has a major and rapid effect on parasite density<sup>41</sup>, thus, precluding judgement on the possibility of direct interaction between parasitized erythrocytes and pulmonary vascular endothelial cells. Finally, electron microscopy of the endothelial barrier was not performed, but this would be the most logical avenue for future research.

In this regard, emphasis should be placed on endothelial cell injury and activation, the glycocalyx and inter-endothelial tight junctions. These would be the most obvious areas of pathology leading to severe fluid leakage. Extrapolating from MA-ARDS, one might

expect endothelial cell injury characterised by cell swelling and necrosis as well denudation of the basement membrane and pinocytotic vesicles<sup>92</sup>. Loss of integrity of the endothelial tight junctions should also be assessed similar to that seen in sepsis<sup>51</sup> as well as possible caveolae as seen in murine babesia<sup>30</sup>. Modification of the glycocalyx may be more difficult to assess but if pinocytotic vesicles are present as in MA-ARDS, this might indicate such changes.

## REFERENCES

1. Aitken EH, Negri EM, Barboza R, et al. Ultrastructure of the lung in a murine model of malaria-associated acute lung injury/acute respiratory distress syndrome. *Malaria journal*. 2014;13: 230.
2. Albertine KH. Ultrastructural abnormalities in increased-permeability pulmonary edema. *Clinics in Chest Medicine*. 1985;6: 345-369.
3. Alibaud L, Llobera R, Al Saati T, March M, Delsol G, Rubin B. A new monoclonal anti-CD3epsilon antibody reactive on paraffin sections. *Journal of Histochemistry & Cytochemistry*. 2000;48: 1609-1616.
4. Ampawong S, Chaisri U, Viriyavejakul P, et al. A potential role for interleukin-33 and  $\gamma$ -epithelium sodium channel in the pathogenesis of human malaria associated lung injury. *Malaria journal*. 2015;14: 389-389.
5. Anstey NM, Handojo T, Pain MC, et al. Lung injury in vivax malaria: pathophysiological evidence for pulmonary vascular sequestration and posttreatment alveolar-capillary inflammation. *Journal of Infectious Diseases*. 2007;195: 589-596.
6. Ashbaugh DG, Bigelow DB, Petty TL, Levine BE. Acute respiratory distress in adults. *Lancet*. 1967;2: 319-323.
7. Bancroft JD, Gamble M. *Theory and practice of histological techniques* Elsevier health sciences; 2008.
8. Barić Rafaj R, Kuleš J, Selanec J, et al. Markers of Coagulation Activation, Endothelial Stimulation, and Inflammation in Dogs with Babesiosis. *Journal of Veterinary Internal Medicine*. 2013;27: 1172-1178.
9. Bernard GR, Artigas A, Brigham KL, et al. The American-European Consensus Conference on ARDS. Definitions, mechanisms, relevant outcomes, and clinical trial coordination. *American journal of respiratory and critical care medicine*. 1994;149: 818-824.
10. Brandtzaeg P, Jones DB, Flavell DJ, Fagerhol MK. Mac 387 antibody and detection of formalin resistant myelomonocytic L1 antigen. *Journal of Clinical Pathology*. 1988;41: 963-970.
11. Carrasco L, Sánchez C, Gómez-Villamandos J, et al. The role of pulmonary intravascular macrophages in the pathogenesis of African horse sickness. *Journal of comparative pathology*. 1999;121: 25-38.
12. Castro CY. ARDS and Diffuse Alveolar Damage: A Pathologist's Perspective. *Seminars in Thoracic and Cardiovascular Surgery*. 2006;18: 13-19.
13. Clark IA, Jacobson LS. Do babesiosis and malaria share a common disease process. *Annals of Tropical Medicine & Parasitology*. 1998;92: 483. Article.

14. Coons AA. The Demonstration of Pneumococcal Antigen in Tissues by the Use of Fluorescent Antibody. *The Journal of Immunology*. 1942;45: 159-170.
15. Cox FE. Heterologous immunity between piroplasms and malaria parasites: the simultaneous elimination of *Plasmodium vinckei* and *Babesia microti* from the blood of doubly infected mice. *Parasitology*. 1978;76: 55-60.
16. Dancey DR, Hayes J, Gomez M, et al. ARDS in patients with thermal injury. *Intensive Care Med*. 1999;25: 1231-1236.
17. Daste T, Lucas MN, Aumann M. Cerebral babesiosis and acute respiratory distress syndrome in a dog. *Journal of veterinary emergency and critical care*. 2013;23: 615-623.
18. Decaro N, Martella V, Buonavoglia C. Canine Adenoviruses and Herpesvirus. *Veterinary Clinics of North America: Small Animal Practice*. 2008;38: 799-814.
19. DeClue AE, Cohn LA. Acute respiratory distress syndrome in dogs and cats: a review of clinical findings and pathophysiology. *Journal of Veterinary Emergency & Critical Care*. 2007;17: 340-347. Article.
20. Dillon AR, Warner AE, Brawner W, Hudson J, Tillson M. Activity of pulmonary intravascular macrophages in cats and dogs with and without adult *Dirofilaria immitis*. *Veterinary Parasitology*. 2008;158: 171-176.
21. Drobotz KJ, Saunders HM, Pugh CR, Hendricks JC. Noncardiogenic pulmonary edema in dogs and cats: 26 cases (1987-1993). *Journal of the American Veterinary Medical Association*. 1995;206: 1732-1736.
22. Ecklund MM, Wahl G, Yamshchikov AV, Smith MS. Journey of a Survivor of Near Drowning, Polymicrobial Pneumonia, and Acute Respiratory Distress Syndrome. *Critical Care Nursing Clinics of North America*. 2012;24: 601-623.
23. El-Assaad F, Wheway J, Mitchell AJ, et al. Cytoadherence of *Plasmodium berghei*-infected red blood cells to murine brain and lung microvascular endothelial cells in vitro. *Infect Immun*. 2013;81: 3984-3991.
24. Ferrer L, Fondevila D, Rabanal R, Ramis A. Detection of T lymphocytes in canine tissue embedded in paraffin wax by means of antibody to CD3 antigen. *Journal of Comparative Pathology*. 1992;106: 311-314.
25. Fiuza C, Bustin M, Talwar S, et al. Inflammation-promoting activity of HMGB1 on human microvascular endothelial cells. *Blood*. 2003;101: 2652-2660.
26. Gadek JE, Pacht ER. The interdependence of lung antioxidants and antiprotease defense in ARDS. *Chest*. 1996;110: 273S-277S.

27. Goddard A, Leisewitz AL, Kjelgaard-Hansen M, Kristensen AT, Schoeman JP. Excessive Pro-Inflammatory Serum Cytokine Concentrations in Virulent Canine Babesiosis. *PloS one*. 2016;11: 1-15. Article.
28. Goddard A, Wiinberg B, Schoeman JP, Kristensen AT, Kjelgaard-Hansen M. Mortality in virulent canine babesiosis is associated with a consumptive coagulopathy. *The Veterinary Journal*. 2013;196: 213-217.
29. Guillaumin J, Hopper K. Successful outcome in a dog with neurological and respiratory signs following smoke inhalation. *Journal of veterinary emergency and critical care*. 2013;23: 328-334.
30. Hemmer RM, Ferrick DA, Conrad PA. Role of T cells and cytokines in fatal and resolving experimental babesiosis: protection in TNFRp55-/- mice infected with the human Babesia WA1 parasite. *The Journal of parasitology*. 2000;86: 736-742.
31. Hemmer RM, Ferrick DA, Conrad PA. Up-regulation of tumor necrosis factor-alpha and interferon-gamma expression in the spleen and lungs of mice infected with the human Babesia isolate WA1. *Parasitology research*. 2000;86: 121-128.
32. Hemmer RM, Wozniak EJ, Lowenstine LJ, Plopper CG, Wong V, Conrad PA. Endothelial cell changes are associated with pulmonary edema and respiratory distress in mice infected with the WA1 human Babesia parasite. *The Journal of parasitology*. 1999;85: 479-489.
33. Henning A: The pathology of the spleen in canine babesiosis. In: Department of Pathology, p. 110. University of Pretoria, University of Pretoria, 2019
34. Herbeck R, Teodorescu Brinzeu D, Giubelan M, Lazar E, Dema A, Ionita H. B-cell transcription factors Pax-5, Oct-2, BOB.1, Bcl-6, and MUM1 are useful markers for the diagnosis of nodular lymphocyte predominant Hodgkin lymphoma. *Romanian Journal of Morphology and Embryology*. 2011;52: 69-74.
35. Hirata K, Kurokawa A. Chlorhexidine gluconate ingestion resulting in fatal respiratory distress syndrome. *Veterinary and human toxicology*. 2002;44: 89-91.
36. Ince C, Mayeux PR, Nguyen T, et al. The Endothelium in Sepsis. *Shock*. 2016;45: 259-270.
37. Irwin PJ, Hutchinson GW. Clinical and pathological findings of Babesia infection in dogs. *Australian veterinary journal*. 1991;68: 204-209.
38. Ishii Y, Takami T, Kokai Y, et al. A novel human B-lymphocyte antigen shared with lymphoid dendritic cells: characterization by monoclonal antibody. *Clinical and Experimental Immunology*. 1985;61: 624-632.
39. Jacobson LS. The South African form of severe and complicated canine babesiosis: clinical advances 1994-2004. *Veterinary Parasitology*. 2006;138: 126-139.

40. Jacobson LS, Clark IA. The pathophysiology of canine babesiosis: new approaches to an old puzzle. *Journal of the South African Veterinary Association*. 1994;65: 134-145.
41. Jacobson LS, Reyers F, Berry WL, Viljoen E. Changes in haematocrit after treatment of uncomplicated canine babesiosis: a comparison between diminazene and trypan blue, and an evaluation of the influence of parasitaemia. *Journal of the South African Veterinary Association*. 1996;67: 77-82.
42. Jarvinen AK, Saario E, Andresen E, Happonen I, Saari S, Rajamaki M. Lung injury leading to respiratory distress syndrome in young Dalmatian dogs. *Journal of Veterinary Internal Medicine*. 1995;9: 162-168.
43. Johnson RP, Huxtable CR. Paraquat poisoning in a dog and cat. *The Veterinary record*. 1976;98: 189-191.
44. Jubala CM, Wojcieszyn JW, Valli VE, et al. CD20 expression in normal canine B cells and in canine non-Hodgkin lymphoma. *Veterinary pathology*. 2005;42: 468-476.
45. Kato Y, Murakami M, Hoshino Y, et al. The class A macrophage scavenger receptor CD204 is a useful immunohistochemical marker of canine histiocytic sarcoma. *J Comp Pathol*. 2013;148: 188-196.
46. Kelmer E, Love LC, Declue AE, et al. Successful treatment of acute respiratory distress syndrome in 2 dogs. *The Canadian Veterinary Journal*. 2012;53: 167-173.
47. Kong D-H, Kim YK, Kim MR, Jang JH, Lee S. Emerging Roles of Vascular Cell Adhesion Molecule-1 (VCAM-1) in Immunological Disorders and Cancer. *Int J Mol Sci*. 2018;19: 1057.
48. Kukielka GL, Hawkins HK, Michael L, et al. Regulation of intercellular adhesion molecule-1 (ICAM-1) in ischemic and reperfused canine myocardium. *Journal of Clinical Investigation*. 1993;92: 1504.
49. Kuleš J, Gotić J, Mrljak V, Barić Rafaj R. Blood markers of fibrinolysis and endothelial activation in canine babesiosis. *BMC veterinary research*. 2017;13: 82.
50. Kumar V, Abbas AK, Aster JC, Robbins SL. *Robbins Basic Pathology*, 9th Edition ed. Philadelphia, PA: Elsevier/Saunders; 2013.
51. Lee WL, Slutsky AS. Sepsis and Endothelial Permeability. *New England Journal of Medicine*. 2010;363: 689-691.
52. Leisewitz A, Goddard A, De Gier J, et al. Disease severity and blood cytokine concentrations in dogs with natural *Babesia rossi* infection. *Parasite Immunology*. 2019;41: e12630.
53. Leisewitz AL, Goddard A, Clift S, et al. A clinical and pathological description of 320 cases of naturally acquired *Babesia rossi* infection in dogs. *Veterinary Parasitology*. 2019;271: 22-30.

54. Leisewitz AL, Jacobson LS, de Morais HSA, Reyers F. The Mixed Acid-Base Disturbances of Severe Canine Babesiosis. *Journal of Veterinary Internal Medicine*. 2001;15: 445-452.
55. Lewis JF, Jobe AH. Surfactant and the adult respiratory distress syndrome. *The American review of respiratory disease*. 1993;147: 218-233.
56. Liebenberg C, Goddard A, Wiinberg B, et al. Hemostatic Abnormalities in Uncomplicated Babesiosis (*Babesia rossi*) in Dogs. *Journal of Veterinary Internal Medicine*. 2013;27: 150-156.
57. Lobetti R, Dvir E, Pearson J. Cardiac Troponins in Canine Babesiosis. *Journal of Veterinary Internal Medicine*. 2002;16: 63-68.
58. Lopez A, Lane IF, Hanna P. Adult respiratory distress syndrome in a dog with necrotizing pancreatitis. *The Canadian Veterinary Journal*. 1995;36: 240-241.
59. Lovegrove FE, Gharib SA, Pena-Castillo L, et al. Parasite burden and CD36-mediated sequestration are determinants of acute lung injury in an experimental malaria model. *Public Library of Science Pathogens*. 2008;4: e1000068.
60. Maegraith B, Gilles HM, Devakul K. Pathological processes in *Babesia canis* infections. *Zeitschrift fur Tropenmedizin und Parasitologie*. 1957;8: 485-514.
61. Maniatis NA, Orfanos SE. The endothelium in acute lung injury/acute respiratory distress syndrome. *Current Opinion in Critical Care*. 2008;14: 22-30.
62. Mathe A, Voros K, Papp L, Reiczigel J. Clinical manifestations of canine babesiosis in Hungary (63 cases). *Acta veterinaria Hungarica*. 2006;54: 367-385.
63. Matthay MA, Zimmerman GA. Acute Lung Injury and the Acute Respiratory Distress Syndrome. *American journal of respiratory cell and molecular biology*. 2005;33: 319-327.
64. McGavin D, Zachary J. *Pathologic Basis of Veterinary Disease*, 5th Edition ed. St.Louis: Elsevier Mosby; 2012.
65. Meban C. Thickness of the air-blood barriers in vertebrate lungs. *Journal of anatomy*. 1980;131: 299.
66. Mitra S, Exline M, Habyarimana F, et al. Microparticulate Caspase 1 Regulates Gasdermin D and Pulmonary Vascular Endothelial Cell Injury. *American journal of respiratory cell and molecular biology*. 2018;59: 56-64.
67. Mohr AJ, Lobetti RG, van der Lugt JJ. Acute pancreatitis: a newly recognised potential complication of canine babesiosis. *Journal of the South African Veterinary Association*. 2000;71: 232-239.
68. Neath PJ, Brockman DJ, King LG. Lung lobe torsion in dogs: 22 cases (1981-1999). *Journal of the American Veterinary Medical Association*. 2000;217: 1041-1044.

69. Neviere R, Mathieu D, Chagnon JL, Lebleu N, Millien JP, Wattel F. Skeletal muscle microvascular blood flow and oxygen transport in patients with severe sepsis. *American journal of respiratory and critical care medicine*. 1996;153: 191-195.
70. O'Dell N: Pathology of fatal natural African Horsesickness virus infection in dogs. *In: Section of Pathology, Department of Paraclinical science, Faculty of Veterinary Science, p. 100. University of Pretoria, University of Pretoria, 2018*
71. Ockenhouse CF, Tegoshi T, Maeno Y, et al. Human vascular endothelial cell adhesion receptors for Plasmodium falciparum-infected erythrocytes: roles for endothelial leukocyte adhesion molecule 1 and vascular cell adhesion molecule 1. *The Journal of experimental medicine*. 1992;176: 1183-1189.
72. Pape H-C, Auf'm Kolk M, Paffrath T, Regel G, Sturm JA, Tscheme H. Primary intramedullary femur fixation in multiple trauma patients with associated lung contusion—a cause of traumatic ARDS? *Journal of Trauma and Acute Care Surgery*. 1993;34: 540-548.
73. Parent C, King LG, Van Winkle TJ, Walker LM. Respiratory function and treatment in dogs with acute respiratory distress syndrome: 19 cases (1985-1993). *Journal of the American Veterinary Medical Association*. 1996;208: 1428-1433.
74. Plopper CG, Mariassy AT, Hill LH. Ultrastructure of the nonciliated bronchiolar epithelial (Clara) cell of mammalian lung: II. A comparison of horse, steer, sheep, dog, and cat. *Exp Lung Res*. 1980;1: 155-169.
75. Ramos-Vara JA. Technical aspects of immunohistochemistry. *Veterinary pathology*. 2005;42: 405-426.
76. Ramos-Vara JA, Miller MA. When Tissue Antigens and Antibodies Get Along: Revisiting the Technical Aspects of Immunohistochemistry—The Red, Brown, and Blue Technique. *Veterinary Pathology Online*. 2014;51: 42-87.
77. Rautenbach Y, Goddard A, Thompson PN, Mellanby RJ, Leisewitz AL. A flow cytometric assessment of the lymphocyte immunophenotypes in dogs naturally infected with Babesia rossi. *Veterinary Parasitology*. 2017;241: 26-34.
78. Sarkar A, Hall MW, Exline M, et al. Caspase-1 Regulates Escherichia coli Sepsis and Splenic B Cell Apoptosis Independently of Interleukin-1 $\beta$  and Interleukin-18. *American journal of respiratory and critical care medicine*. 2006;174: 1003-1010.
79. Schmidt EP, Yang Y, Janssen WJ, et al. The pulmonary endothelial glycocalyx regulates neutrophil adhesion and lung injury during experimental sepsis. *Nature Medicine*. 2012;18: 1217-1223.



80. Singh B, Pearce JW, Gamage LN, Janardhan K, Caldwell S. Depletion of pulmonary intravascular macrophages inhibits acute lung inflammation. *American Journal of Physiology-Lung Cellular and Molecular Physiology*. 2004;286: L363-L372.
81. Sirivisoot S, Techangamsuwan S, Tangkawattana S, Rungsipipat A. Pax5 as a potential candidate marker for canine B-cell lymphoma. *Veterinárni Medicína*. 2017;62: 74-80. Article.
82. Snyder PW. Chapter 5 - Diseases of Immunity1. In: Zachary JF, ed. *Pathologic Basis of Veterinary Disease (Sixth Edition)*. Mosby; 2017:242-285.e245.
83. Sone Y, Serikov VB, Staub NC. Intravascular macrophage depletion attenuates endotoxin lung injury in anesthetized sheep. *Journal of Applied Physiology*. 1999;87: 1354-1359.
84. Souza MC, Silva JD, Padua TA, Capelozzi VL, Rocco PR, Henriques M. Early and late acute lung injury and their association with distal organ damage in murine malaria. *Respiratory physiology & neurobiology*. 2013;186: 65-72.
85. Spitz S. The pathology of acute falciparum malaria. *Military Surgery*. 1946;99: 555-572.
86. Stalker M, Hayes M, Maxie M. *Jubb, Kennedy, and Palmer's pathology of domestic animals*, 5th Edition ed., vol. 2; 2007.
87. Steinvall I, Bak Z, Sjoberg F. Acute respiratory distress syndrome is as important as inhalation injury for the development of respiratory dysfunction in major burns. *Burns*. 2008;34: 441-451.
88. Sweers L, Kirberger RM, Leisewitz AL, Dormehl IC, Killian E, Naudé F. The scintigraphic evaluation of the pulmonary perfusion pattern of dogs hospitalised with babesiosis. *Journal of the South African Veterinary Association*. 2008;79: 76-83.
89. Taylor WR, Hanson J, Turner GD, White NJ, Dondorp AM. Respiratory manifestations of malaria. *CHEST Journal*. 2012;142: 492-505.
90. Thille AW, Esteban A, Fernández-Segoviano P, et al. Chronology of histological lesions in acute respiratory distress syndrome with diffuse alveolar damage: a prospective cohort study of clinical autopsies. *The Lancet Respiratory Medicine*. 2013;1: 395-401.
91. Thomovsky EJ, Bach J. Incidence of acute lung injury in dogs receiving transfusions. *Journal of the American Veterinary Medical Association*. 2014;244: 170-174.
92. Tomaszewski Jr JF. Pulmonary pathology of acute respiratory distress syndrome. *Clinics in Chest Medicine*. 2000;21: 435-466.
93. Turk J, Miller M, Brown T, et al. Coliform septicemia and pulmonary disease associated with canine parvoviral enteritis: 88 cases (1987-1988).

- Journal of the American Veterinary Medical Association*. 1990;196: 771-773.
94. Van den Steen PE, Deroost K, Deckers J, Van Herck E, Struyf S, Opdenakker G. Pathogenesis of malaria-associated acute respiratory distress syndrome. *Trends in parasitology*. 2013;29: 346-358.
95. Van den Steen PE, Geurts N, Deroost K, et al. Immunopathology and dexamethasone therapy in a new model for malaria-associated acute respiratory distress syndrome. *American journal of respiratory and critical care medicine*. 2010;181: 957-968.
96. Van Rensberg IB, De Clerk J, Groenewald HB, Botha WS. An outbreak of African horsesickness in dogs. *Journal of the South African Veterinary Association*. 1981;52: 323-325.
97. Van Sittert SJ, Drew TM, Kotze JL, Strydom T, Weyer CT, Guthrie AJ. Occurrence of African horse sickness in a domestic dog without apparent ingestion of horse meat. *Journal of the South African Veterinary Association*. 2013;84.
98. Vannier E, Gewurz BE, Krause PJ. Human Babesiosis. *Infectious Disease Clinics of North America*. 2008;22: 469-488.
99. Vannier EG, Diuk-Wasser MA, Ben Mamoun C, Krause PJ. Babesiosis. *Infectious Disease Clinics*. 2015;29: 357-370.
100. Walker T, Tidwell AS, Rozanski EA, DeLaforcade A, Hoffman AM. Imaging diagnosis: acute lung injury following massive bee envenomation in a dog. *Veterinary radiology & ultrasound : the official journal of the American College of Veterinary Radiology and the International Veterinary Radiology Association*. 2005;46: 300-303.
101. Ware LB: Pathophysiology of acute lung injury and the acute respiratory distress syndrome. *In: Seminars in Respiratory and Critical Care medicine*, pp. 337-349. New York: Thieme Medical Publishers, c1994-, 2006
102. Ware LB, Matthay MA. The acute respiratory distress syndrome. *New England Journal of Medicine*. 2000;342: 1334-1349.
103. Welzl C, Leisewitz AL, Jacobson LS, Vaughan-Scott T, Myburgh E. Systemic inflammatory response syndrome and multiple-organ damage/dysfunction in complicated canine babesiosis. *Journal of the South African Veterinary Association*. 2001;72: 158-162.
104. White DJ, Talarico J, Chang HG, Birkhead GS, Heimberger T, Morse DL. Human babesiosis in New York State: Review of 139 hospitalized cases and analysis of prognostic factors. *Archives of internal medicine*. 1998;158: 2149-2154.
105. Wilkins PA, Otto CM, Baumgardner JE, et al. Acute lung injury and acute respiratory distress syndromes in veterinary medicine: consensus definitions: The Dorothy Russell Havemeyer Working Group on ALI and

- ARDS in Veterinary Medicine. *Journal of Veterinary Emergency & Critical Care*. 2007;17: 333-339. Article.
106. Winkler GC. Review of the significance of pulmonary intravascular macrophages with respect to animal species and age. *Experimental Cell Biology*. 1989;57: 281-286.
107. Woo C-H, Lim J-H, Kim J-H. VCAM-1 upregulation via PKC $\delta$ -p38 kinase-linked cascade mediates the TNF- $\alpha$ -induced leukocyte adhesion and emigration in the lung airway epithelium. *American Journal of Physiology - Lung Cellular and Molecular Physiology*. 2005;288: L307-L316. Journal Article.
108. Wu Y, Szeszak T, Stins M, Craig AG. Amplification of *P. falciparum* Cytoadherence through induction of a pro-adhesive state in host endothelium. *Public Library of Science One*. 2011;6: e24784.
109. Zachary JF, McGavin MD. *Pathologic Basis of Veterinary Disease*, 6th Edition ed.Elsevier Health Sciences; 2016.
110. Zimmerman GA, Albertine KH, Carveth HJ, et al. Endothelial activation in ARDS. *Chest*. 1999;116: 18S-24S.

## APPENDICES

# Appendix 1: O'Dell lung scoring system grading criteria<sup>70</sup>

## APPENDIX 2

Table 1: Grading criteria for histological lesions.

Parameter	Grading	Criteria
<b>Autolysis</b>		
<b>Severity</b>	Mild	Anatomical architecture easily distinguishable, cellular morphology well-defined
	Moderate	Anatomical architecture still easily distinguishable, cellular morphology not well-defined, red blood cells still preserved, small numbers of putrefactive (Clostridial) bacteria may be present in some fields
	Severe	Cellular morphology cannot be defined, anatomical architecture barely distinguishable, red blood cells lysed and difficult to identify, numerous putrefactive (Clostridial) bacteria present
<b>Histopathology (All changes in comparison with normal control lung [Figure 9 and 10])</b>		
<b>Lesion distribution</b>	Focal	Single well circumscribed area affected
	Multifocal	Multiple non-overlapping areas affected
	Coalescing	Multiple overlapping areas affected
	Diffuse	Entire lung tissue OR all specific anatomical sites affected [Figure 11 and 12]
<b>Hyperaemia/congestion</b>	Mild	Single layer of erythrocytes in capillaries with open spaces in between [Figure 13]
	Moderate	Single layer of erythrocytes in capillaries with no open spaces
	Severe	Double layer or more of erythrocytes in capillaries with no open spaces [Figure 14]
<b>Inflammatory cell infiltrate* (monocyte-macrophages, lymphocytes, plasma cells, neutrophils, eosinophils)</b> - perivascular interstitium - peribronchiolar interstitium - sub-pleural interstitium	Mild	Single leukocytes present without notable expansion of the interstitial anatomy [Figure 29, 43 and 49]
	Moderate	Two to three layers of leukocytes present resulting in slight expansion of the interstitial anatomy
	Severe	More than three layers of leukocytes present resulting in marked expansion of the interstitial anatomy [Figure 30]
<b>Inflammatory cell infiltrate* (monocyte-macrophages, lymphocytes, plasma cells, neutrophils, eosinophils)</b> - alveolar wall	Mild	Single extravascular leukocytes without notable expansion of the alveolar wall [Figure 15]
	Moderate	Slight expansion of the alveolar wall by extravascular leukocytes (double normal thickness) [Figure 16]
	Severe	Marked expansion of the alveolar wall by extravascular leukocytes (more than double normal thickness) [Figure 17]
<b>Inflammatory cell infiltrate* (monocyte-macrophages, lymphocytes, plasma cells, neutrophils, eosinophils)</b> - alveolar lumen - bronchiolar lumen	Mild	≤1 leukocytes observed in >50% of the alveolar/bronchiolar lumens [Figure 21]
	Moderate	2-5 leukocytes observed in >50% of the alveolar/bronchiolar lumens
	Severe	≥6 leukocytes observed in >50% of the alveolar/bronchiolar lumens [Figure 22]
<b>Fibrin</b>	Mild	Affecting less than a third of the anatomic location [Figure 31, 53 and 54]
	Moderate	Affecting more than a third to two thirds of the anatomic location [Figure 24]
	Severe	Affecting more than two thirds of the anatomic location [Figure 32]
<b>Haemorrhage* - perivascular interstitium</b>	Mild	Single extravasated erythrocytes present without notable expansion of the interstitial anatomy [Figure 33 and 50]

- peribronchiolar interstitium - sub-pleural interstitium	Moderate	Slight expansion of the interstitial anatomy by extravasated erythrocytes (double normal thickness) [Figure 34 and 44]
	Severe	Marked expansion of the interstitial anatomy by extravasated erythrocytes (more than double normal thickness) [Figure 35]
<b>Haemorrhage*</b> - bronchiolar lumen - alveolar lumen	Mild	Small numbers of extravasated erythrocytes present in less than 50% of alveolar/bronchiolar lumens [Figure 25]
	Moderate	Small numbers of extravasated erythrocytes present in more than 50% of alveolar/bronchiolar lumens OR less than 50% of alveolar/bronchiolar lumens are filled with extravasated erythrocytes multifocally [Figure 26]
	Severe	>50% of alveolar/bronchiolar lumens are filled with extravasated erythrocytes [Figure 27]
<b>Oedema*</b> (amorphous clear to eosinophilic extravascular fluid) - perivascular interstitium - peribronchiolar interstitium - sub-pleural interstitium	Mild	Slight expansion (1x) of the interstitium by oedema fluid [Figure 36, 45 and 51]
	Moderate	Moderate expansion (2-3x) of the interstitium by oedema fluid [Figure 37 and 46]
	Severe	Marked expansion (>3x) of the interstitium by oedema fluid [Figure 38 and 47]
<b>Oedema*</b> (amorphous clear to eosinophilic extravascular fluid) - bronchiolar lumen - alveolar lumen	Mild	Affecting less than a third of alveolar/bronchiolar lumens
	Moderate	Affecting a third to two thirds of alveolar/bronchiolar lumens
	Severe	Affecting more than two thirds of alveolar/bronchiolar lumens [Figure 28 and 56]
<b>Microvascular endothelial cell activation</b> (endothelial cell nucleus thickness is double or more the normal thickness)	Mild	Less than a third of endothelial cells display nuclear activation/hypertrophy
	Moderate	A third to two thirds of endothelial cells display nuclear activation/hypertrophy
	Severe	More than two thirds of endothelial cells display nuclear activation/hypertrophy [Figure 20 and 41]
<b>Lymphatic vessel distention</b>	Mild	Distension of less than a third of lymphatic vessels
	Moderate	Distension of a third to two thirds of lymphatic vessels [Figure 39]
	Severe	Distension of more than a third of lymphatic vessels
<b>Apoptosis</b> (clusters of closely aggregated dark purple nuclear fragments [Figure 19]) - alveolar wall	Mild	≤1 apoptotic cells per HPF
	Moderate	2-5 apoptotic cells per HPF
	Severe	≥6 apoptotic cells per HPF [Figure 18]
<b>Immunohistochemistry</b>		
<b>Degree of labelling</b>	1+	≤1 clearly labelling cells per HPF
	2+	2-5 clearly labelling cells per HPF
	3+	≥6 clearly labelling cells per HPF [Figure 58 and 60]

\* Criteria for the evaluation of inflammatory cell infiltrate, haemorrhage and oedema varied dependent on anatomical location.

HPF: High power field (400x magnification)

**Appendix 2: Modified O'Dell Lung scoring system for use  
in *Babesia*-associated ALI/ARDS**

O'Dell lung scoring system for Babesia associated canine ALI/ARDS -						
Case ID	Adapted from Pathology of natural Horsesickness virus infection in dogs by Nicolize O'Dell					
Anatomical Region / Parameter			Scoring			
<b>Autolysis</b>			Absent	Mild	Moderate	Severe
<b>Lesion distribution</b>			Focal	Multifocal	Coalescing	Diffuse
<b>Congestion</b>			Absent	Mild	Moderate	Severe
<b>Alveolar walls</b>	Cell infiltrate	Monocyte-macrophages	Absent	Mild	Moderate	Severe
		Lymphocytes	Absent	Mild	Moderate	Severe
		Plasma cells	Absent	Mild	Moderate	Severe
		neutrophils	Absent	Mild	Moderate	Severe
		Eosinophils	Absent	Mild	Moderate	Severe
	Apoptosis		Absent	Mild	Moderate	Severe
	Microvascular endothelial cell activation	Nuclear hypertrophy/activation	Absent	Mild	Moderate	Severe
	Thombosis				Present	Absent
<b>Alveolar lumen</b>	Cell infiltrate	Monocyte-macrophages	Absent	Mild	Moderate	Severe
		Lymphocytes	Absent	Mild	Moderate	Severe
		Plasma cells	Absent	Mild	Moderate	Severe
		neutrophils	Absent	Mild	Moderate	Severe
		Eosinophils	Absent	Mild	Moderate	Severe
	Fibrin		Absent	Mild	Moderate	Severe
	Haemorrhage		Absent	Mild	Moderate	Severe
			Focal	Multifocal	Coalescing	Diffuse
	Oedema		Absent	Mild	Moderate	Severe
	Hyaline membrane				Absent	Present
<b>Perivascular interstitium</b>	Cell infiltrate	Monocyte-macrophages	Absent	Mild	Moderate	Severe
		Lymphocytes	Absent	Mild	Moderate	Severe
		Plasma cells	Absent	Mild	Moderate	Severe
		neutrophils	Absent	Mild	Moderate	Severe
		Eosinophils	Absent	Mild	Moderate	Severe
	Fibrin		Absent	Mild	Moderate	Severe
	Haemorrhage		Absent	Mild	Moderate	Severe
			Focal	Multifocal	Coalescing	Diffuse
	Oedema		Absent	Mild	Moderate	Severe
	Microvascular endothelial cell activation	Nuclear hypertrophy/activation	Absent	Mild	Moderate	Severe



	Lymphatic vessel distension	Distension	Absent	Mild	Moderate	Leukocytes
		Content	Oedema	Haemorrhage	Fibrin	Severe
<b>Subpleural interstitium</b>	Cell infiltrate	Monocyte-macrophages	Absent	Mild	Moderate	Severe
		Lymphocytes	Absent	Mild	Moderate	Severe
		Plasma cells	Absent	Mild	Moderate	Severe
		neutrophils	Absent	Mild	Moderate	Severe
		Eosinophils	Absent	Mild	Moderate	Severe
	Fibrin		Absent	Mild	Moderate	Severe
	Haemorrhage		Absent	Mild	Moderate	Severe
			Focal	Multifocal	Coalescing	Diffuse
	Oedema		Absent	Mild	Moderate	Severe
	<b>Pleural mesothelium</b>	Hypertrophy/activation			Present	Absent
<b>Peribronchiolar interstitium</b>	Cell infiltrate	Monocyte-macrophages	Absent	Mild	Moderate	Severe
		Lymphocytes	Absent	Mild	Moderate	Severe
		Plasma cells	Absent	Mild	Moderate	Severe
		neutrophils	Absent	Mild	Moderate	Severe
		Eosinophils	Absent	Mild	Moderate	Severe
	Fibrin		Absent	Mild	Moderate	Severe
	Haemorrhage		Absent	Mild	Moderate	Severe
			Focal	Multifocal	Coalescing	Diffuse
	Oedema		Absent	Mild	Moderate	Severe
	Anthraxis				Present	absent
	BALT activity				Hyperplastic	Normal
<b>Bronchiolar lumen</b>	Cell infiltrate	Monocyte-macrophages	Absent	Mild	Moderate	Severe
		Lymphocytes	Absent	Mild	Moderate	Severe
		Plasma cells	Absent	Mild	Moderate	Severe
		neutrophils	Absent	Mild	Moderate	Severe
		Eosinophils	Absent	Mild	Moderate	Severe
	Fibrin		Absent	Mild	Moderate	Severe
	Haemorrhage		Absent	Mild	Moderate	Severe
			Focal	Multifocal	Coalescing	Diffuse
	Oedema		Absent	Mild	Moderate	Severe

### Appendix 3: Immunohistochemistry score sheet for *Babesia*-associated ALI/ARDS

Immunohistochemistry score sheet for the pathology of babesia-related ALI/ARDS in dogs												
Case ID		Region					Case Average		Total Average	Standard Deviation	Min	Max
Test cases	IHC marker....	1	2	3	4	5		Alveoli				
Case 1	Alveoli							Alveolar wall				
	Alveolar wall							Peribronchial				
	Peribronchial											
Case 2	Alveoli											
	Alveolar wall											
	Peribronchial											
Case 3	Alveoli											
	Alveolar wall											
	Peribronchial											
Case 4	Alveoli											
	Alveolar wall											
	Peribronchial											
Case 5	Alveoli											
	Alveolar wall											
	Peribronchial											
Case 6	Alveoli											
	Alveolar wall											
	Peribronchial											
Case 7	Alveoli											
	Alveolar wall											
	Peribronchial											
Case 8	Alveoli											
	Alveolar wall											
	Peribronchial											
Case 9	Alveoli											
	Alveolar wall											
	Peribronchial											
Case 10	Alveoli											
	Alveolar wall											
	Peribronchial											
Case 11	Alveoli											
	Alveolar wall											
	Peribronchial											

## Appendix 4: Informed consent

*(To be completed by the patient's owner / authorized agent)*

### Encircle Yes or No where necessary

1. Have you read the information sheet on canine babesiosis? Yes No
2. Have you had the opportunity to ask questions about the research project? Yes No
3. Have you received satisfactory answers to your questions? Yes No
4. Have you received enough information about this study? Yes No
5. Supply the name of the person to whom you have spoken to:  
.....
6. Do you grant consent that blood and urine samples can be drawn from your dog? Yes No
7. Do you grant consent that a post mortem examination can be performed in the case of death?  
Yes No

I, ....., hereby give permission that my dog ....., a ..... may participate in this clinical study conducted at the Onderstepoort Veterinary Academic Hospital.

I understand that this study will in no way harm my dog. Furthermore I understand that the costs of the additional tests will be borne by the trial fund, and that I will only be liable for costs pertaining the treatment that would in any event be required by my dog, including any complications that may arise as a result of canine babesiosis.

Signed at Onderstepoort on the ..... day of ..... 20.....

Signature Owner/Agent .....

Home Tel: .....

Work Tel: .....

Cell No: .....

## **Appendix 5: Individual case reports**

### **5.1. Case 1 – S6/15 – Carter Leibrandt**

Macroscopically, the lungs showed dark red mottling, especially in the cranial lobes. The caudal lobes were diffusely dark red and oozed froth on cut surface. There was also an increased, rubbery consistency. Histologically, the alveoli showed extensive atelectasis accompanied by a marked increase in the number of alveolar macrophages as well as low protein content pulmonary oedema. There were multifocal areas of mild to moderate haemorrhage per diapedesis along with fibrin exudation into the alveolar spaces. Multifocal areas of complete alveolar plugging by fibrin exudate was noted and this was also accompanied by some cellular debris. Alveolar macrophages were foamy, and a few contained small quantities of dark brown granular pigment consistent with haemosiderin. Scattered neutrophils were also observed within the alveolar spaces as well as within the alveolar ducts. The interstitium was severely expanded due to the presence of mononuclear leukocytes accompanied by severe congestion/hyperaemia. Segmental areas of fibrin deposition were observed within the vascular capillaries. Mild perivascular oedema was noted and there is also marked congestion within the bronchiolar arterioles and venules. Moderate haemorrhage was present in the interstitium surrounding a few bronchiolar venules as well as in the subcapsular regions. Moderate mononuclear leukostasis was noted in the bronchial blood vessels with a mild accumulation of large lymphocytes and plasma cells in a perivascular distribution multifocally. The endothelial cells were plump and activated with ovoid nuclei. The bronchioles contained moderate quantities of oedema as well as haemorrhage and fibrin with alveolar macrophages and lesser numbers of neutrophils.

### **5.2. Case 2 – S400/15 – Brono Arlow**

The lungs showed mottling with multifocal to coalescing dark red to black discolouration representing haemorrhage especially in the caudodorsal lobes. There are multifocal small pink areas of alveolar emphysema on the periphery. Histologically, the lung tissue showed multifocal, isolated areas of moderate to severe alveolar and interstitial haemorrhage with fibrin deposition accompanied by small segmental areas of alveolar wall necrosis. The alveoli showed a mild increase in the number of alveolar macrophages, some of which showed erthrophagocytic activity and others also contained small quantities of brown to black, granular pigment (consistent with haemosiderin). The alveolar capillaries showed marked to severe leukostasis consisting primarily of mononuclear cells. These mononuclear cells had a plasmacytoid appearance as well as lymphocytoid and monocytoid appearance. Some of the monocytic cells possessed expanded, vacuolated cytoplasm often containing granular, slightly basophilic material (potentially consistent with phagocytosed *B. rossi* remnants). Sections of the interstitium especially near the bronchial vasculature showed expansion by accumulations of mononuclear cells in a perivascular cuffing by mononuclear cells with mild expansion due to oedema. In area's, scattered apoptotic cells with visible karyorhexis and karyolysis. Some inflammatory cells showed active mitosis. Scattered erythrocytes do contain intracytoplasmic piroplasm's (consistent

with *B. rossi*). Mild peribronchial anthracosis was also noted. The bronchiolar arterioles and venules showed severe leukostasis with a pavinging or “rafting” of leukocytes with a few scattered erythrocytes between the cells along with a small quantity of plasma. These cells were mostly monocytes with a decreased nucleocytoplasmic ration and slightly grainy to vacuolated cytoplasm, often containing small quantities of granular basophilic material. Endothelial cells were plump appearance with nuclei containing coarsely stippled to marginated chromatin. The alveolar ducts, bronchioles and bronchi also contained a few erythrocytes, alveolar macrophages and moderately proteinaceous pulmonary oedema.

### 5.3. Case 3 – S1063/15 – Lexy Strydom

Macroscopically, the lungs showed multifocal to coalescing areas of haemorrhage throughout with the caudal lobes appearing worse affected. Severe tracheal froth was present as well. Histologically, the lung tissue showed diffuse accumulation of markedly protein rich pulmonary oedema in the alveoli accompanied by mild haemorrhage per diapedesis. Additionally, there was a mild increase in alveolar macrophages, some of which showed erythrophagocytosis. The interstitium was mildly expanded due to accumulation of oedema but there was also moderate, diffuse accumulation of mononuclear inflammatory cells within the interstitium accompanied by a marked alveolar capillary leukostasis. The inflammatory cells consisted primarily of monocytes and lymphocytes. The monocytes possessed slightly granular to vacuolated cytoplasm with frequent evidence of erythrophagocytosis. The nuclei were often expanded with coarsely stippled to marginated chromatin. There were scattered larger, blastic leukocytes visible as well. The alveolar capillary endothelium was plump with hypertrophic ovoid nuclei with coarse chromatin. Scattered inflammatory cells also showed karyorhexis and karyolysis. The bronchial vasculature showed severe leukostasis, predominantly comprising monocytes with indented nuclei. Few red blood cells and plasma separated the cells. Occasional monocytes had what appeared to be phagocytosed piroplasm's. Several erythrocytes possessed round to ovoid *B. rossi* piroplasms. Moderate to severe perivascular oedema was noted around the bronchial arterioles. The alveolar ducts, bronchioles and bronchi contained a large quantity of protein-rich pulmonary oedema as well as alveolar macrophages. Fibrin strands were visible in the bronchioles. Foci of severe atelectasis were present and there was a marked increase in the number of alveolar macrophages in these regions. Moderate subcapsular oedema was also present and small areas of perivascular lymphoplasmacytic accumulation were noted multifocally.

### 5.4. Case 4 – S2447/15 - Lemo Motsepe

Macroscopically, the lungs showed mottling with severe, multifocal haemorrhages with interspersed, raised pink areas. There was a moderate increase in weight and marked tracheal froth and oozing on lung cut surface. Macroscopically, the alveoli possessed protein-rich pulmonary oedema accompanied by multifocal areas of mild atelectasis,

and mild to moderate foci of haemorrhage per diapedesis. Scattered areas of alveolar fibrin exudation were noted especially near the bronchial vasculature accompanied by a moderately increased alveolar macrophage, some of which were slightly vacuolated, whilst others showed prominent karyorhexis and karyolysis. A few of these macrophages contained light brown dusty pigment (consistent with haemosiderin) as well as refractory carbon pigment. There was a mild mononuclear leukostasis accompanied by severe congestion in the alveolar capillaries as well as bronchial blood vessels. A few do show karyorhexis and karyolysis. Focal segments of alveolar wall expansion due to mononuclear cell accumulation associated with the fibrin exudation into the surrounding alveoli were noted. Other sections also exhibited perivascular accumulations of lymphocytes and plasma cells. The alveolar ducts and bronchioles also contained low to high protein content pulmonary oedema. Mild vascular oedema was noted around the bronchial vasculature. The bronchi and bronchioles contained a few intraluminal erythrocytes along with a few alveolar macrophages. Occasional large immature leukocytes and megakaryocytes were noted in the vasculature.

#### **5.5. Case 5 – S7382/14 – Chico Rambaya**

Macroscopically, the lungs showed severe mottling with multifocal to coalescing bright red haemorrhage with interspersed sunken, dark red areas (atelectasis). There was also mildly increased consistency and red tinged froth present in the trachea and bronchi. Histologically, there was multifocal areas of severe atelectasis accompanied by intervening areas of emphysema. There was severe diffuse high protein content pulmonary oedema. The alveoli also showed a mild increase of macrophages (some of which are foamy) with small quantities of fibrin as well as mild haemorrhage per diapedesis, but areas of obvious moderate haemorrhage were visible as well multifocally. Alveolar macrophages showed active erythrophagocytosis and accumulation of small quantities of dark brown crystalline pigment consistent with haemosiderin pigment. The alveolar interstitium showed a mild increase in the number of intravascular mononuclear cells and was also accompanied by marked congestion. The bronchiolar blood vessels showed marked accumulation of fibrin with numerous enmeshed neutrophils and macrophages and these cells had a slightly smudged appearance. Margination of mononuclear cells was also observed in some segments while other segments showed endothelial cell swelling with plump, hyperchromatic nuclei. The bronchioles and bronchi showed marked accumulation of high protein content pulmonary oedema as well as red blood cells and scattered alveolar macrophages with the rare neutrophil. There was severe congestion in the alveolar capillaries and bronchial blood vessels. Macrophages in the bronchial associated lymphoid tissue contained refractile carbon pigment.

#### **5.6. Case 6 – S7485/14 – Blowey Manthosi**

Macroscopically, the lungs showed mottling with multifocal to coalescing areas of bright red haemorrhage and accentuated lobulation with well demarcated 3mm petechiations. The caudal lungs lobes showed the most prominent petechiations.

Histologically, the alveoli showed diffuse high protein content pulmonary oedema accompanied by multifocal mild atelectasis with a mild increase in the number of alveolar macrophages and mild to moderate multifocal haemorrhage per diapedesis. Scattered areas of alveolar fibrin exudation were noted especially around the bronchial blood vessels accompanied by a moderate increase in alveolar macrophages, some of which appeared to be mildly vacuolated, others showed karyorhexis and karyolysis. A few of these macrophages haemosiderin and carbon. There was mild mononuclear leukostasis, including some karyorhexis and karyolysis, but also severe congestion in the alveolar capillaries and bronchial blood vessels. Multifocal segments of alveolar walls were thickened due to mononuclear cell accumulation with associated fibrin exudation into the surrounding alveoli. Other sections showed perivascular accumulation of lymphocytes and plasma cells. Alveolar ducts and bronchioles also contained low to high protein content pulmonary oedema. Mild oedema was noted around the bronchial vasculature. Bronchi and bronchioles showed a few intraluminal erythrocytes and alveolar macrophages. Occasional large immature leukocytes and megakaryocytes were note intravascularly.

#### **5.7. Case 7 – S3822/15 – Puddles Hansen**

Macroscopically, the lungs were relatively normal. Histologically, the alveoli showed variable low to high protein content pulmonary oedema throughout accompanied interspersed by emphysema and atelectasis. The alveolar wall was thickened due to accumulation of mononuclear leukocytes and leukostasis. Multifocal areas of marked intra-alveolar haemorrhage and fibrin were encountered. Occasional megakaryocytes were noted in the alveolar capillaries. Bronchiolar lumens contained necrotic debris and colonies of coccoid bacteria. Bronchial blood vessels showed mild mononuclear leukostasis. There was a mild increase in alveolar macrophages, some with haemosiderin pigment. There was occasional of carbon within scattered macrophages in the bronchial associated lymphoid tissue. Moderate to severe perivascular oedema was also present.

#### **5.8. Case 8 – S3544/15 – Spot Bruyns**

Macroscopically, there was multifocal to coalescing dark to bright red areas representing haemorrhage. Mild tracheal froth accumulation was noted as well as oozing from lung cut surface. Histologically, the alveoli showed marked accumulation of high protein content pulmonary oedema diffusely throughout accompanied by multifocal areas of severe fibrin exudation. These areas were accompanied by numerous alveolar macrophages with scattered neutrophils and there was also moderate haemorrhage per diapedesis. The alveolar macrophages had a vacuolated appearance with open, vesiculated nuclei and a few contained cytoplasmic, granular dark brown pigment (consistent with haemosiderin). Segments of the alveolar ducts and alveoli were also lined by eosinophilic material consistent with fibrin. The interstitium is moderately expanded by mononuclear cells, while the alveolar capillaries also contained monocytes as well as a few scattered megakaryocytes and

some blastic leucocytes. The alveolar capillary endothelium had a plump appearance with ovoid nuclei containing coarse chromatin. Segments of the bronchial arterioles showed marked margination of mononuclear cells and occasional neutrophils accompanied by perivascular oedema as well as areas of karyorrhexis and karyolysis. Surrounding macrophages also occasionally contained carbon. The remaining alveolar interstitium was moderately expanded due to oedema as well as mononuclear cell accumulation. Some bronchial blood vessels also showed moderate congestion as well as mononuclear leukostasis and scattered erythrophagocytosis was noted along with an increase in mitotic frequency. Mild surrounding perivascular interstitial haemorrhage and oedema was noted as well. The peribronchiolar alveoli showed a moderate increase in macrophages and the bronchial lumens contained a low protein content pulmonary oedema.

#### **5.9. Case 9 – S9932/14 – Sasha Proctor**

Macroscopically, there was severe, multifocal to coalescing, well demarcated, dark red areas of haemorrhage. Some of the foci were surrounded by thin bright red halo and larger foci were also sunken representing atelectasis. Some areas were pink and raised indicating emphysema and there is a mild increase in weight and consistency. Histologically, the alveoli possessed moderate to severe haemorrhage multifocally and this was accompanied by the presence of marked high protein pulmonary oedema and severe atelectasis. There was a mild increase in the number of alveolar macrophages. Multifocal areas also showed severe haemorrhage and fibrin accumulation within the alveolar ducts as well as bronchioles and this was accompanied by a few alveolar macrophages. The interstitium showed marked expansion due to the presence of mononuclear leukocytes and there was also a moderate mononuclear leukostasis in the alveolar capillaries. The mononuclear cells have slightly foamy to granular eosinophilic cytoplasm. The nuclei were ovoid with fine chromatin and there was a mild to moderate increase in number of visible mitotic figures as well as apoptotic cells. Megakaryocytes were observed multifocally within the vascular capillaries. The alveolar capillaries did not show any sign of active erythrophagocytosis or haemosiderin pigment formation. The bronchiolar vasculature showed marked mononuclear leukostasis with visible active erythrophagocytosis and the endothelial cells appear plump and active. There was mild accumulation of dark brown crystalline pigment within the bronchiolar associated lymphoid tissue consistent with carbon. Mild perivascular oedema was also present.

#### **5.10. Case 10 – S3541/15 – Eddie Loggenberg**

Macroscopically, the lungs showed diffuse dark red discolouration and there is moderate light red pleural effusion. There was a mild increase in weight and visible froth in the trachea. Histologically, most alveoli contained low protein content pulmonary oedema but there was moderate haemorrhage per diapedesis and there were scattered alveolar macrophages, some of which contained haemosiderin. The interstitium showed moderate to severe generalised congestion and there were a few



scattered megakaryocytes noted along with occasional mononuclear cells present in the alveolar capillaries. There was mild to moderate perivascular oedema around the bronchiolar and bronchial vasculature. Activated endothelial cells were visible in segments and there was some mononuclear cell margination. Macrophages in the bronchiolar associated lymphoid tissue showed moderate carbon accumulation. The bronchioles and alveolar ducts contained low protein content pulmonary oedema.

#### 5.11. Case 11 – S8095/14 – Rotty Hecker

Macroscopically, the lungs showed mottling with multifocal to coalescing dark red discolouration with a surrounding, light red halo. Histologically, the alveoli showed multifocal areas of moderate haemorrhage per diapedesis with areas of severe haemorrhage and fibrin exudation. This was also accompanied by marked high protein content pulmonary oedema in most alveoli. There was also a mild to moderate increase in the number of alveolar macrophages some of which showed erythrophagocytosis and contained small quantities of haemosiderin. The interstitium was markedly expanded due to the presence of mononuclear cells as well as oedema. The mononuclear cells had expanded, slightly granulated vacuolated cytoplasm and ovoid to indented nuclei with coarsely stippled chromatin. Several the cells also contained *B. rossi* piroplasms. The interstitium also contained a few scattered multinucleated cells consistent with megakaryocytes. The bronchial vasculature also showed severe, pavingting/rafting leukostasis mostly with mononuclear cells which have expanded cytoplasm and active erythrophagocytosis and golden yellow to brown intracytoplasmic pigment in some cells (haemosiderin) with a small number of red blood cells and plasma separating the cells. Scattered karyorhexis and karyolysis were noted in the inflammatory cells. The bronchial vasculature showed multiple thrombi with entrapped mononuclear cells as well as few red blood cells but there was marked monocytic accumulation on the surface. The enmeshed cells in the thrombus were monocytic with expanded cytoplasm and showed active erythrophagocytosis. The alveolar capillary endothelium often had a plump appearance with ovoid nuclei with coarse chromatin. Carbon was noted with in macrophages of the bronchial associated lymphoid tissue. Mild perivascular oedema was also present and there were also scattered areas of mild atelectasis. The alveolar ducts and bronchioles contained low protein content pulmonary oedema. There were scattered intravascular larger immature leukocytes.

